

POLITECNICO DI MILANO

Scuola di Ingegneria Industriale e dell'Informazione

Corso di Laurea Magistrale in Ingegneria Elettrica



**ANALYSIS AND PRELIMINARY REALIZATION
OF A BRAKE PAD CONTACT DETECTION
SYSTEM**

Relatore: Professore Francesco Castelli Dezza

Correlatore : Professore Stefano - Melzi

Tesi di Laurea Magistrale di:

MATTIA FEDERICO LEVA

Matricola 858334

ANNO ACCADEMICO 2017-2018

Contents

Introduction	1
Chapter 1	2
1 Electrical contact system	2
1.1 Electrical contact	2
1.2 Electrical contact surfaces	3
1.3 Contact resistance	4
1.4 Theoretical contact resistance evaluation through a-spots	5
1.5 Film resistance	8
1.6 Temperature influence	9
2 Mechanical brake system	10
2.1 How the braking system works	11
2.2 Friction theory	12
2.3 Types of Friction Braking Systems	12
2.3.1 Drum Brakes	13
2.3.2 Disc Brakes	13
2.3.3 Disc brake components	14
2.4 Wear pad sensors	22
2.4.1 Squealer type	22
2.4.2 Resistive circuit type	23
2.4.3 Electronic parking motion type	24
Chapter 2	25
1.1 Electrical conductive characterization of mechanical components	25
2.1 Components characterization	26
3.1 Capacity test with frequency sweep	44
3.2 Incremental distance	53
3.3 Single pad analysis of the complete system	56
Chapter 3	59
1.1 FEM analysis	59

2.1 Simulation setup	59
2.2 Simulation configuration process	60
3.1 DC Conduction	62
3.2 Current density distribution	70
4.1 Electrostatic Simulations	75
4.2 Capacitance matrix	75
4.3 Simulation setup	78
4.4 Final impedance value	87
Chapter 4	88
4.1 AD5933 system description	89
4.2 Measurement setup	92
4.3 Advantages versus disadvantages	93
4.4 Experimental test on the EVAL-AD5933EB board	94
Conclusion	105
Bibliography References	106
Appendix	107

Abstract

Up to now, when thinking about advancing the efficiency of a vehicle, all the components under investigation are purely related to the engine, aerodynamics and tire compounds. The importance of the braking system is usually underestimated. In addition another element scarcely taken into account is the pollution produced by the brake pad components during braking. Braking system is a mechanical device, one of the most important elements for the right functioning of a vehicle. It inhibits motion by converting kinetic energy into heat or in the newest hybrid cars in electrical energy storable in batteries. The aim of this thesis is to identify the presence of unwanted contacts between brake disc and brake pads when braking is not requested by the driver. More precisely, a deep experimental analysis, is made on the electrical characterization of the brake pad studying it as one electrical element component, on the possible unwanted contacts configurations and the evaluation of these through an impedance variation. The solution proposed consists in comparing the measurements taken between a set of brake pads with a series of reference impedance values in order to obtain the relative distance between pad and disc. Three approaches have been adopted: the first one is an experimental one, the second one based on electronic simulations and the third one related to the production of an industrial product.

Figure Index

Figure 1: Surface contact spots

Figure 2: Resistivity-Temperature trend

Figure 3: Automotive braking system

Figure 4: Drum brake components

Figure 5: Fixed caliper

Figure 6: Floating caliper

Figure 7: Brake disc comparison

Figure 8: Brake pads typologies

Figure 9: Squealer wear indicator

Figure 10: Resistance value of a cast iron ring

Figure 11: 1:1 Scale brake pad

Figure 12: Four quarter of the brake pad during the 1/24 analysis

Figure 13: First quarter impedance measurement

Figure 14: Scotch tape pre-cut stage

Figure 15a: Outside 1cm border impedance

Figure 15b: Inside 1cm border impedance

Figure 16: Lateral extremes impedance

Figure 17: Horizontal stripes

Figure 18: 8th order impedance characterization curve

Figure 19: Connection clamps points

Figure 20: 4 pressure points versus 2 pressure points configuration

Figure 21a: Pad right to the designated slot

Figure 21b: Pad above half right slot

Figure 21c: Pad above the slot

Figure 21d: Pad above half left slot

Figure 21e: Pad left to the designated slot

Figure 22: Pads placed on same surface configuration

Figure 23: Capacitance measurement with pad position configuration 180° above and side to side bottom

Figure 24: simplified pad positioning (above) versus real pad positioning (below)

Figure 25: Short-circuiting the right pad

Figure 26: Short-circuited equivalent circuit (left) compared to the complete equivalent circuit (right)

Figure 27: DC conduction applied voltages

Figure 28: Complete pad-disc contact

Figure 29: Quarter pad-disc contact

Figure 30: Half quarter pad-disc contact

Figure 31: Current density distribution with total contact

Figure 32: Ratio between current density distribution over different contact areas

Figure 33: Electrical equivalent system of the braking system

Figure 34: Region setup comparison

Figure 35: AD5933 board block diagram

Figure 36: System connections

Figure 37: Automotive system connections

Figure 38: Calibration setup of the EvalAD5933EBZ board

Figure 39: Software parameter for board calibration

Figure 40: Impedance measurement setup

Figure 41: 11 impedance simulation with EvalAD5933EBZ board

Table Index

Table 1: Relationship between a-spots shape and Resistance

Table 2: Relation between a-spot radius and resistance value

Table 3: Pie chart of pad materials

Table 4: Cast iron bulk resistivity

Table 5: Resistance values of the pad divided in 24 parts

Table 6: Four quadrant impedance

Table 7: Half quarter impedance vertical case

Table 8: Half quarter impedance horizontal case

Table 9: Border impedance

Table 10: Left-Right/Center impedance

Table 11: Horizontal section impedance

Table 12 (a, b, c, d, e, f, g): Resistance and Capacitance values over three main setup

Table 13: Quadrant area values

Table 14: Resistance values expressed in ohm of the over mentioned configurations

Table 15: Resistance times relative area values

Table 16: Parameters comparison

Table 17: Capacitance frequency sweep results

Table 18: Frequency sweep resistance-capacitance analysis in six different configurations

Table 19: Capacitance measurement with same surface and angle displacement

Table 20: Incremental distance comparison between the two configurations

Table 21: Numerical results of short-circuiting one pad

Table 22: Material characters

Table 23: Relation between pad contact cases and total loss

Table 24: Relation between pad contact cases and resistance

Table 25: Iterative process for conductivity value

Table 26: Final total loss and resistance values with definitive bulk conductivity

Table 27: Comparison between same surface and opposite surface capacitive behavior

Table 28: Long distance capacitance measurements

Table 29: Comparison between simulation and experimental results

Table 30: Peak to peak voltage of the output signal

Table 31: Impedance at incremental distance

Graph Index

Graph 1: Four quadrant impedance

Graph 2: Case b and c impedance comparison

Graph 3: Total configurations impedance measurement comparison

Graph 4: Resistance times area behavior

Graph 5: Same surface incremental distance capacitance

Graph 6: Opposite surface incremental distance capacitance

Graph 7: Comparison between graph 5 and 6

Graph 8: Relation between pad contact area and total loss

Graph 9: Iterative conductivity identification process

Graph 10: Capacitive simulation trend at different percentage errors

Graph 11: Same surface versus Opposite surface capacitive trend

Graph 12: Simulation versus experimental tests

Graph 13: Impedance at incremental distance

Introduction

This thesis deals with the possibility to improve and increase the global automotive efficiency by installing an electronic devices which measures the impedance of the wheel brake setup. The presented solution is one of the possible approaches to the problem and it aims to reduce unwanted contacts during ordinary driving, so increase vehicle efficiency in terms of eco-sustainability both in a reduction of fuel consumption, pads wear and fine dust particles emissions.

The analysis has been structured in four chapters

The first chapter is subdivided in two parts. The first one explains how electric contact works and how resistance can be measured depending on the environmental conditions. The second one, on the other hand, treats the mechanical features of the braking system of a vehicle. The focus is set especially on disc brake components and brake pad composition.

In the second chapter, an experimental approach has been opted for the braking system in order to evaluate the possibility to establish a closed electrical circuit and define the electro-mechanical characters. In particular the electrical ones are bulk conductivity, permittivity and impedance in terms of resistance and capacitance.

The third chapter exposes the results of the finite element method (FEM) simulations. In order to accomplish this task the software used are Ansys Electronics and Solidwork2016 for the system design. Two main different setup are considered: DC conduction for current density distribution and Electrostatic analysis for the capacitance matrix configuration.

The fourth chapter proposes a possible solution to the measurement problem, by the use of an evaluation board which allows to detect the presence of unwanted contacts. The solution is both explained in a theoretical way and through an experimental frequency sweep analysis.

Chapter 1

Electrical contact system

1.1 Electrical contact

An electrical contact is defined as the interface between the current-carrying members of electrical devices that assure the continuity of electric circuit. The current-carrying members in contact, often made of solids, are called contact members or contact parts, meanwhile the current-receiving ones can be both solids or liquids. The contact members connected to the respective positive and negative circuit clamps are called anode and cathode.

Electrical contacts provide electrical connection between parts and they perform many functions. The primary purpose of an electrical connection is to allow the uninterrupted passage of electrical current across the contact interface. The best possible connection can only be achieved when a metal-to-metal contact is established. Although the nature of the contact processes may differ from one to another, they are all governed by the same fundamental phenomena. The most important are degradation of the contacting interface and the associated changes in contact resistance, load, temperature, and other parameters of a multipoint contact.

Electrical contacts can be classified according to their nature, surface geometry, kinematics, design and technology features, current load, application, and by others means.

In general, electrical contacts can be divided into two basic categories: stationary and moving.

- Stationary contacts, contact members are connected rigidly or elastically to the stationary unit of a device to provide the permanent joint. They are divided into non-separable or all-metal (welded, soldered, and glued), and clamped (bolted, screwed, and wrapped).

1. Non-separable(permanent) joints have a high mechanical strength and provide the stable electrical contact with a low transition

resistance. A non-separable joint is often formed within one contact member.

2. Clamped contacts are made by mechanically joining conductors directly with bolts or screws or using intermediate parts called clamps. These contacts may be assembled or disassembled without damaging the joint integrity.

- Moving contacts are characterized by at least one rigid or elastic contact member connected to the moving unit of a device. Depending on their operating conditions, these contacts are divided into two categories: commutating and sliding.

1. Commutating contacts intermittently control the electric circuit. They fall into two categories: separable (various plug connectors, circuit breakers) and breaking.

2. In sliding contacts, the contacting parts of the conductors slide one over the other without separation. Current passage through the contact zone is followed by physical phenomena (electrical, electromechanical, and thermal) that produce changes on the surface layers of the contacting members. The severity of the processes occurring at contact interface depends on the magnitude and character of the current passing through the contact points, the applied voltage, operating conditions, and contact materials used .

1.2 Electrical contact surfaces

Ideal surfaces are completely flat and homogeneous in all its points. Real surfaces on the other hand are not uniform and plain but includes many asperities and defects.

Therefore, when contact is made between two surfaces, in our case between brake pads and brake disc, all the imperfections and asperities with maximum height of both members come into contact. Higher the braking load is

required, higher will be the amount of defects come in contact forming spots. The overall area of these spots is known as the real contact area. This area depends both on the mechanical behavior of the surface layers and their roughness. It is continuously changing and at each braking pressure applied it modifies itself. Once the braking is released the contact are should be zero, and an air gap is formed between contact surfaces. This process of contact and detachment can be seen as an electrical switch characterized by a varying impedance.

This process leads to the evaluation of the electrical impedance.

1.3Contact resistance

As mentioned before solid surfaces are always rough. The dimension of asperities and defects can vary from the length of the sample to the atomic scale. By convention, the surface irregularities are classified into errors in form, waviness, roughness, and sub-roughness (nano-scale roughness). Those levels of roughness are associated with corresponding types of contact area (apparent, real, and physical area of contact). Study of these areas follows the general trend of mechanics from the macroscopic models up to the current attempts to understand the micro/nano scale processes in the contact of solids. The surface topography affects all the contact characteristics but primarily the mechanical ones. Another important factor affecting the contact behavior is the presence of various films (such as oxides, contaminant dusts, reaction products and water) which interfere in the system.

The hypothetical electrical circuit evaluated should be an ensemble of mechanical components involving the automotive mechanical braking system. The “closing circuit component” is the connection of pads with the rotating disc.

The current passes through the “a-spots” that are smaller than the theoretical contact spots when braking is in course, meanwhile an open circuit is present when braking is not applied.

Since the electrical current lines are constricted to allow them to pass through the a-spots ,as shown in Figure (1), the electrical resistance increases. This increase is defined as the constriction resistance. Moreover if contaminant films are considered, on the mating surfaces an increase the resistance of a-spots is noticed. The total resistance due to constriction and contaminant films determines the contact resistance.

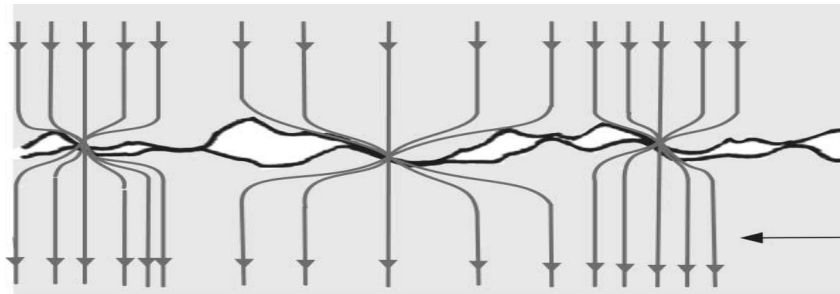


Figure 1: Surface contact spots

The fundamental monograph of Holm considered most of the contact phenomena important for mechanical and electrical aspects. Holm’s approach is focus on the description of the factors of either electrical or thermal origin affecting the contact resistance. In the case of isotropic roughness topographies, the a-spots are assumed to be circular or noncircular when the roughness has a directional characteristic (e.g., in rolled-metal sheets or extruded rods).

1.4 Theoretical contact resistance evaluation through a-spots

Lets start by considering two cylinders C_1 and C_2 , defining their contact surfaces A_{s1} A_{s2} and their theoretical contact surface A_a . Due to the presence of imperfections and asperities of surfaces C_1 and C_2 the real contact surface is defined as A_c . The current flux flows from the cathode A_{s1} to the anode A_{s2} through A_c . This phenomena brings to what is called constriction resistance between two points, a and b, of the cylinders. It is evaluated as:

$$R_{ab} = \frac{U_{ab}}{I} \quad (1.1)$$

Considering one cylinder and assuming the total area A_a is made of perfectly conductive material, so that the current flux flows parallel to the cylinder, the ideal total contact resistance (R^0_{ab}) can be determined by applying a voltage potentials between a and b.

The constriction resistance and the applied voltage are defined as:

$$R = R_{ab} - R^0 \quad (1.2)$$

$$U = R * I \quad (1.3)$$

In case of simple contact, without any type of film on the surface, R is simply defined as contact resistance. In case a film is present, for example iron oxide on disc rotor, the contact resistance R should be the sum of the constriction resistances of both conductors plus the film resistance

$$R = R_{constriction1} + R_{constriction2} + R_{film} \quad (1.4)$$

Where :

$$R_{constriction1} = \frac{\rho_1}{a*n} \quad R_{constriction2} = \frac{\rho_2}{a*n} \quad (1.5)$$

“n” corresponds to the number of a- spots and “a” to their section. The film resistance for instance is expressed as:

$$R_{film} = \frac{\sigma}{A_c} \quad (1.6)$$

Constriction resistance for a single a-spot between two conductors of semi infinite length is given by:

$$R_{construction} = \frac{\rho}{2d} \quad (1.7)$$

And considering both conductors it becomes:

$$R_{construction} = \frac{\rho}{d} \quad (1.8)$$

Respectively the resistivity of the conductor (ρ), and the conductor asperity diameter (d).

If different materials have been used for the two conductors, such as the case we are going to study, it is possible to rewrite the above mentioned resistance as:

$$R_{construction} = \frac{\rho_1}{a * n} + \frac{\rho_2}{a * n} = \frac{\rho_1 + \rho_2}{2} \quad (1.9)$$

In more detail, construction resistance of one circular asperities with radius “a” of cylindrical conductor with radius R can be rated as the solution of the Laplace equation:

$$R_c = \frac{\rho}{2a} \left[1 - 1.41581 \left(\frac{a}{R} \right) + 0.06322 \left(\frac{a}{R} \right)^2 + 0.15261 \left(\frac{a}{R} \right)^3 + 0.19998 \left(\frac{a}{R} \right)^4 \right] \quad (1.10)$$

Constriction resistance is function of the number and the dimension and the shape of the a-spots. Supposing to have different a-spots shapes we can get different resistance values as it is reported in Table 1:

a-spot shape	Radius [μm]	Length [μm]	Width [μm]	Ring thickness [μm]	Resistance [Ω]
Circular	5.64				$1.55 * 10^{-3}$
Squared		10	10		$3.04 * 10^{-3}$
Rectangular		50	2		$0.43 * 10^{-3}$
Ring	16.41			1	$0.71 * 10^{-3}$

Table 1: Relationship between a-spots shape and Resistance

Once the a-spots are defined, in an electric contact the number of asperities depends from the braking force required, so by a mechanical load. It is

possible that some of these deformity get together forming a group called cluster. In this situation a new equation is labeled. Always taking into account the circular geometry of the a-spots it results:

$$R_{constriction} = \frac{\rho}{nd} + \frac{\rho}{D} \quad (1.11)$$

The cluster radius is also called Holm radius and is indicated with a . In Table 2 are reported some interesting values regarding the above formula progressively increasing the a-spots radius.

a-spot radius [μm]	a-spot resistance [Ω]	Holm radius (a) [μm]	Cluster resistance [Ω]	Single a-spot radius equivalent resistance [Ω]
0.02	0.3289	5.34	0.0937	1.18
0.04	0.1645	5.36	0.0932	1.94
0.1	0.0685	5.42	0.0923	3.16
0.2	0.0329	5.50	0.0909	4.04
0.5	0.0132	5.68	0.0880	4.94

Table 2: Relation between a-spot radius and resistance value

The real contact area depends on the mechanical applied load. The deformation of the parts in contact can be of two types: plastic or elastic. The difference between the two consists in the contact pressure which follows the Hertz theory.

1.5 Film resistance

The film resistance takes into account of the contribute of the contact resistance due to the presence of contaminated layers on the contact surface. These films can be: oxidation layers, lubricants, water and corrosive agents

which due to their high resistivity tends to limited conduction and so the current flows.

Conduction is not prohibited, these layer are really thin , on average less than 10^{-10} m, and can conduct thanks to the tunnel effect. In traditional mechanic energy conservation law states that a particle can't overcome an obstacle if it doesn't have to energy to do it. On the other hand quantum mechanics allows a probability, a really small one, to the particle to be able to overcome the barrier. Since it is a probability, the tunnel effect resistivity is independent to the film composition.

Calling ρ_f the contaminated layer resistivity, s the layer width and with Σa the summation of all the contaminated areas, resistance can be written as:

$$R_f = \frac{\rho_f s}{\Sigma a} \quad (1.16)$$

Hypothesizing an uniform distribution of the layer above the contact surface, meaning that $\Sigma a=A$, it is possible to rewrite film resistance as:

$$R_f = \frac{\rho_f s H}{F} \quad (1.17)$$

where H is the hardness of the contaminant layer and F the applied load. The relationship between F and H is defined by the law:

$$F = A_{contact} * H \quad (1.18)$$

1.6 Temperature influence

In the previous formula contact resistance has been found in relation with resistivity ρ of the material. Resistivity is function of temperature:

$$\rho_T = \rho_0 [1 + \alpha(T - T_0)] \quad (1.19)$$

ρ_0 is the resistivity at standard temperature, ρ_T the one at the desired temperature, T_0 the reference temperature and α the temperature coefficient.

When temperature increases the vibrations of the metal ions in the lattice structure increases. These vibrations bring to collision between free electrons and the other electrons. Each collision scoops out a bit of energy from free electrons and causes electrons inability motion. This process reduces the movements of the delocalized electrons and drift velocity. As a consequence resistivity of the conductive material increases and current flow decreased. In the Figure (2) is depicted the behavior of resistivity as function of temperature for conductors

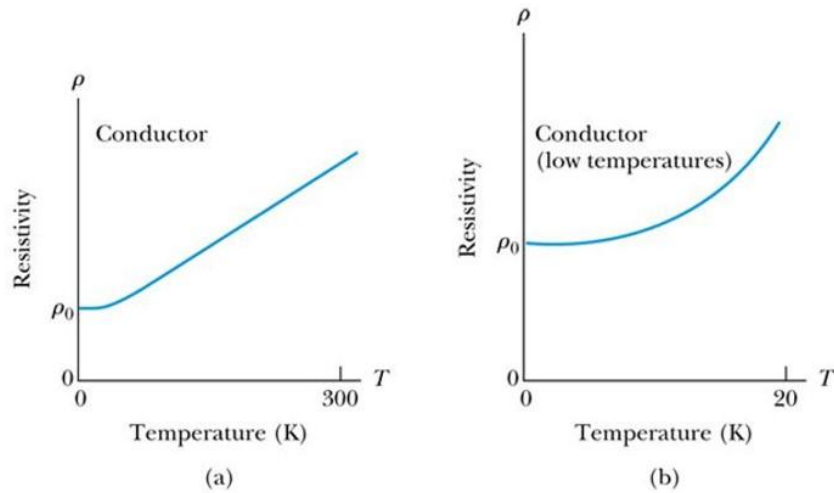


Figure 2: Resistivity-Temperature trend

Mechanical brake system

In order to slow or stop a vehicle the kinetic and any potential energy of the vehicle's motion must be dissipated in heat or converted into electrical energy. Friction brakes operate by converting the energy of the vehicle's motion into heat and dissipating it to the atmosphere. This process is an irreversible process that is nowadays is been reduced by hybrid and full

electric vehicle. Despite the constant increase of this new generation vehicle (electric and hybrid-electric vehicles) and re-generative braking technology, friction brakes are always used in every kind of automotive braking systems shown in Figure (3). Due to this, research continues to improve the braking system in each aspect: materials, thermal dissipation, weight reduction and safety through electrical sensors.

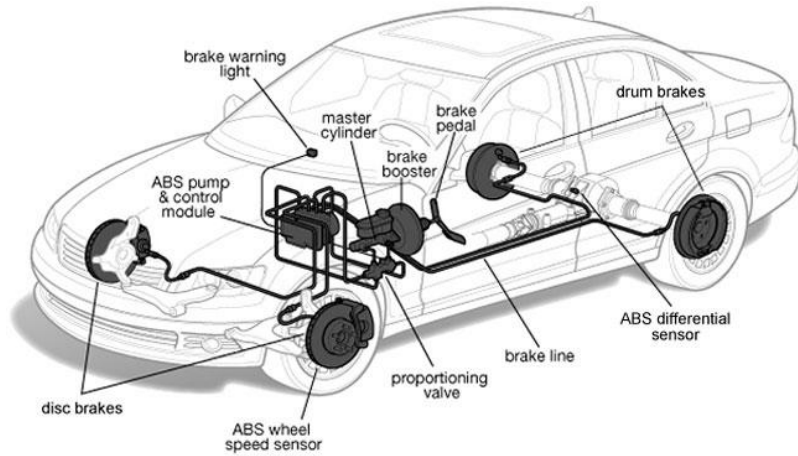


Figure 3: Automotive braking system

2.1 How the braking system works

Brake system is characterized by two important principles: Friction and Heat. When friction is applied from the stator (pads, shoes), through a pneumatic system, to the rotor (drum, disc), the vehicle slows down and stops and heat is generated. The kinetic energy present in the moving vehicle has been converted to heat. The rate of conversion depends on vehicle weight, braking force and breaking surface area. On the other hand is not to be underestimated how the system is capable to apply force and how to disperse heat. During braking, a large amount of heat is created and has to be absorbed by the rotor firstly and then from the surrounding components. They can be seen as temporary thermal storage devices (rotor, pads), and cooling (fresh air flow). The combination of the two has to satisfy the braking system performance.

2.2 Friction theory

Friction is a phenomena that happens when two surfaces in relative motion get in contact and a resistance to movement is gained. The automotive braking system applies this principle in order to control the vehicle momentum of inertia and speed, so kinetic energy.

Friction is generated when the braking slip force is applied to the system. Slip force is proportional to the perpendicular forces applied to the involved braking components.

$$F = \mu F_{perpendicular} \quad (1.20)$$

Considering that

$$F_{braking} = F_{deceleration} \quad (1.21)$$

and according to Newton's law:

$$\mu F_{perpendicular} = \frac{F_{perpendicular}}{g} * a \quad (1.22)$$

where g stands for the gravitational constant and a for the deceleration. This leads the definition of friction coefficient μ .

$$\mu = \frac{a}{g} \quad (1.23)$$

2.3Types of Friction Braking Systems

Two types of automotive brakes exist: drum and disc.

The main difference is their working principle. Drum brakes operate by pressing shoes (stator) radially outwards against a rotating drum (rotor), while disc brakes operate by axially compressing pads (stator) against a rotating disc (rotor). An advanced form of the disc brake is the ventilated or vented disc,

which is characterized by internal cooling: with this solution the air flows through radial passages or vanes in the disc.

2.3.1 Drum Brakes

Early automotive brake systems used the drum setup on all four wheels. They were called drum brakes because the components, depicted in the cutaway in Figure (4), were housed in a round drum that rotates along with the wheel. Inside there is an hydraulic piston that, when braking, forces a pair of shoes against the drum and slows down the wheel. In order to limit heat shoes are made of a heat-resistant friction material similar to that used on clutch plates.

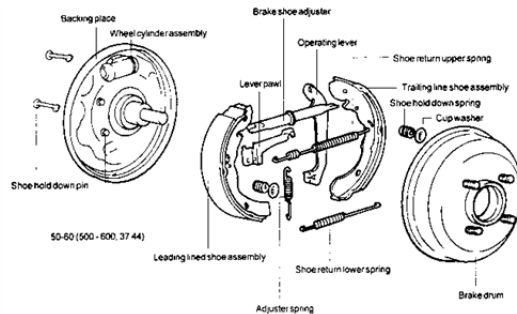


Figure 4: Drum brake components

This basic design is able to withstand all the circumstances, but it had one major defect. Under high braking conditions, like descending a steep hill with a heavy load or repeated high-speed slow downs, drum brakes would often fade and lose effectiveness. Usually this fading was the result of too much heat build-up within the drum. This because drum brakes can only operate as long as they can absorb heat ,once the brake components themselves become saturated with heat, they lose the ability to stop a vehicle. Nowadays they are used only the rear axles in low power car.

2.3.2 Disc Brakes

The design of discs brakes is far superior to that of drum ones. Instead of housing the major components within a metal drum, disc brakes is made up

by a rotor and a caliper and a pair of pads, one on each side of the rotor. The main advantages of disc brake over drum are:

- The rubbing surfaces of the disc brake and the pair pads are exposed to the atmosphere providing better cooling and reducing the possibility of thermal failure.
- In drum brakes, expansion of the drum at elevated temperatures will result in longer pedal travel and a roundness which doesn't make perfect contact between the drum and shoes in following braking. In disc brakes elevated temperatures cause an increase in disc thickness, enlarging the heat absorption area with no adverse effect in braking.
- Disc brake adjustment is achieved automatically whereas drum brakes need to be adjusted as the friction material wears.
- Disc brakes are less sensitive to high temperatures and can operate safely at temperatures of up to 1000°C. Drum brakes due to their geometry and effects on their friction co-efficient, should not exceed 500-600°C. A really big difference especially when repetitive braking is applied.

Brake discs both solid and ventilated can be cast from an iron alloy and machined to the required finish specifications or made with carbon-ceramic composite materials.

2.3.3 Disc brake components

Ones defined the two system, only disc brake components are evaluated: calipers, discs and brake pads.

Calipers

The brake caliper is the brake component which houses brake pads and the small pistons. The last ones are moved by an hydraulic system activated by the brake pedal. They are usually made in aluminum or chrome-plated steel and in some cases in plastic material. Calipers which have to withstand high temperature are made in cast iron. Two types exists: fixed and floating relative shown in Figure (5) and Figure (6). The main difference between the two in the relative motion with respect to the disc.

Fixed calipers don't move with respect to the disc which leads to fabricated much more accurate, with few imperfections discs. Pairs of opposing pistons are used to clamp the disc from both sides. The use of this type of calipers is much more expensive and complex than a floating type.

Floating calipers, also known as "sliding calipers" move with respect to the disc along a line parallel to the disc rotation axis. Only one piston on one side of the disc pushes the inner brake pad until it makes contact with the braking disc, then pulls the caliper body opposite way with the outer brake pad. In this way pressure is applied to both sides of the disc. Floating caliper (single piston) designs are subject to sticking failure, caused by dirt, dust and corrosion interacting with at least one mounting mechanism and blocking it from its normal movement. This leads to unwanted contacts and precocious wear of brake pads. In particular brake pads start to rub the disc with an angle different from the desired one and to generate constant undesired friction to the movement of the vehicle.

The condition of sticking can result from infrequent vehicle use, failure or high wear of seals and rubber protection allowing debris to entry. This unwanted phenomena implies many consequences such as reduced fuel efficiency, extreme heating of the disc or excessive wear on the affected pad and steering vibration.

Another type of floating caliper is a swinging caliper. The main difference stands in how the caliper is attached to the car: instead of using two horizontal bolts that allow the caliper to move straight in and out relative to the car body, a swinging caliper utilizes a single vertical pivot bolt located. When braking is applied, the brake piston pushes the inside piston and rotates the whole caliper inward. Because the swinging caliper's piston angle changes relative to the disc, this design uses wedge-shaped pads that are narrower in the rear on the outside and narrower on the front on the inside.

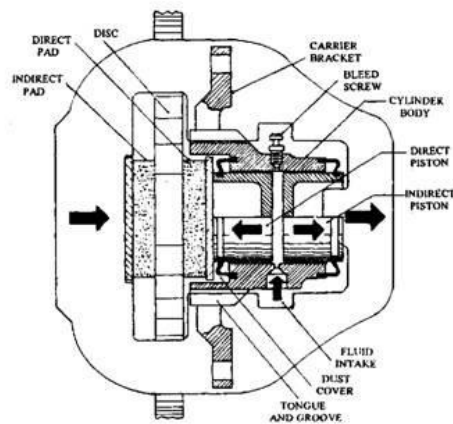


Figure 5: Fixed caliper

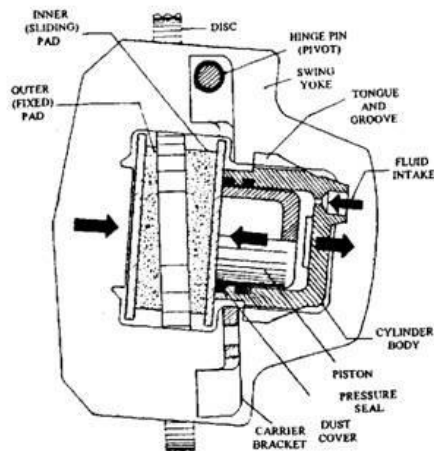


Figure 6: Floating caliper

Discs

The brake rotor, disc, is the rotating part of the braking system assembly. Both of the surfaces are used for the braking aim and here is where the pads are squeezed onto. The material used for rotors is known as cast grey iron and is cast iron mixed with Graphitic structures.

There are mainly 2 type of rotor and 4 sub categories:

1. Solid rotor
2. Ventilated or vented rotor

The difference stands on the capability of heat dissipation, vented disc in fact has a higher potential due to its design. Many ducts are created inside the disc in order to let air flowing inside and better cool down temperature.

Subcategories

- Blank or smooth: characterized by smooth and plain surface
- Drilled: characterized by drills in the brake surface area
- Slotted: characterized by straight or curved lines in the surface area
- Drilled and slotted: characterized by both holes and lines on the braking surface area

This subcategories except from the blank have a lower surface contact with the pads but a better air flow. The difference between drilled and slotted is a matter of brake pad in use on the system. Their performance is higher to respect of the smooth ones but they suffer of cracking. Figure (7) shows all the rotor subcategories.



Figure 7: Brake disc comparison

Brake pads

Brake pads are the last component of the brake wheel compartment. They are the element of contact with the disc and they have the aim is gripping the brake discs to reduce their rotational speed. They are placed in brake calipers., Brake pads are defined as consumables, so they suffer from wear, and need to be replaced before they go below a minimum level. Wear is measured by the thickness of the layer of friction material. This mixture of components is what helps a brake disc slow down and stop whenever the brakes are used, but also when traction control or ESP kicks in to slow down one of the wheels.

The friction material is the main characteristic used to determines brake pads type. All brake pads rely on a metallic plate that has friction compound on it and the composition of the said material determines how those pads will operate. There is no general rule regarding brake pad composition to say which one is the best or the worst. The best brake pads for the vehicle depend on the usage. Some pads are better for day-to-day driving in all weather conditions, while others are designed only to be used on the track. In the case of the latter, even if their level of performance is incredible when compared to regular ones, it is illegal to use them on public roads. The reason lies in the composition of racing brake pads, which is designed to operate in particular conditions, which are incompatible with day-to-day use.

Till 1970s asbestos was one of the main material used in the production of pads, but when was proven its dangerousness to human health it had been banned.

Brake pads are made by 5 different types of materials:

1. Binding materials (binders)
2. Abrasive materials
3. Performance materials that are included in precise amounts to enhance certain braking characteristics, including temperature specific lubricants
4. Filler materials
5. Structural materials, which help the pad maintain proper shape during use

Their percentage is represented in the following Table (3):

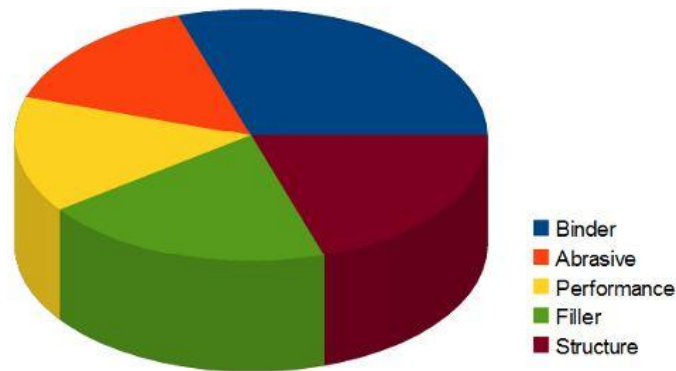


Table 3: Pie chart of pad materials

These five types of materials encompass more than 2,000 substances and only each brake pad manufacturer knows the specific composition.

Depending on the required specification given from the automotive manufacturer each car has its own pad. So depending on the utilization compounds used are present in different percentages. Here three examples characterized by their composition are illustrated:

1) ORGANIC, NON-ASBESTOS(NAO) AND FULLY ORGANIC

NAO brake pads contains 10-30% of metals, plant derived fibers and fillers like carbon, rubber, glass and Kevlar, bonded in resin. The fillers and plant fibers are used to dissipate heat and dampen vibrations. This type of pads are used on many vehicles due to their efficiency. Furthermore they are cheap and quiet but as a drawback they're soft and generally don't last as long as other more expensive formulations. The main difference between organic and fully organic in the amount of metals: organic have an higher amount which enhances heat transfer capability.

- Pros: Inexpensive, quiet
- Cons: Wear quickly

2) SEMI-METALLIC

Called “semi-metals” by the pros, semi-metallic brake pads are filled with metal fibers, between 30-65% in total weight, such as copper, steel, Graphite and brass bonded with resin. The fibers pull heat away from the rotor and transfer it to the metal back plate to reduce overheating and brake split. That’s why semi-metallic pads provide ultimate stopping power.

Since they’re the hardest of all pad materials, semi-metallic brake pads tend to wear rotors faster and to produce noise. During stops and soft braking are characterized by a notorious squeal . Due to the presence of metals, when they get wet they produce rust, so the first braking won’t be as good as expected.

- Pros: Stopping power
- Cons: Noisy, dusty

3) CERAMIC

Ceramic brake pads are the evolution of semi-metallic and organic brake pads. They are designed in order to overcome the braking performance of semi-metallic brake pads, remove noise, dust, and the worn excessive brake rotor issues. A large percentage of new cars are equipped with ceramic brake pads right from the factory. They are made with a ceramic dense materials mixed with metal fibers such as copper and steel. This kind of pads are more expensive but gives better braking efficiency.

- Pros: Stopping power
- Cons: Range in quality

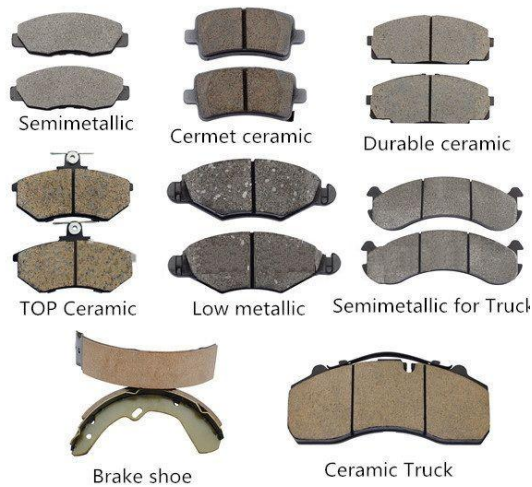


Figure 8: Brake pads typologies

To sum up here is a Figure (8) of all the different subclasses of brake pads and brake shoes.

2.4 Wear pad sensors

There are 3 main kinds of braking wear pad sensors which adopts mechanical and electrical strategies are:

- Squealer type
- Resistive circuit types
- Electronic parking motion type

2.4.1 Squealer type

This is the first invented system to evaluate brake pads lifespan. On each brake pad an hardened steel clip is fixed to the pad holder as shown in Figure (9). When the pad gets consumed, the clip starts scraping on the disc brake producing a scraping noise. This method let us known only if brake pads are usable or not safe during driving.

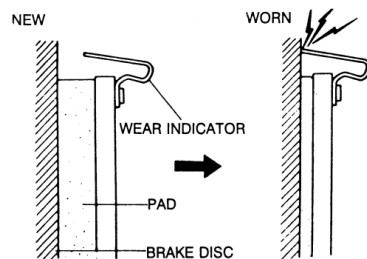


Figure 9: Squealer wear indicator

2.4.2 Resistive circuit type

1) Single resistive circuit

In the late 1970s this system had been developed using an electrical approach. An electric circuit made up by a wire loop is sank inside the brake pad and fed with a small current. At the ends of the wire loop a sensor measures the resistance value and rectifier circuit compares it with the threshold value (2000 ohms). When the threshold value is exceeded the rectifier senses the wire loop as an open circuit and gives a signal to the dashboard by turning on a light. This system is really reliable in terms of resistance measurements, but suffers physical damages and connectors corrosion.

As well as the squealer type this solution is an ON-OFF evaluation.

2) Double resistive circuit

Modern brake pad wear sensors interact with the entire braking system and can estimate the mileage until the pads are worn out.

New generation wear sensors are characterized by two resistive circuits in parallel sank inside the brake pad and placed at different depths. This allows to define one additional condition to the two previous models (squealer and single resistive): no more ON-OFF conditions but ON1, ON2 and OFF.

When the first circuit (less deep in the pad) brakes down, the sensor will feel an increase in the resistance value due to the parallel structure. As a response it doesn't set a warning to the driver but estimates the pad remaining lifespan. This processes of estimation is gathered not just by the cut circuit but through other information such as wheel speed, mileage, brake pressure, brake disc temperature and brake operating time.

The remaining lifespan can be displayed in two ways:

- Warning dashboard led-light characterized by 2 colors: yellow for half wear, red for total wear
- Indicative mileage available until pads change displayed during start up

When both the parallel circuits get cut off, the sensor will see an open circuit and a red light in both configuration will be displayed.

2.4.3 Electronic parking motion type

Electronic parking motion sensors have been developed from the early 2000s when electronic park brakes started to appear in vehicles. The system involves both front and rear brakes and it is characterized by specific caliper design: inside each caliper a stepper motor is placed. When electronic parking brake is applied the braking system actuates the stepper motors which push the pads toward the discs and stop the vehicle. A sensor placed on the stepper motor measure the angle or the number of rotation needed to engage the contact. The angle is then converted into a length which corresponds to the movement of the pad in order to reach the disc.

With this technology it is possible to evaluate each time the system works the exact amount of wear of each pad. The limitation of the strategy is that it the pad always get in parallel contact with the disc.

Chapter 2

1.1 Electrical conductive characterization of mechanical components

In order to define the mechanical components an experimental approach has been used. All of the components are analyzed in terms of their materials and electrical features. Each component once mechanically defined is then compared to the complete system, evaluating the behaviors at different specifications. The brake components under investigation are: brake disc, brake pad and pad plate. In particular the last two mentioned ,pad and plate, are examined considering them as two mechanical components but as an unique piece for electrical measures since there are glued together.

Laboratory set up

All tests are done in the laboratory of Electrical Drives in Politecnico of Milan , in Bovisa Campus, at specified temperature of 22°C during the winter time period. The data collection are taken through an electronic device used to evaluate many electrical parameters, such as: R/Q, C/D, C/R, L/Q, respectively resistance (R), capacitance(C), inductance (L) ,quality factor (Q) and dissipation factor (D), and elaborated through excel and matlab and design and simulation software.

The equipment given by the structure and used is a high precision LCR meter series -819/829 (12-100k Hz) in combination with the LCR-06A probes The main test modes used are the R/Q and R/C ones. The first method has been adopted for the brake disc material characterization, meanwhile the second for the pad one. The mechanical parts under test are a brake disc rotor and a brake pad.

The instrument configuration mainly is:

- Frequency 12Hz
- Voltage 1 V

- AUTO MODE
- Speed FAST
- Display value
- MODE R/Q & R/C
- CIRCUIT parallel

Depending on the parameter to be measured Speed can vary from SLOW (used to perform capacitance measurements), MEDIUM to FAST(used to evaluate resistance measurements).

Here the data sheet is reported:

https://www.csulb.edu/sites/default/files/groups/college-of-engineering/About/gwinstek_lcr_meter.pdf

2.1 Components characterization

Brake disc

The brake disc under test is a Brembo ventilated disc defined by its serial number: A213 423 03 12 35 16 AAL301 AA MIN TH 0.945"=24 mm 6D Brembo. As explained in the previous chapter it is classified as drilled and slotted vented disc, so it is a high performance rotor. The evaluation from a material characteristic point of view is studied by the representation of a section of a scaled rotor ring. The LCR is connected to the ring at its section edges by the 06A probes. In this measures the R/Q mode at the lower frequency possible: 12 Hz.

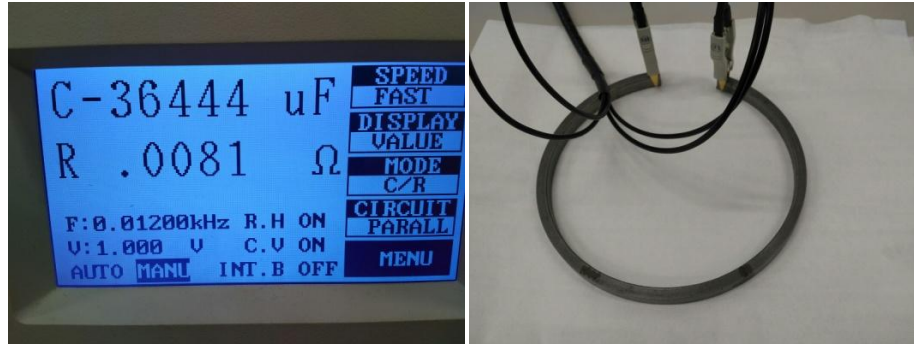


Figure 10: Resistance value of a cast iron ring

The characterization of the disc is made by considering resistivity of the material taken into account: a section of ring with specific data:

$$\text{Extrnal diameter} = 155\text{mm}$$

$$\text{Internal diameter} = 167\text{mm}$$

$$\text{Disc section} = (6 * 9.9)\text{mm}$$

$$\text{Circular length in degree} = 330^\circ$$

From the experimental data shown in Figure (10), the resistance value is

$$R = 0.0081 \text{ ohm}$$

The average radius is then calculated

$$R_{av} = \frac{\text{external diameter} + \text{internal diameter}}{2} \quad (2.1)$$

$$\text{The total current path is given by: } l = 2\pi * R_{av} \quad (2.2)$$

$$\text{Then the effective length of the disc section: } l_{tot} = l - \left(\frac{11}{12}\right)l \quad (2.3)$$

Reminding that resistivity is:

$$\rho = \frac{R * S}{l_{tot}} = \frac{0.0081\text{ohm} * 59.4\text{mm}^2}{463.64\text{mm}} \quad (2.4)$$

$$\rho = 1.038 * 10^{-6} \text{ohm} * m$$

Comparing the obtained value with the one in Table below (4), it is evident that the two values are practically the same. This means that the disc section is made by cast iron. By analogy , since the ring and the disc are made from the same material, the brake disc is made of cast iron too.

Cast iron	100×10^{-8}	Ωm
-----------	----------------------	------------------

Table 4: Cast iron bulk resistivity

Brake pad

The brake pad is the most difficult component to estimate since its composition varies between each manufacturer, more 2000 components are used and no info has been given. To Figure out the material nature many experiments have been done. Firstly it is extremely important to investigate how the disc and the pad behave when they get in contact, in particular in the situation of unwanted contacts between the parts then understand the possible situation which can occur most of the time.

The approach adopted in order to detect the pad resistivity is divided in few steps:

1. Design pad on a Graphic software
2. Evaluates its surface area and volume
3. Divide it surface in slots and measure resistance through R/Q mode
4. Change mode to R/C for an impedance control
5. First approach: resistivity through impedance tests
6. Second approach: resistivity through impedance tests in pressed condition
7. Characterization

1.Design

The design of the brake pad is done through Solidwork 2016 software. In this way it is easy to asses points 2,3. The design as depicted in Figure (11)

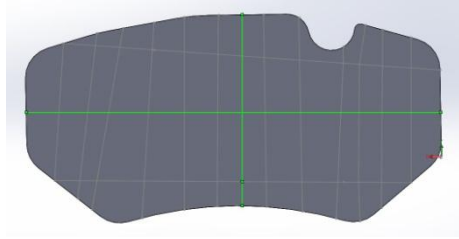


Figure 11: 1:1 Scale brake pad

The pad is represented in a 1:1 scale and the attribution of the material for the FEM analysis is given at the end as last step.

2.Evaluation of areas

Once the 3D-model is created, its surface has been calculated in mm^2 and then has been divided in parts according to predefined models: equal areas, offset perimeter, vertical and horizontal stripes, quarters, 1/6 of quarters . Different kind of measures are taken and with different approaches in order to get different aspects results.

For each type of measure a double test is done and corresponding Tables are created. The first test is limited to the pad itself, meanwhile the second on the system totality.

3.Surface division and conductive test

The main purpose of this procedure is to get as many concrete values as possible for a better material estimation. The measures are always done with the LRC instrument and set at the frequency of 12Hz. In the first approach it is important to understand if the pad is made up of a conductive or insulator material, so for this test the R/Q modes was adopted. The two probes are connected respectively one to fixed point such as the eyelet present on the pad plate and the other on the point of interest by applying a finger pressure. Here in Table(5) are shown the values corresponding the each selected quarter of area the 1/24 area analysis of the resistances expressed in ohm.

R [Ω]	1 st quarter values			2 nd quarter values		
	5.01	3.81	8.56	3.65	hole	5.26
	2.42	3.54	3.76	4.35	6.75	4.34
	3 rd quarter values			4 th quarter values		
	5.01	6.23	9.01	6.01	4.76	3.74
	5.68	6.47	3.62	2.58	6.46	3.5

Table 5: Resistance values of the pad divided in 24 parts

It is noticeable that one slot is characterized by a “hole”, this due to the pad shape. In this particular case in that spot was not possible to get a value.

Since a small resistance has been found we assume the pad to be composed of the mixture of materials that consider as a whole is conductive.

In Figure (12) is shown how the four quadrant are divided in and some spots where measurement have been taken. Finger pressure is not present for a better understand of the images. Important to notice is that the eyelet is always the same and not interchanged with the other one.

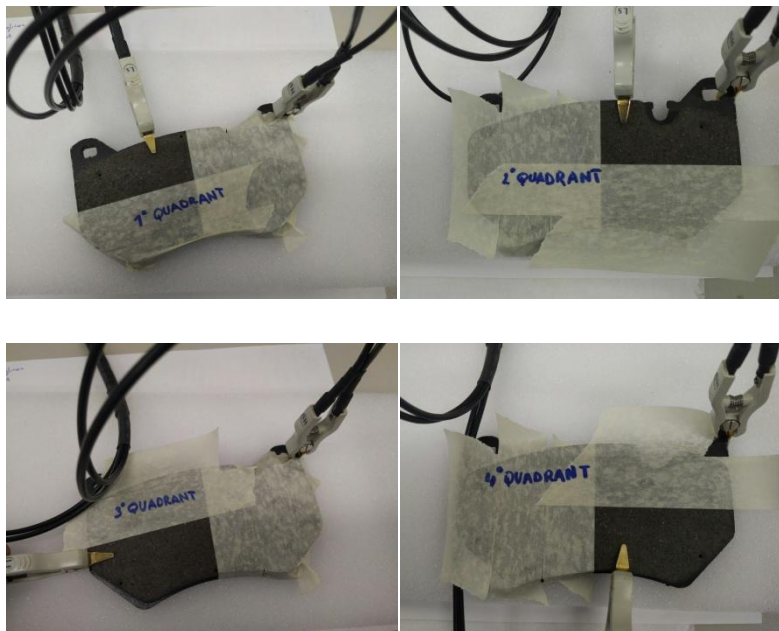


Figure 12: Four quarter of the brake pad during the 1/24 analysis

4.Impedance control

Conductivity is established, so the next step is to change mode and pass from R/Q to R/C one. This switch permits to obtain resistance and capacitance of the respective pad. Now the system changes, it is no more only the brake pad, but the set up of brake disc and pad. The impedance measurements are calculated later once all R/C values are collected.

The different configurations are:

- a) 1/4 division (4 values)
- b) left- right division (2 values)
- c) up-down division (2 values)
- d) 1cm offset from perimeter, both cases (2 values)
- e) 1,5cm vertical cut-off on both sides and vice versa (2 values)
- f) 2,5 cm horizontal cut-off both sides and vice versa (2 values)

All the values collected in Tables are then compared highlighting the relation between the absolute values of the impedance (Z complex number) and the corresponding areas (A). For a better evaluation of these values, the position of probes and pad on the disc are always the same. They have been marked in order to reduce position errors

For example test “a” is made by covering with an insulating Scotch tape each time 3 of the 4 sections of the surface leaving undercover the interested area. The measure is taken connecting the two probes respectively to the eyelet of the pad pate and a fixed point of the disc. This is done for each quarter.

5.First approach :Impedance analysis

a)in this test the quarter pad sectors are considered. Three quarters are covered with scotch tape meanwhile the remaining one leaved uncovered.

Since brake pressure should not act any kind of weight is not used. The only weight acting on the system is the pad one. Figure (13) highlights the setup of the impedance measurement.

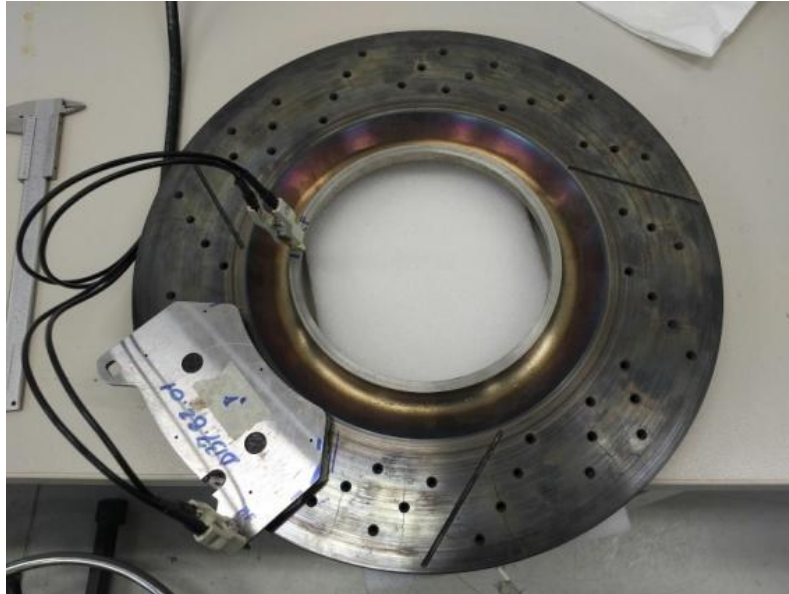


Figure 13: First quarter impedance measurement

The four impedances results obtained are: and shown in Table (6)

Impedance/ quarter area	R [Ω]	X [Ω]
1 st Quarter	52.82	0.107
2 nd Quarter	62.22	0.142
3 rd Quarter	62.51	0.034
4 th Quarter	48.14	0.118

Table 6: Four quarter impedance

where the quarters are defined as:

- 1 = top left quarter
- 2 = top right quarter
- 3 = bottom left quarter
- 4 = bottom right quarter

and the Graph (1) comparison is:



Graph 1: Four quadrant impedance

b) this test divides the pad in two parts: left side and right side. In both configuration the impedance test is measured and shown in Table(7):

impedance/ half area	R [Ω]	X [Ω]
Left [sx]	28.25	0.110378
Right [dx]	24.63	0.070617

Table 7: Half quarter impedance vertical case



Figure 14: Scotch tape pre-cut stage

For sake of simplicity scotch tape is not perfectly shaped along the pad border as it had been done for the quarter configuration, but with some excesses (in Figure(14)) possible is to be see the pre-cut stage where scotch tape

is). The small excess doesn't affect the measurement since the established insulation is guaranteed.

c) is the same test as case b where the pad is divided in two equal parts: upper part and bottom part. For upper and bottom part is intended the portion of pad area divided by an horizontal line. The result are written in Table(8):

impedance/ half area	R [Ω]	X [Ω]
Upper part	19.26	0.14744
Bottom part	25.36	0.120633

Table 8: Half quarter impedance horizontal case

Since case b) and c) have similar results in terms of impedance, just one Graph (2) is performed:



Graph 2: Case b and c impedance comparison

d) in this case the border is analyzed. A 1cm border is defined as region to study. Two opposite configurations seen in Figure (15a, 15b) have been set and measured. The impedance values are represented in Table(9):

impedance/Border	R [Ω]	X [Ω]
OutsideBorder	15.39	0.055722
Inside Border	20.85	0.382521

Table 9:Border impedance



Figure 15a: Outside 1cm border impedance

The cuts of the scotch are made directly with a sharp knife on the pad. Moreover during setup in order not to scrap, produce cavities or small holes on the surface a really sharp knife has been adopted with a small pressure applied.



Figure 15b: Inside 1cm border impedance

The last two examples are related to the horizontal and vertical relative motion between rotor and stator, respectively disc and pads. Assuming the disc fixed, the pad is the relative moving element.

e) left-right contact depicted in Figure(16) allows to evaluate small contact due to non parallelism between pad and disc



Figure 16: Lateral extremes impedance

The opposite configuration is not pictured but can be easily imagined as the same as the previous one changing white part with black one and viceversa.

From a numerical point of view Table (10) shows the measured values:

impedance/sides	R [Ω]	X [Ω]
Vertical sided	77340	13.26964
Vertical inside	11.5	0.082497

Table 10: Left-Right/Center impedance

It is evident that when the inside part is taped and the sides considered, an open circuit is present since resistance is around 77 kOhm.

f) this configuration is characterized by an horizontal section (h sections). The main problem noticed is during up-down measure, the positioning of the pad: the changing of posing the pad let a contact of the sides or not a contact. Since we want to verify unwanted contacts, without knowing the real position, the pad has been positioned and then moved a bit rising the contact. In particular Figure(17) shows a central unwanted contact meanwhile the opposite configuration the other two possible unwanted contacts rising during not parallel set up. The values of this two configurations are inserted in Table(11)



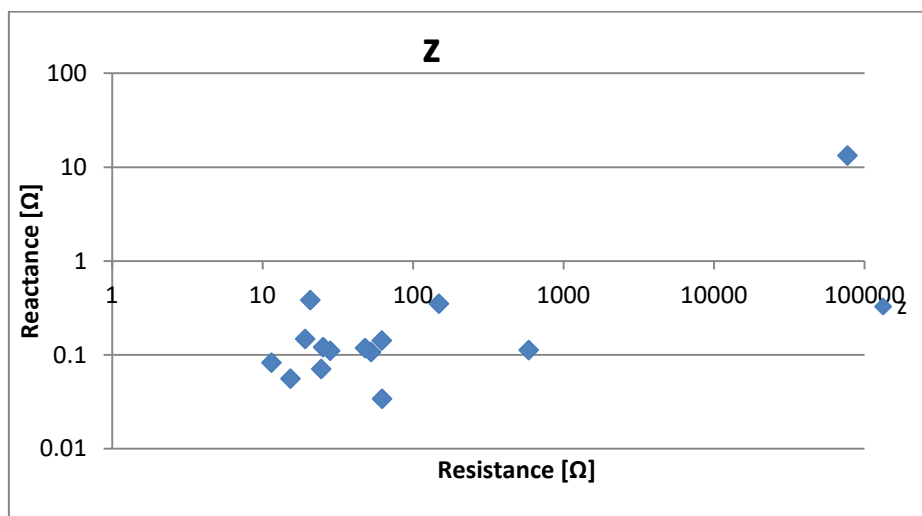
Figure 17: Horizontal stripes

impedance/h-sections	R [Ω]	X [Ω]
Horizontal sides	589	0.11264
Horizontal inside	149.1	0.350122

Table 11: Horizontal section impedance

The last two configurations are the ones with a huge impedance gap between all the others and this is due to the fact that the contact is absent (type e-sides) and the contact is less present even if same percentage of surface area are considered.

In the following Graph (3)e is depicted the Graph considering all impedance values expressing both R and Z in logarithmic scale:



Graph 3: Total configurations impedance measurement comparison

The extreme right value is the one of no contact, meanwhile the rest represent a partial contact. This allows us to understand the difference between contact and no-contact, but not a clean difference between each type of contact.

A characterization curve of all the data has been elaborated through matlab software. An eighth order function is found ,shown in Figure(18), but it has an important non linear behavior. Due to this non-linearity it is not possible to establish a relationship between impedance over surface contact area.

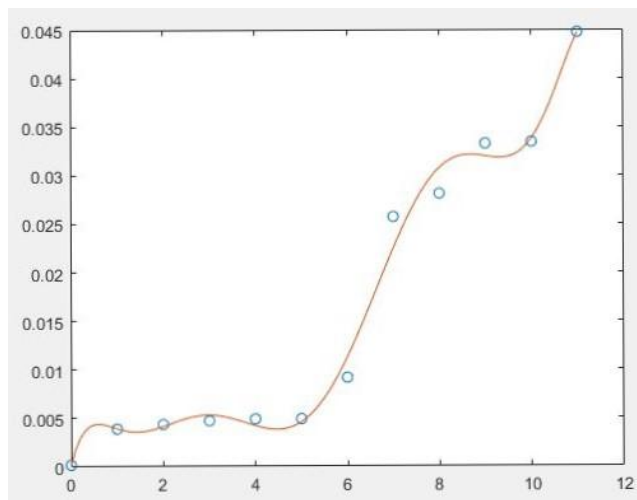


Figure 18: 8th order impedance characterization curve

6.Second approach: impedance analysis through pressure

The first approach was not successful in terms of defining the resistivity of the pad so a new technique has been adopted. It differs from the previous one by two important factors:

- Pressure applied between disc and pad
- Point of connection of both probes

In this second test brake disc and brake pad are pressed together with the use of clamps in order to create a much wider contact between parts and so a better measurement. These new values are taken connecting the probes

respectively one to the same eyelet as the previous test, the other to the disc in eight different positions.

The eight spots are: left to the pad, right to the pad, hole cavity expressed by "0", the other eyelet (left one), and the remaining four on the four elements inside the vented conducts. Here a Figure(19) for a better explanation:

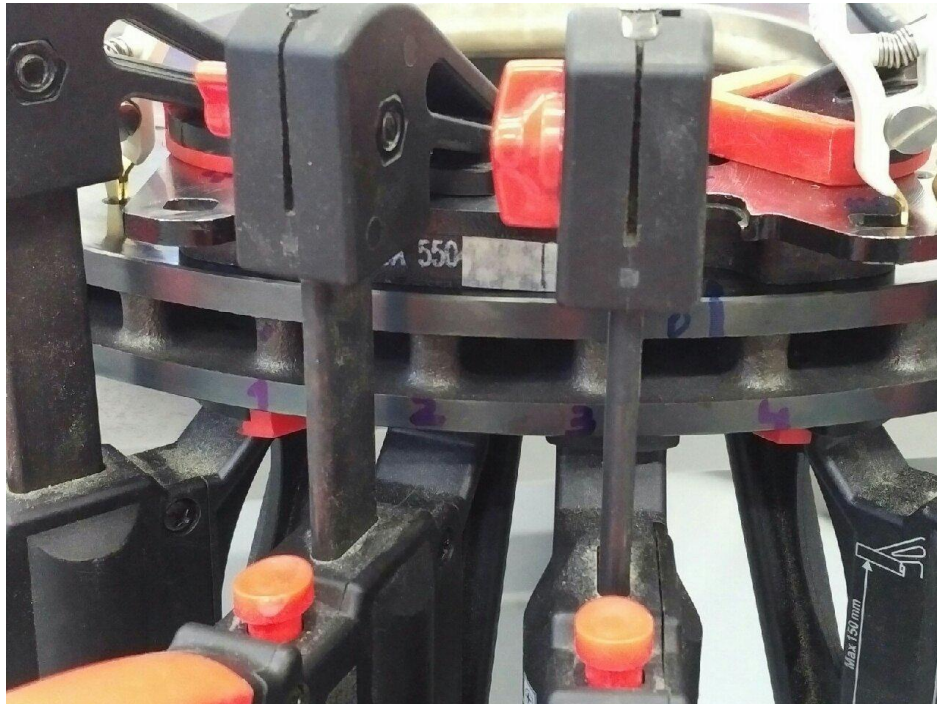


Figure 19: Connection clamps points

To the top right the fixed probe and on the disc the clip points of the measurements indicated by numbers and letters.

The left eyelet setup has been measure in order to verify that in all the configurations the setup of the clamps wasn't interfering.

Cases 1.1 and 1.2 differs by the number of clamps used to press the pad to the disc, in the first case four clamps (4PP), in the second two clamps (2PP). In both configurations, the central clamps are located on the pistons position, the other two at the pad extremity.

Figure(20) shows the two cases: 1.1 at left and 1.2 at right

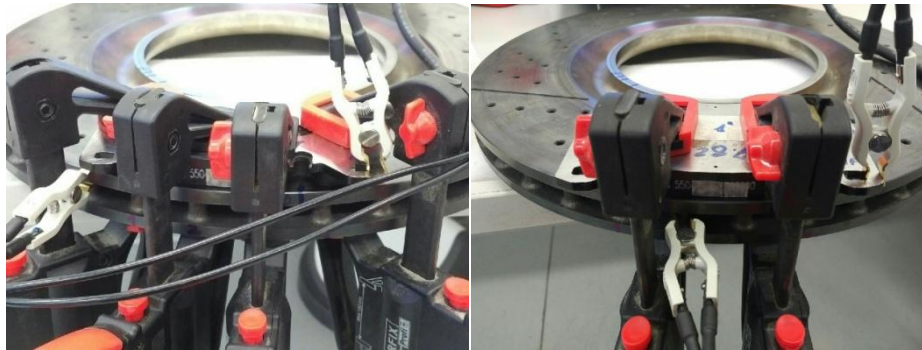


Figure20: 4 pressure points versus 2 pressure points configuration

From the results reported in the following Tables (12) it is noticeable that in both cases the measure doesn't depend on the contact position of the "free" probe both for resistances and capacitances.

New layouts are considered in cases 2, with four pressure points (4PP), where different contact areas are inspected: left side (HPVRC), right side (HPVLC), upper part (HPHUC) and lower part (HPHLC). These are the same configurations adopted in first approach.

In the last case, case 3, the pad is entirely covered with tape.

Case 1.1: 4 Pressure points (4PP)

Position/Z	Left to the pad	eyelet sx	Right to the pad	Positon 1	Position 2	Position 3	Position 4	Hole Pad	
R	0.7198	0.0028	0.7223	0.7213	0.7219	0.7218	0.7218	0.7269	[Ω]
C	-2.3529	over	-2.4961	-2.6438	-2.2047	-2.2169	-2.1852	-2.4457	[μF]

Table 12a: 4 pressure points

Case 1.2: 2 Pressure points (2PP)

Position/Z	Left to the pad	eyelet sx	Right to the pad	Positon 1	Position 2	Position 3	Position 4	Hole Pad	
R	0.7936	0.0028	0.7868	0.7847	0.7838	0.7806	0.7815	0.7788	[Ω]
C	-1.8353	over	-1.7973	-1.4673	-1.7871	-1.9002	-1.7998	-1.8674	[μF]

Table 12b: 2 pressure points

Case 2.1: Half pad far from the reference eyelet vertical covered with scotch tape (HPVLC)

Position/Z	Left to the pad	eyelet sx	Right to the pad	Position 1	Position 2	Position 3	Position 4	Hole Pad	
R	1.27	0.0028	1.265	1.268	1.275	1.262	1.248	1.248	[Ω]
C	-0.2682	over	-0.2796	-0.2300	-0.2681	-0.2511	-0.2481	-0.2823	[μF]

Table 12c: 4 pressure points with partial insulation

Case 2.2: Half pad near to the eyelet vertical covered with scotch tape (HPVRC)

Position/Z	Left to the pad	eyelet sx	Right to the pad	Position 1	Position 2	Position 3	Position 4	Hole Pad	
R	1.672	0.0028	1.633	1.635	1.623	1.626	1.626	1.608	[Ω]
C	0.19835	over	0.13666	0.14094	0.17795	-0.1956	-0.1916	0.11543	[μF]

Table 12d: 4 pressure points with partial insulation

Case 2.3: Half pad horizontally upper part covered (HPHUC)

Position/Z	Left to the pad	eyelet sx	Right to the pad	Position 1	Position 2	Position 3	Position 4	Hole Pad	
R	2.366	0.0027	2.292	2.262	2.208	2.216	2.199	2.195	[Ω]
C	0.11173	over	0.0187	0.1296	0.10848	0.12991	0.11048	0.10745	[μF]

Table 12e: 4 pressure points with partial insulation

Case 2.4: Half pad horizontally lower part covered (HPHLC)

Position/Z	Left to the pad	eyelet sx	Right to the pad	Position 1	Position 2	Position 3	Position 4	Hole Pad	
R	1.643	0.0028	1.619	1.521	1.497	1.473	1.408	1.423	[Ω]
C	0.17736	over	0.19596	0.14363	0.10706	0.17626	0.12642	0.1561	[μF]

Table 12f: 4 pressure points with partial insulation

Case 3: Complete insulated pad (TC)

Position/Z	Left to the pad	eyelet sx	Right to the pad	Position 1	Position 2	Position 3	Position 4	Hole Pad	
R	1.643	0.0028	1.619	1.521	1.497	1.473	1.408	1.423	[Ω]
C	0.17736	over	0.19596	0.14363	0.10706	0.17626	0.12642	0.1561	[μF]

Table 12g: 4 pressure points with total insulation

In the previous approach now impedances are evaluated, but since capacitance are small (μF) we can just consider resistances.

Starting from the four quadrant areas expressed in mm^2 Table(13):

1 st Quadrant [mm^2]	2 nd Quadrant [mm^2]
1879.82	1870.93
3 rd Quadrant [mm^2]	4 th Quadrant [mm^2]
1870.14	1871.77

Table 13: Quadrant area values

The total area (S) equals to 7492.66 mm^2 and the synthetic resistance Table (14) not including case 3 is:

¹ Cases	Left to the pad	Right to the pad	Position 1	Position 2	Position 3	Position 4	hole pad
4PP	0.7198	0.7223	0.7213	0.7219	0.7218	0.7218	0.7269
2PP	0.7936	0.7868	0.7847	0.7838	0.7806	0.7815	0.7788
50%PVLC	1.27	1.265	1.268	1.275	1.262	1.248	1.248
50%PVRC	1.672	1.633	1.635	1.623	1.626	1.626	1.608
50%PHUC	2.366	2.292	2.262	2.208	2.216	2.199	2.195
50%PHLC	1.643	1.619	1.521	1.497	1.473	1.408	1.423

Table 14: Resistance values expressed in ohm of the over mentioned configurations

is possible to calculate the product resistance times contact surface area [$\Omega \cdot \text{mm}^2$]:

$$R * S_{eq} \quad (2.5)$$

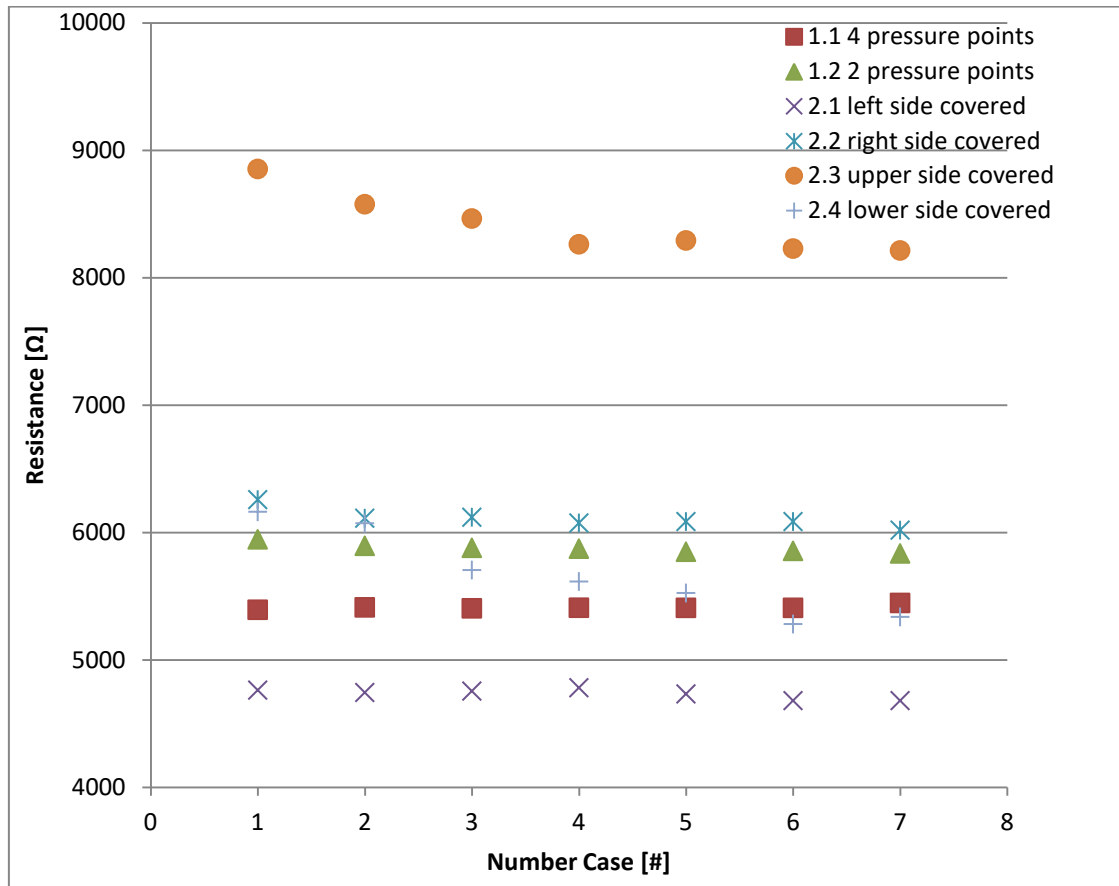
and represent it in Table (15).

Cases	Resistance times area [$\Omega \cdot \text{mm}^2$]						
	Left to the pad	Right to the pad	Position 1	Position 2	Position 3	Position 4	hole pad
4PP	5393.217	5411.948	5404.456	5408.951	5408.202	5408.202	5446.415
2PP	5946.175	5895.225	5879.490	5872.747	5848.770	5855.514	5835.284
50%PVLC	4762.449	4743.699	4754.949	4781.199	4732.450	4679.950	4679.950
50%PVRC	6257.794	6111.829	6119.315	6074.402	6085.630	6085.630	6018.262
50%PHUC	8853.359	8576.458	8464.200	8262.137	8292.073	8228.460	8213.492
50%PHLC	6162.482	6072.464	5704.891	5614.873	5524.855	5281.056	5337.317

Table 15: Resistance times relative area values

“PP”: pressure points;
 “PVRC”: pad vertically right covered
 “PVLC”: pad vertically left covered

“PHUC”:pad horizontally upper covered
 “PHLC”:pad horizontally lower covered
 Giving shape to the Table values in a Graph(4)



Graph 4: Resistance times area behavior

A linear behavior is highlighted in every configuration except from the 2.4 (“+” symbols) with a little decay of the values.

In each setup is considered:

Cases/parameters	Min [Ω]	Max [Ω]	Delta [Ω]	Mean [Ω]
4PP	5393.217	5446.415	53.19785	5411.627
2PP	5835.284	5946.175	110.891	5876.172
50%PVRC	4679.95	4781.199	101.249	4733.521
50%PVLC	6018.262	6257.794	239.5324	6107.552
50%PHUC	8213.492	8853.359	639.8671	8412.883
50%PHLC	5281.056	6162.482	881.4263	5671.134

Table 16: Parameters comparison

Considering three different mean values:

1. All cases except 2.3 = 5560.001 [Ω]
2. Cases 1.1 and 1.2 = 5643.900 [Ω]
3. All cases = 6035.481 [Ω]

Mean number 2 is taken as reference, and in terms of percentage, the other two differs respectively: 1 by 1.5% and 3 by 8%. The second percentage is higher due to case 2.3 where the contact is in worst condition since clamps are all located externally to the disc.

Now resistivity can be calculated with (2.4) as:

$$\rho = \frac{R * S}{l} \quad 2.5$$

where the height of the pad is $l=10\text{mm}$, and at the numerator is taken mean value number 2

$$\rho = \frac{5643.9\Omega\text{mm}^2}{10\text{mm}} = 0.564[\Omega\text{m}]$$

The parameter of our interest is conductivity

$$\sigma = \frac{1}{\rho} = 1.77305 \left[\frac{S}{m} \right] \quad (2.6)$$

3.1 Capacity test with frequency sweep

When braking is not requested by the driver, any contact is established between the rotor and stator and an air gap is present. The air gap can be seen as an insulator and a capacitor is made up: the two armature are respectively rotor and stator, meanwhile the dielectric in the middle is air.(cool or hot) Since the rotor disc tested has not a flat surface but characterized by slots and drills, it is important to measure how capacitance behaves in different sections of the disc.

To realize this test, the brake pad is covered with a layer of scotch tape and settled on the disc surface. The LCR instrument probes are connected to the fixed position of the disc and to the eyelet of the pad. Frequency is very important in order to evaluate capacity, so measurement have been taken at three frequencies: 12Hz, the lower one the instrument can handle, 50 Hz, the common European frequency and 1kHz.

Three drills are present on the disc and for a better probes contacts the examined one is the one left to the fixed disc probe position. In particular five different position, as shown in Figure (21 a, b, c, d, e) are set:

1. Pad right to the designated slot
2. Pad above half right slot
3. Pad above the slot
4. Pad above half left slot
5. Pad left to the designated slot

In the photos below are represented the 5 configuration listed before:

Since the capacitance value is really small is important to be sure that the capacitance measurements are not affected by errors. To avoid this possible issue the used procedure is:

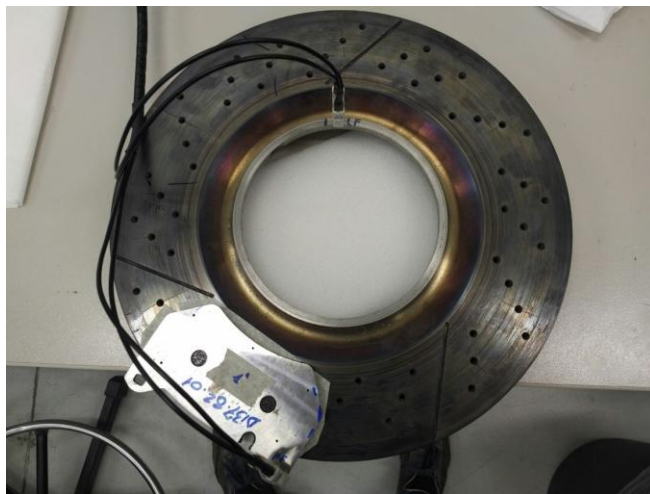


Figure 21a: Pad right to the designated slot

First place the pad over the disc in the correspondent position. Then fix the clamps respectively one on the disc previously defined reference point and the other one to the reference pad eyelet (right eyelet).

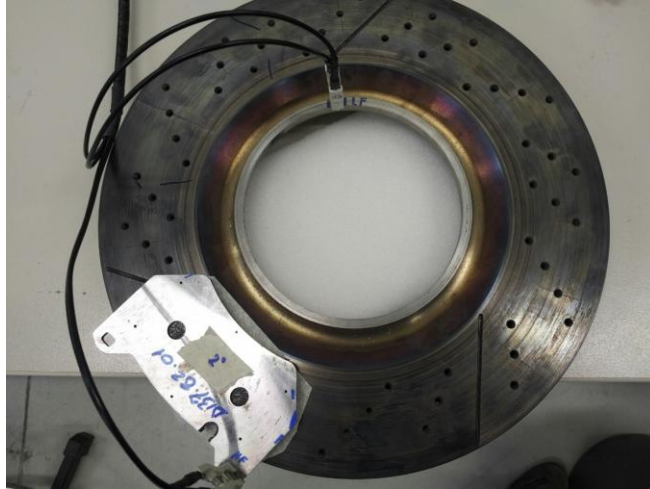


Figure 21b: Pad above half right slot

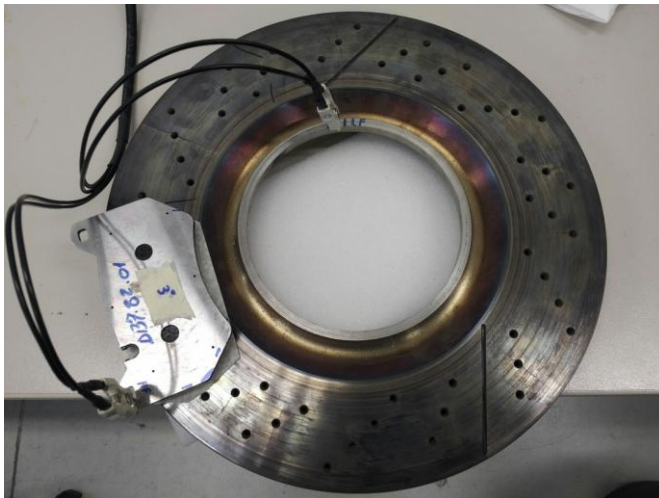


Figure 21c: Pad above the slot

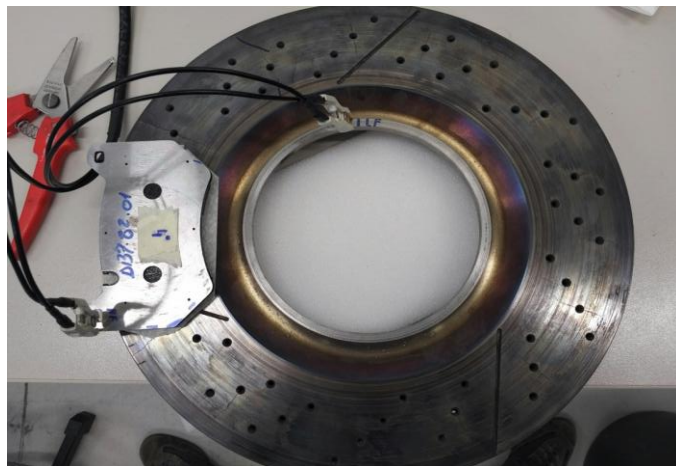


Figure 21d: Pad above half left slot

Once the system is fixed is possible to apply the frequency sweep. Three values of capacitance are taken. The process is finished, and the new position configuration can be performed.

Before any numerical analysis, the five cases can be divided in three groups: group 1 where there is not interaction between slot and pad (position 1 and 5), group 2 where there is partial interaction (position 2 and 4) and group 3 where maximum interference should occur (position 3).

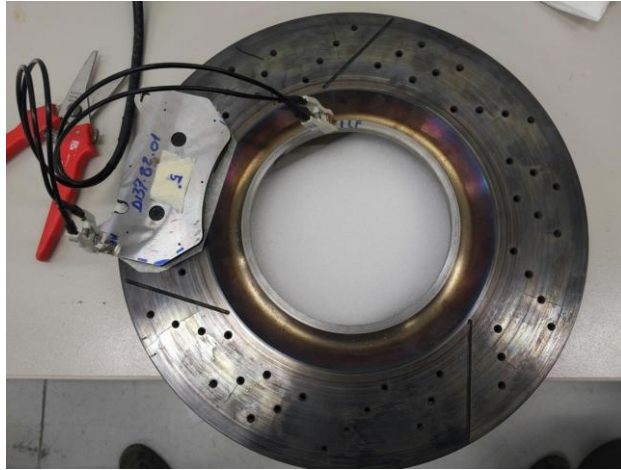


Figure 21e: Pad left to the designated slot

From Table (17) is evident that even changing the frequency, the obtained values are of the same order of magnitude (nF) This means that the established set up doesn't interact with the disc surface shape .

Frequency/position	12Hz	50Hz	1kHz	Position description
P1=PRS	0.56 nF	0.65 nF	0.49 nF	Pad right to slot
P2=PAHRS	0.53 nF	0.62 nF	0.46 nF	Pad above half right slot
P3=PAS	0.56 nF	0.62 nF	0.49 nF	Pad above slot
P4=PAHLS	0.59 nF	0.41 nF	0.49 nF	Pad above half left slot
P5=PLS	0.58 nF	0.42 nF	0.49 nF	Pad left to slot

Table 17: Capacitance frequency sweep results

Once established that the rotor surface design doesn't interact with the interested measures, new tests have been made considering the total disc-pad system.

Disc-pads electric circuit test

The aim of this test is to evaluate through capacitance measures the possibility to detect two threshold values for the three possible working conditions:

- No contact between pads and disc
- Contacts between both pads and disc

- Only one pad touches the disc

Tests setup is not the same as the real braking system one, the two pads lay down on the disc as shown in Figure(22) and not one on each side of the rotor.



Figure 22: Pads placed on same surface configuration

Six configuration have been defined, each one characterized by a different surface contact area (as insulator scotch tape has been used):

1. Not insulated pads: both of the pads are completely touching the surface of the disc (NI)
2. Left pad insulated, right pad not insulated (LI)
3. Right pad insulated, left pad not insulated (RI)
4. Both pads insulated (BI)
5. Insulating left part of both pads (LPBI)
6. Insulating right part of both pads (RPBI)

The probes are connected respectively to the external eyelet of each pad and the R/C mode is used, in particular in SLOW speed for capacitance values and FAST speed for resistance values.

For every configuration four frequency are taken into account: the smallest one the equipment can hold (12Hz), the common European one (50Hz), double the common (100Hz) and a high frequency (1kHz). Moreover four measurements have been taken for every single frequency.

Here is a Table (18) of the obtained results:

R [Ω]	12Hz	50Hz	100Hz	1kHz	C	12Hz	50Hz	100Hz	1kHz
NI 1	27.76	22.26	23.73	24.57		0.08045	0.06	0.0047	0.00035
NI 2	24.87	21.83	27.38	21.22		0.132	0.064	0.0075	0.00064
NI 3	24.78	23.92	23.58	26.55		0.083	0.008	0.0058	0.0003
NI 4	22.56	22.1	21.86	21.68		0.08765	0.011	0.0066	0.00057
LI 1	over	over	over	over		0.427	0.32	0.366	0.36
LI 2	over	over	over	over		0.415	0.37	0.377	0.363
LI 3	over	over	over	over		0.39	0.45	0.37	0.363
LI 4	over	over	over	over		0.43	0.44	0.38	0.372
RI 1	over	over	over	over		0.484	0.456	0.444	0.424
RI 2	over	over	over	over		0.484	0.456	0.444	0.424
RI 3	over	over	over	over		0.483	0.454	0.444	0.424
RI 4	over	over	over	over		0.216	0.203	0.198	0.188
BI 1	over	over	over	over		0.21	0.148	0.198	0.187
BI 2	over	over	over	over		0.215	0.236	0.196	0.188
BI 3	over	over	over	over		0.216	0.226	0.198	0.188
BI 4	over	over	over	over		0.216	0.203	0.198	0.188
LPBI 1	32.14	32.36	37.21	36.23		0.049	0.00248	0.00244	0.00036
LPBI 2	40.54	39.25	38.68	36.58		0.047	0.011	0.00548	0.0001
LPBI 3	105	102	101	98		0.017	0.004	0.00126	0.00043
LPBI 4	56.47	55.66	55.97	55.42		0.049	0.0055	0.0035	0.0003
RPBI 1	58.53	58.76	56.74	51.16		0.056	0.006	0.0132	0.00022
RPBI 2	54.49	54.16	49.26	48.02		0.044	0.008	0.005	0.0025
RPBI 3	38.23	40.41	55.53	54.81		0.028	0.005	0.011	0.00018
RPBI 4	57.4	55.01	56.88	51.41		0.045	0.005	0.005	0.00012

Table 18: Frequency sweep resistance-capacitance analysis in six different configurations ²

“NI”: not insulated pad
“LI”: left pad insulated
“RI”: right pad insulated
“BI”: both pads insulated
“LPBI”: both left pad parts insulated
“RPBI”: both right pad parts insulated

In particular in the table resistances are expressed in ohm, meanwhile capacitances are expressed in μF (white values) and nF (blue values)

These six configurations can be divided in two groups depending on the surface contact area:

1. Both pads have a portion of area touching the disc (conf. 1,5,6)
2. Only one or no one pad is touching the disc (conf. 2, 3, 4)

It is of our interest investigate on how the capacitance changes along this tests.

Considering the two above mentioned groups, it is evident how unit of measurements differs by 3 orders of magnitude, from 10^{-6} in group 1 to 10^{-9} in group 2.

During capacitance measurement tests, the LCR visualized capacitance value didn't always give a precise number, but many oscillations occurred. On average the variations stay inside 10% with some peaks around 15%. This phenomena rose mostly in group 1 especially in configurations 5 and 6 where contact was partial and a little imperceptible movement or vibration from outside could have interfered. On the other hand capacitance measurement of group 2 were less affected by this uncertainty with a maximum variation of 5%.

Taking only four measure is not enough to define a good characteristic behavior since a trend 3 out of 4 is not successfully satisfactory, so other six measurements have been taken. In particular no more an R_C measure but only C in two pads position:

- A: 180° displacement, same surface (upper Figure 24)
- B: One near the other, same surface (lower Figure 24)

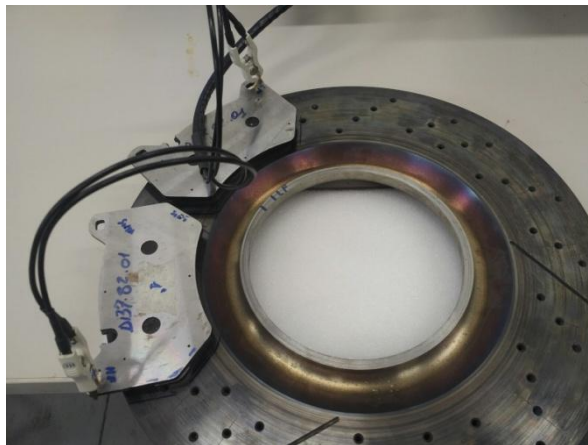
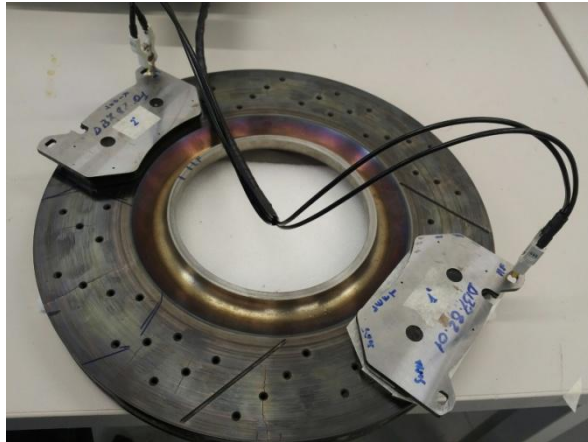


Figure 23: Capacitance measurement with pad position configuration 180° above and side to side bottom

Here is the Table(19) results:

C[nF]	12Hz	50Hz	100Hz	1k Hz
A				
LI 5	0.464	0.45	0.452	0.43
LI 6	0.488	0.485	0.451	0.431
LI 7	0.475	0.478	0.451	0.433
LI 8	0.493	0.48	0.455	0.433
LI 9	0.511	0.55	0.457	0.433
LI 10	0.501	0.49	0.457	0.434
B				
	0.455	0.48	0.403	0.383
	0.442	0.35	0.403	0.388
	0.423	0.443	0.404	0.389
	0.431	0.484	0.405	0.389
	0.438	0.32	0.409	0.389
	0.453	0.29	0.41	0.389

C[nF]	12Hz	50Hz	100Hz	1k Hz		12 Hz	50 Hz	100 Hz	1k Hz
-------	------	------	-------	-------	--	-------	-------	--------	-------

RI 5	0.416	0.393	0.387	0.372
RI 6	0.418	0.399	0.388	0.372
RI 7	0.419	0.4	0.389	0.373
RI 8	0.418	0.394	0.389	0.373
RI 9	0.419	0.395	0.388	0.373
RI 10	0.42	0.396	0.388	0.373

0.458	0.429	0.422	0.405
0.458	0.428	0.422	0.404
0.457	0.43	0.422	0.404
0.457	0.432	0.423	0.405
0.458	0.43	0.423	0.405
0.456	0.428	0.423	0.404

BI 5	0.213	0.175	0.201	0.193
BI 6	0.217	0.185	0.204	0.194
BI 7	0.218	0.204	0.202	0.194
BI 8	0.213	0.187	0.203	0.194
BI 9	0.218	0.198	0.204	0.194
BI 10	0.223	0.192	0.205	0.195

0.215	0.233	0.196	0.187
0.218	0.221	0.194	0.186
0.216	0.226	0.197	0.187
0.219	0.225	0.197	0.187
0.217	0.266	0.197	0.188
0.213	0.226	0.195	0.188

Table 19: Capacitance measurement with same surface and angle displacement

“LI”: Left pad insulated

“RI”: Right pad insulated

“BI”: Both pads insulated

All capacitance are expressed in nF, configuration A is to the left, configuration B to the right

Even changing position the variation in not significant. However is clear the difference between one insulated pad an both pads: capacitance is half the other.

The best values to take as references are one at 100Hz since their oscillation values is the smallest one around 0.5pF

From now the LCR sampling frequency is fixed at 100Hz, even if a comparative measurement is always done at the lower instrument frequency of 12Hz.

3.2 Incremental distance

Once the capacitance measure reached a stable value, after ten capacitive measurements for each configuration, a new test has been done comparing how the capacitance values react to brake pads-disc distance.

In order to perform this test it is fundamental to define how distance is fixed and how to maintain it constant. From previous researches the mean distance between brake pads and discs, when braking pressure is not applied, is around 1,0mm. This value is what we define as maximum distance between the parts. The other extreme to fix is the minimum distance we can experimentally apply in the laboratory set up. Since in the previous tests scotch tape has been used, in order to be able to compare of all the test results, is evident that the minimum distance is given by the scotch tape thickness, which is 0.1 mm.

Since the minimum distance step is 0,1 mm, ten measurements are available. Each values is taken by adding layer by layer on both pads and measuring the capacitance value of the system : one clamp on one pad eyelet and the other clamp to the other pad eyelet. The instrument set up is fixed in R/C MODE , FAST speed and sampling frequency at 100Hz.

Two different configuration are settled:

- Pads placed on the same disc surface (simplified position case)
- Pads place one facing the other on the disc surfaces (ideal position case)

In the first configuration brake pads are placed over the same disc surface so that the pressure aging on the disc, which is given only by the pad weight, is the same in both pads.

In the second configuration instead the pads are respectively facing each other and placed on the two disc contact surfaces.

From a theoretical point of view

Here in Figure (24) the two different setup are depicted:

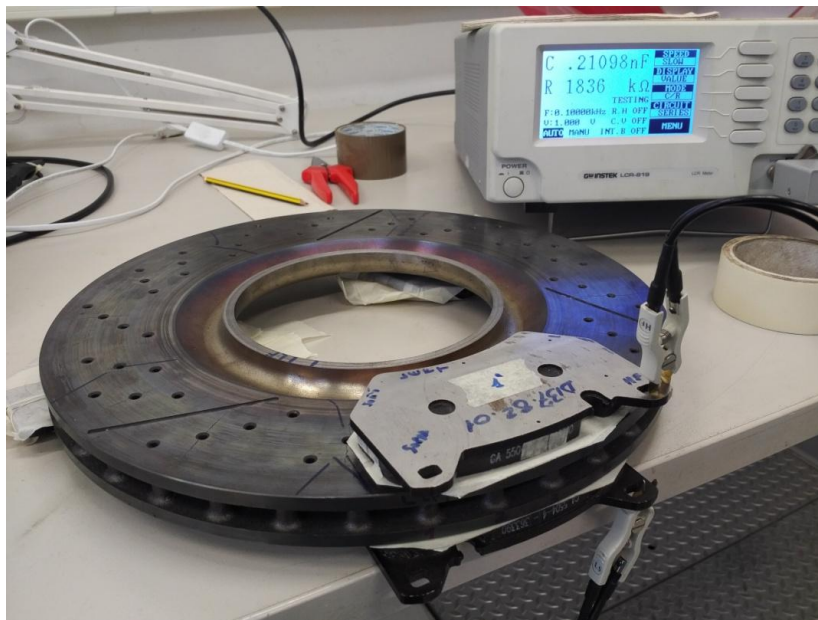
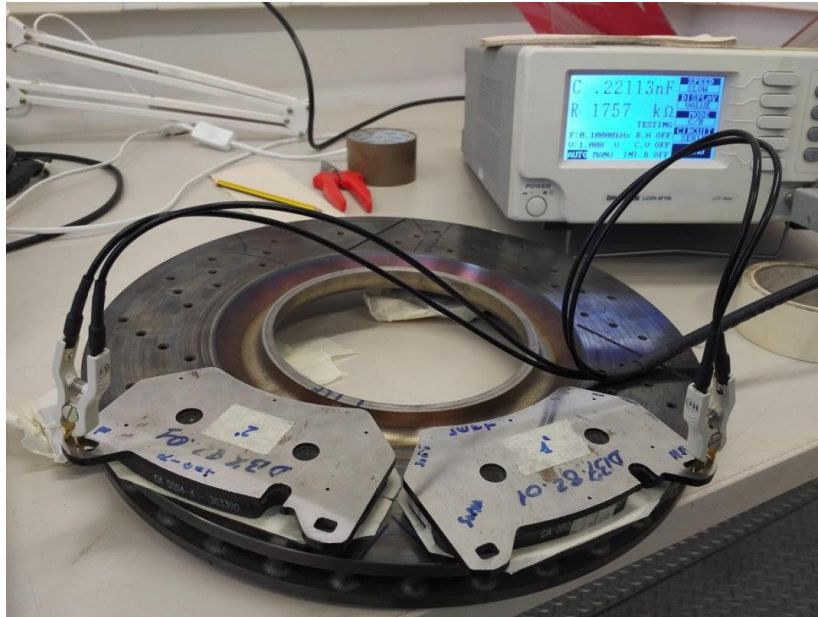


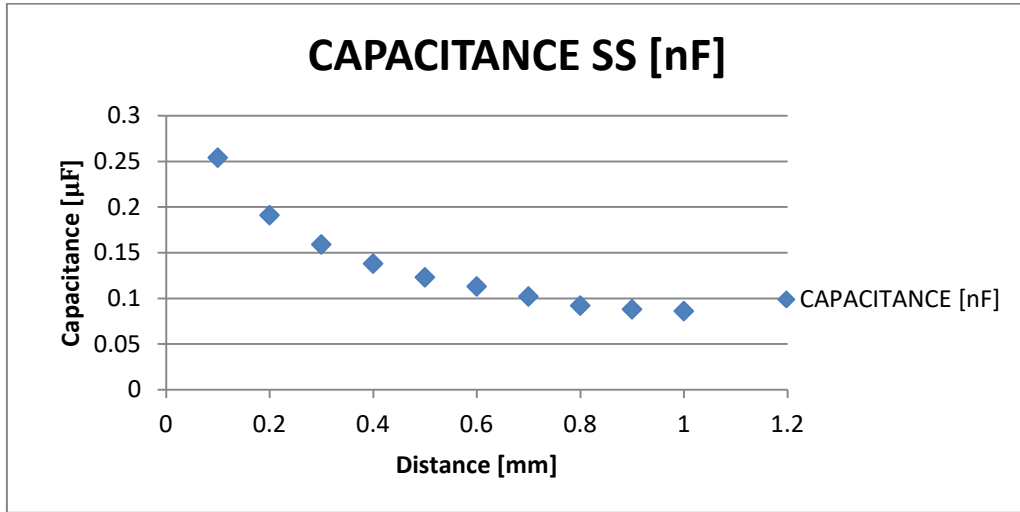
Figure 24: simplified pad positioning (above) versus real pad positioning (below)

The comparison between the two settings permits to understand the electrical circuit behavior inside the disc.

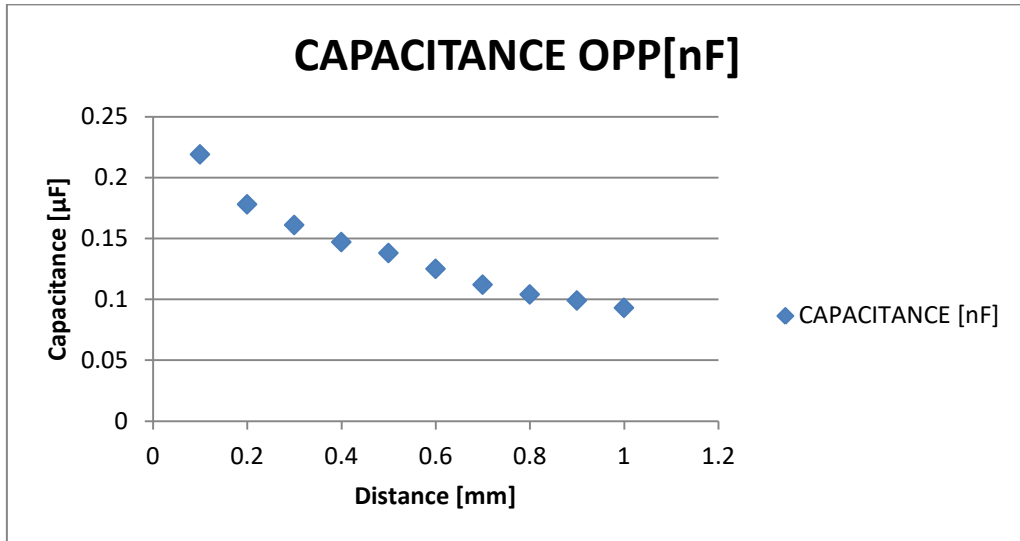
Defining the first configuration as SAME SURFACE and the second as OPPOSITE, the result are shown in the Table (20) and relative Graphs (5 and 6) below:

DISTANCE [mm]	0.1	0.2	0.3	0.4	0.5	0.6	0.7	0.8	0.9	1
CAPACITANCE [nF] SAME SURFACE	0.254	0.191	0.159	0.138	0.123	0.113	0.102	0.092	0.088	0.086
CAPACITANCE [nF] OPPOSITE SURFACE	0.219	0.178	0.161	0.147	0.138	0.125	0.112	0.104	0.099	0.093

Table 20: Incremental distance comparison between the two configurations

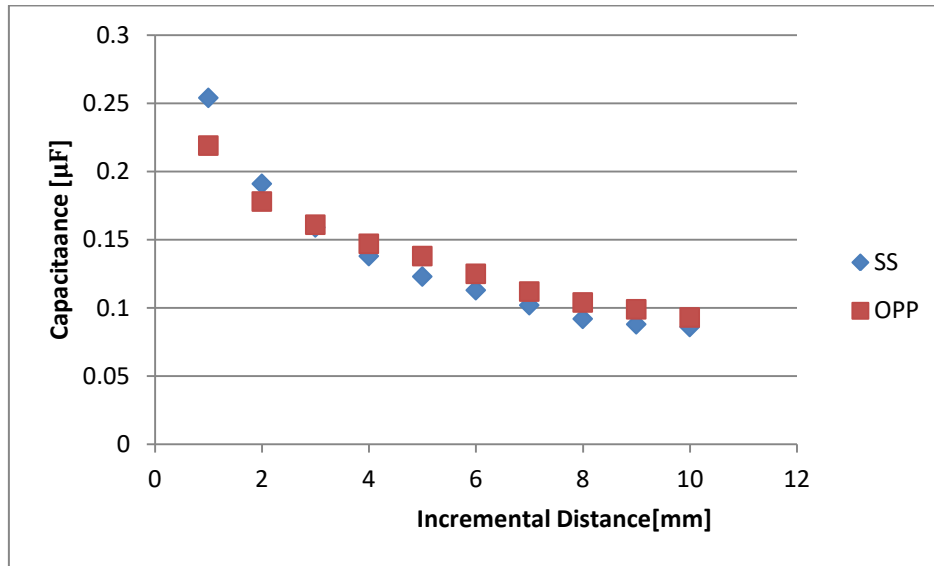


Graph 5: Same surface incremental distance capacitance



Graph 6: Opposite surface incremental distance capacitance

Comparing the obtain result in a comparative Graph (7):



Graph 7: Comparison between graph 5 and 6

It is possible to see that the two curves are two similar hyperbolas with the same decay capacity value over distance. The range is not particularly wide in fact in 1 mm thickness the variation is around 0.168 nF. Moreover since the two curves are so similar seems that there is not a particular influence in positioning the pads respect to the disc faces.

3.3 Single pad analysis of the complete system

In the previous paragraph a capacitance-distance relationship has been found. Now the aim is to understand how the two pads interact within the system: control how the capacity changes by short-circuiting a pad giving same potential to one pad and the disc. It can be seen as something previously treated but in this case the system is passed from 1 pad system to a 2 pads one.

The Same Surface setup is taken into account for a sake of construction simplicity and the short-circuit is made by the connection of 2.5mm² green-yellow wire to the probe and the disc as shown in Figure(25). The probe is connected as well to the pad eyelet, creating in this way a common potential.

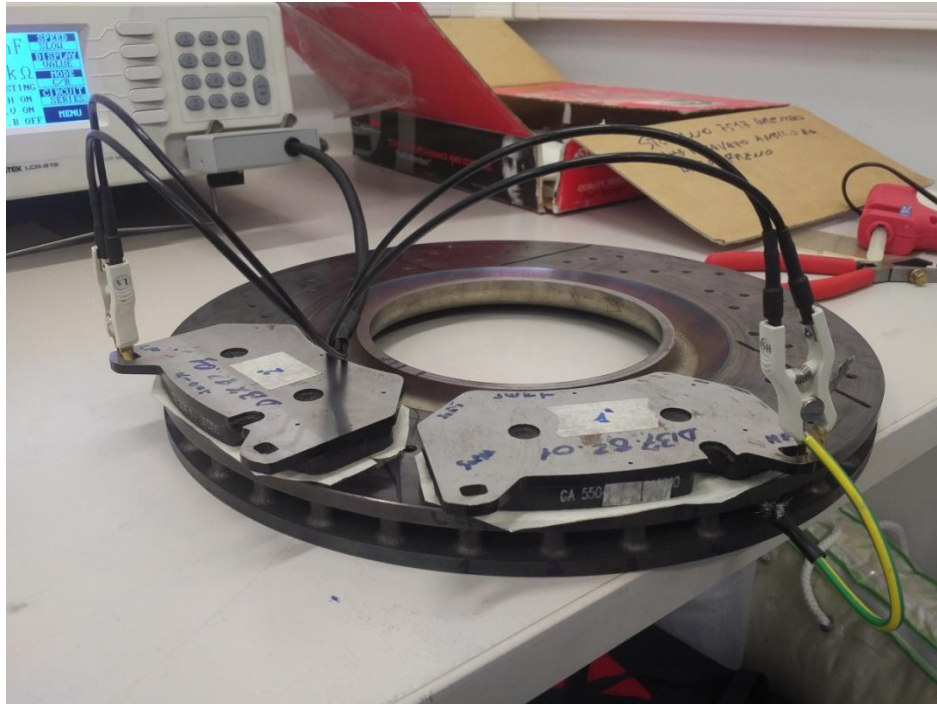


Figure 25: Short-circuiting the right pad

From a theoretical point of view short-circuiting a pad means that given same voltage to the system and assuming that the two pads are equals, the capacitance should double in value.

If we consider two electrical circuits made up by a voltage source V and respectively the first one with only a capacitor meanwhile the second one with two series capacitors, shown in Figure (26), it is possible to verify the previous statement.

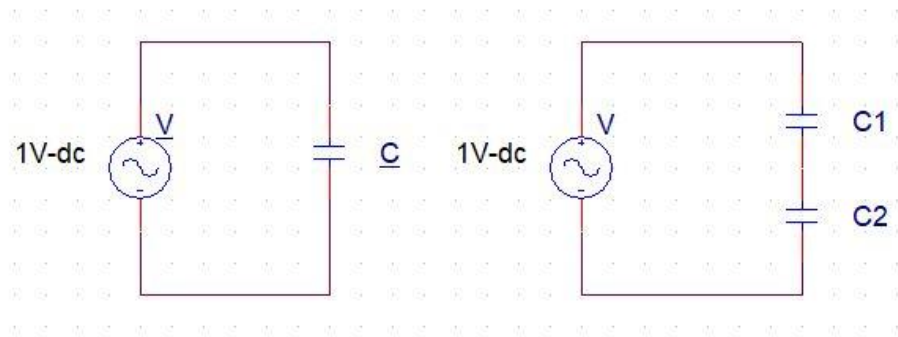


Figure 26: Short-circuited equivalent circuit (left) compared to the complete equivalent circuit (right)

In order to compare the two it is important to remind how to calculate series capacitors:

$$\frac{1}{C_{eq}} = \sum_{i=1}^n \frac{1}{C_i} = \frac{1}{C_1} + \frac{1}{C_2} \quad (2.7)$$

Assuming C_1 equals C_2 , the equivalent capacitance of the right circuit is:

$$\frac{1}{C_{eq}} = \frac{1}{C_1} + \frac{1}{C_2} = \frac{C_1 + C_2}{C_1 * C_2} = \frac{2 * C_1}{C_1^2} = \frac{2}{C_1} \quad (2.8)$$

Since the applied voltage is the same in the two circuits, it is possible to represent the capacitance comparison as:

$$\frac{1}{C} = \frac{2}{C_1} \quad (2.9)$$

and

$$C_1 = C_2 = 2C \quad (2.10)$$

In terms of numerical values and experimental tests the results are shown in the Table (21) below:

DISTANCE [mm]	CAPACITANCE [nF]	Settings
0.1	0.254	2 pads
0.1	0.512	1 pad short-circuited

Table 21: Numerical results of short-circuiting one pad

Writing in the capacitance comparison formula previously obtained the experimental capacitance values:

$$\frac{1}{0.254} = \frac{2}{0.512}$$

The two rational numbers differs by less than 1%, so it is possible to confirm that the experimental taken measurements are correct.

Chapter 3

1.1 FEM Analysis

In this chapter finite element method is used with the aim to verify the experimental values obtained in laboratory measurement sessions with a numerical problem solving software.

Finite element method (FEM) is a method of solving problems in engineering and science fields. It is mainly used for those situations where no exact solution, expressible in terms of mathematical formulation, is available. It is based on a numerical method and can be defined as a piece-wise process. The analysis can be applied to one-dimensional systems, but more usually there is an area or volume within which the solution is required, so 2D and 3D are more often evaluated. The sketch of the system to simulate, once imported from design software or defined inside the FEM software, is split into a number of smaller areas (for 2D simulations) or volumes (for 3D simulations) which are called finite elements. This process is known as discretisation. Each finite element is then analyzed and once all elements are evaluated, an assembling process is made, forming a mesh and giving a numerical solution to the input requests.

The software in use to perform the FEM simulations is Ansys Electronics version 16.2

2.1 Simulation setup

Ansys Electronics is a FEM software which allows to perform resistive and capacitive simulation of 3D models. Since the software offers the possibility to import system models from Graphic software, Solidworks 2016 has been used for the design of every single parts of the system and all the configurations to be tested.

In terms of FEM analysis, the solution types defined in order to perform resistive and capacitive calculations are “Electrostatic” for the evaluation of

capacitance matrix and “DC Conduction” for the calculation of ohmic losses and therefore resistance values.

2.2 Simulation configuration process

For every simulation a series of steps need to be done before being able to launch it. Here are listed all the steps needed:

1. Choose type of simulation (Maxwell 3D design)
2. Design/Import the system to study (import STEP Files)
3. Define solution type (Electrostatic & DC Conduction)
4. Assign materials properties (creation of materials with specific characteristics)
5. Assign excitation (Voltages)
6. Create result matrix (Capacitance/Total Loss/Ohmic Loss)
7. Define solution setup (n° of steps and percent energy error)
8. Results/Fields overview (voltage/current density distribution/ohmic loss distribution/electric and dielectric fields distributions)

Type of simulation: is the first step which characterizes the type of project is going to be treated.

Design/import: is the phase in which the system is drawn or imported by a design software.

Solution type: 2 main kinds of solution type are present: Electrostatic and Magnetostatic. The one of our interest is the first one. In Electrostatic it is possible to perform three different simulations:

- Electrostatic
- DC conduction
- Electric transient

Material assignment: each system component should be characterized by its physical properties. In this step it is also possible to create a surrounding system region to be included in the simulation process.

Excitation: it is possible to assign voltages to system components.

Result matrix: creation of a matrix where results are inserted.

Solution setup: define how precise the analysis should be in terms of percentage error and maximum number of steps to be performed if the error is not reached.

Result/Fields: is the final step where the results of the simulation and where Graphs are implemented.

All steps are fundamental for a correct simulation, but the most important one is step number three because it allows to determine which are the parameters to investigate on and to establish which are the output variables.

To create the simulation as similar as possible to the experimental tests shown in chapter 2, new materials have been added to the default ones. These materials are shown in the following Table(22):

Properties/Materials	Conductivity [S/m]	Relative permittivity
Cast iron	963391.1	1
Pad composite	1.77305	1

Table 22: Material characters

Cast iron is attributed to brake pad plates and disc, meanwhile pad composite to the brake pads.

3.1 DC Conduction

DC Conduction simulation allows to evaluated inside an electric circuit how total losses are spread and to perform the current density distribution in the system. Through these output variables is then possible to calculate the system resistance value and the bulk conductivity.

Bulk conductivity analysis

All simulations have been studied in the case of pads placed on the same disc surface. Once materials have been assigned, the voltages applied are respectively 1V (red) to one pad plate and 0V(blue) to the other one as depicted in Figure (27)

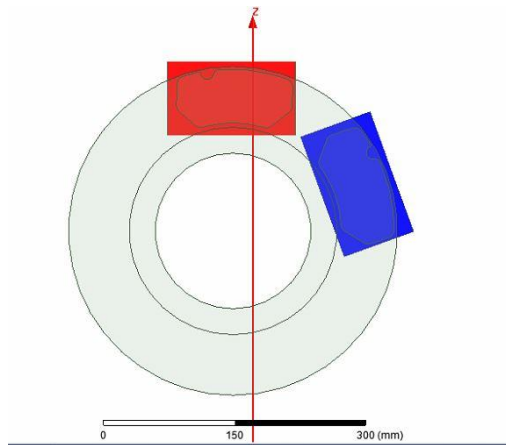


Figure 27: DC conduction applied voltages

This setup is followed by nine different cases, each one characterized by a different contact area between disc brake and brake pads, but with same analysis description of 30 steps and losses percentage error of 0.05%.

The nine cases can be divided into three subgroups, each one with a specific contact area:

1. Total contact: one case
2. Quarter contact: four cases
3. Half contact: four cases

The total contact simulation has been done in order to get a comparison with the values obtained in the previous chapter, when resistance results were obtained by pressing the pad to the disc with four clamps. This case is defined as case 0 and will be the reference for all the following ones.

Quarter contact have been designed dividing the pads in four equal area parts and realizing the contact with just one sector: case 1 (upper left), case 2 (upper right), case 3(lower left) and case 4 (lower right).

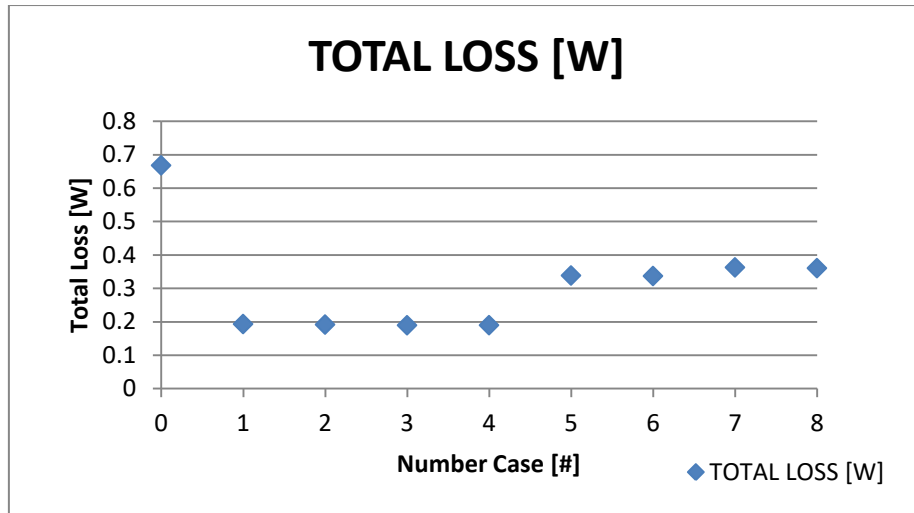
Half contact have been done dividing the pads in two equal area parts computing other four cases: case 5 (left side), case 6 (right side), case 7 (upper part) and case 8 (lower part).

Once simulated all the cases the results in terms of total losses [W] are represented in the following Table(23):

N° case	TOTAL LOSS [W]
0	0.66822
1	0.19342
2	0.19176
3	0.18971
4	0.18997
5	0.33864
6	0.33709
7	0.3629
8	0.36065

Table 23: Relation between pad contact cases and total loss

And the relative Graph(8):



Graph 8: Relation between pad contact area and total loss

The Graph shows a how the three subgroups are divided and how the contact area influences the total loss value. To better understand this situation the total loss distribution come in help. In the following Figures(28, 29, 30), one for each case, is evident how losses spread along the pads as a function of the contact area.

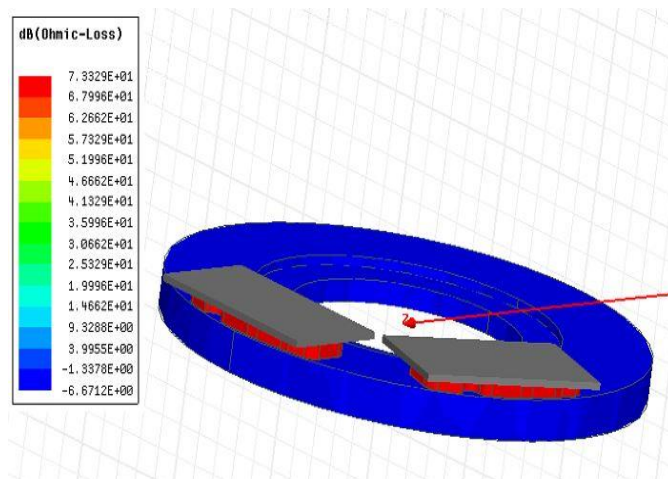


Figure 28: Complete pad- disc contact

The first subgroup, made up by the complete contact situation, shows the interesting behavior of ohmic losses which are totally inside the pads.

This means that from a material properties point of view the composite pad material is not as conductive as cast iron and it is where the current density increases.

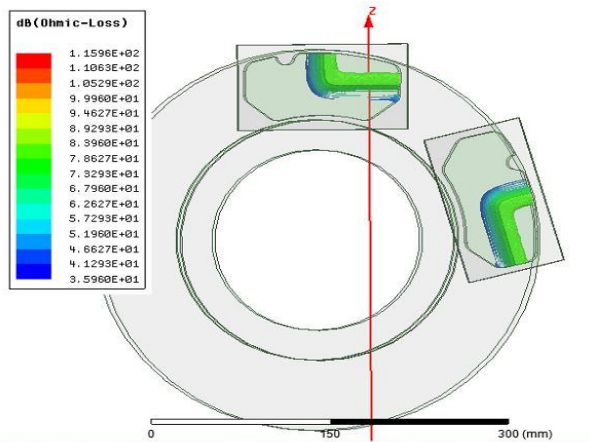


Figure 29a: Upper right quarter contact

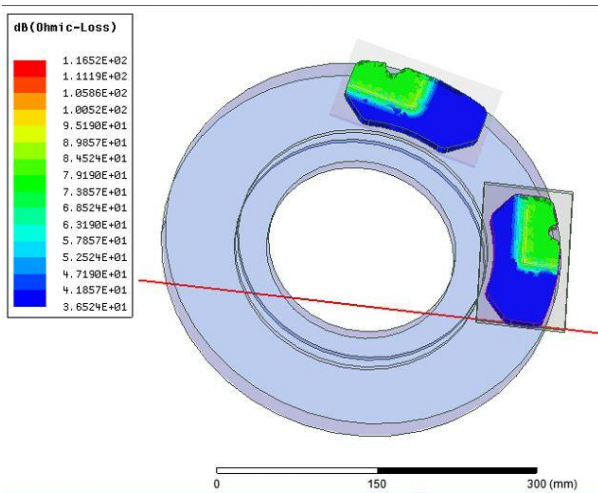


Figure 29b: Upper left quarter contact

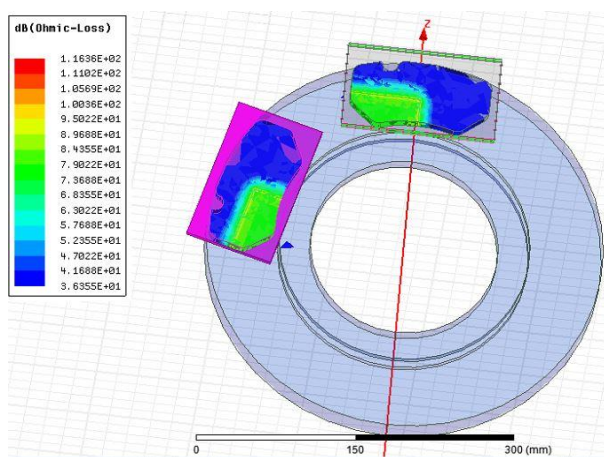


Figure 29c: Lower left quarter contact

The second subgroup is characterized by one of the four quarter pad area in contact with the disc. In all four configurations the ohmic losses are widely spread over the interested contact area with an extremely low value

where no contact happens and the highest value on the contact edges. The phenomena can be seen in the first of the four images where propagation is more pronounced: blue lines represent the three out of quadrant which don't get in contact with the disc (no loss),

red lines are the contact edge (high loss) and green ones express the transition from the two ends.

Even if the quarters are different in shape, the loss distribution inside the pad is practically the same.

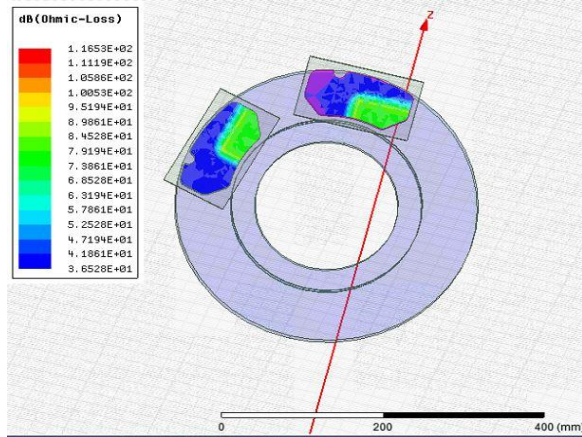


Figure 29d: Lower right quarter contact

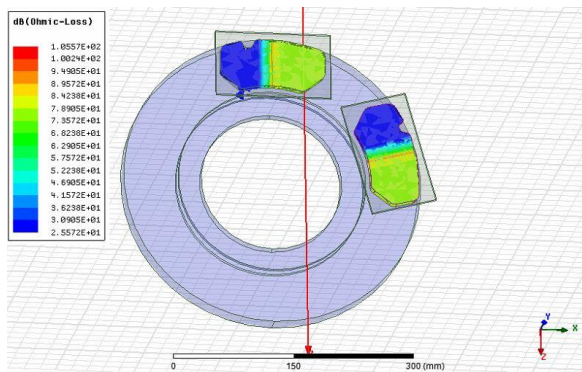


Figure 30a: Right half contact

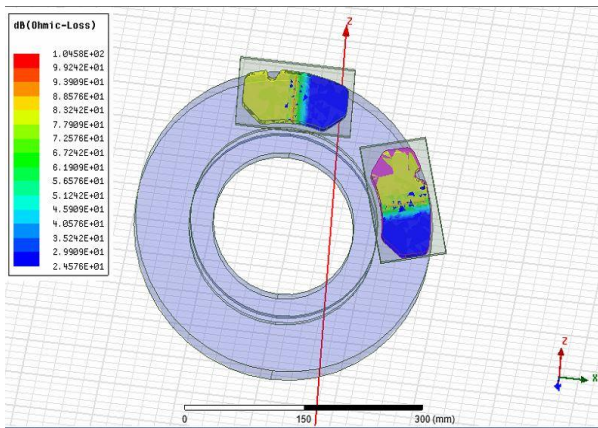


Figure 30b: Left half contact

The last subgroup characterized by the other four configurations is similar to the second subgroup but the spectrum is completely different. The main difference is in how the spectrum is spread on the c surface: ohmic losses are no more only on the contact area but also in the fractional part adjacent.

In case 5 and 6 (left and right contact) the distribution doesn't change meanwhile in case 7 and 8 (upper and lower contact) the region with a very low content of total loss (blue area) has a 10% difference.

The maximum value of all four cases compared to the previous subsystem is lower. This is correct since the contact surface area has increased. Comparing the maximum values of the three systems we can establish which is the relationship between surface contact area and total loss value. In particular the amounts are:

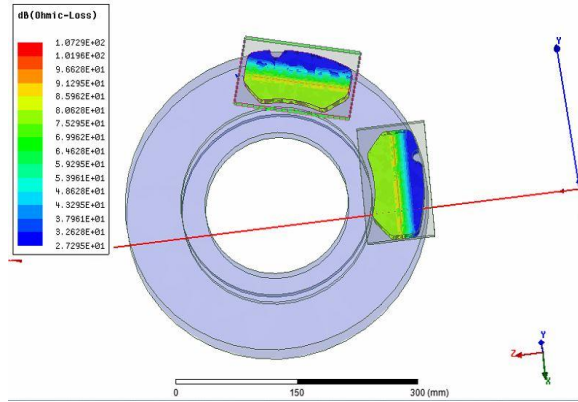


Figure 30c: Lower half contact

7.33 dB for [1]

116 dB for [2]

105 dB for [3]

With this comparison is evident the order of magnitude difference between total contact and partial one,

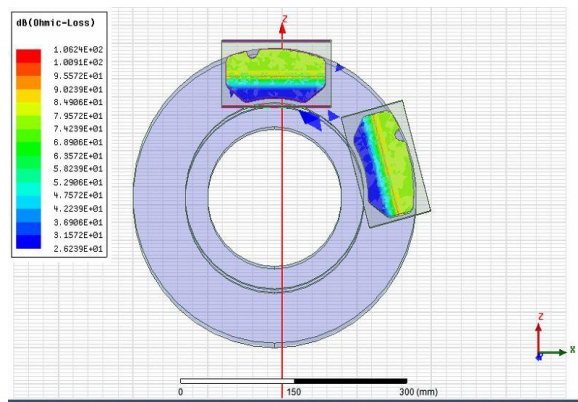


Figure 30d: Higher half contact

Reminding that the total loss equals the total electric power we can establish that:

$$P_{loss} = P_{el} = V * I \quad (3.1)$$

And that ohm law is:

$$V = R * I \quad (3.2)$$

The evaluation of resistance can be performed:

$$R = \frac{V^2}{P_{loss}} \quad (3.3)$$

Since $V=1$,

$$R = \frac{1}{P_{loss}} \quad (3.4)$$

Resistance values are then listed in the next Table(24):

N° case	RESISTANCE [Ω]
0	1.496513
1	5.170096
2	5.214852
3	5.271203
4	5.263989
5	2.952988
6	2.966567
7	2.75558
8	2.772771

Table24: Relation between pad contact cases and resistance

If the resistance value of case 0 (1.496513 ohm) is taken into account and compared to the laboratory second approach (four points pressure configuration) which gave a result of 0.720 ohm, a divergence is present. The reason which allows to obtain two different values stays in the assignment of materials step, particularly the insertion of the bulk conductivity of brake pads. They, in fact, are the most difficult studied components, not easily and extremely accurate measured due to impossibility to separate them from their plate.

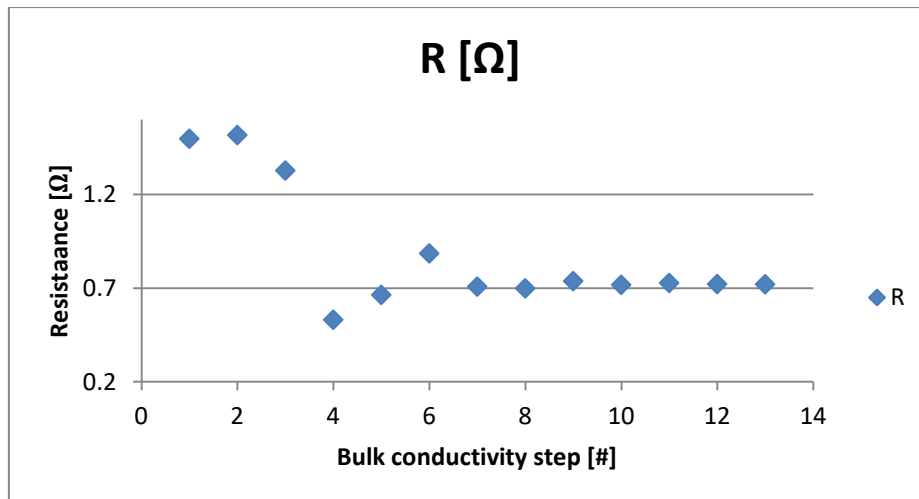
if the experimental value is fixed as reference, and assuming that brake pad plates and disc resistance is negligible respect to the pad one (two order of magnitude smaller than the brake pad) it is possible to vary bulk conductivity and achieve the results . it is not an immediate transition conductivity-resistance, but as it was explained before after having imposed material properties in order to get resistance value voltages have to be imposed and total losses calculated.

Starting from 1.496513 ohm, the target is to reach 0.720 ohm. The iterative process has been done only for case 0, which is as previously said the reference case. When the goal is gained and then settled, all the other simulation have been repeated with the new bulk conductivity value. In the following Table(25) is described the above mentioned mechanism.

TARGET : 0.72 Ω		
BULK CONDUCTIVITY [S/m]	TOTAL LOSS [W]	R [Ω]
1.77305	0.66822	1.496513
1.75	0.65954	1.5162
2	0.75365	1.3269
5	1.884	0.5308
4	1.5075	0.6633
3	1.1303	0.8847
3.75	1.4132	0.7076
3.8	1.4321	0.6983
3.6	1.3567	0.7371
3.7	1.3944	0.7172
3.65	1.3756	0.7270
3.68	1.3869	0.7210
3.685	1.3887	0.7201

Table 25: Iterative process for conductivity value

From a graphical point of view Graph (9) explains the process iteration by iteration of the output parameter.



Graph 9: Iterative conductivity identification process

Twelve iterations have been done before reaching the wanted values with an error less than 0.01%

The new bulk conductivity value defined to us to repeat the DC conduction simulations is:

$$\sigma = 3.685 \left[\frac{S}{m} \right]$$

The new total loss and then resistance Table(26) is:

N° case	TOTAL LOSS [W]	RESISTANCE [Ω]
0	1.3887	0.720098
1	0.40198	2.487686
2	0.3985	2.50941
3	0.39428	2.536269
4	0.39481	2.532864
5	0.70408	1.420293
6	0.70057	1.427409
7	0.75422	1.325873
8	0.74955	1.334134

Table 26: Final total loss and resistance values with definitive bulk conductivity

All these parameters and simulations have been done by assuming that the two pads are placed on the same disc surface and no pressure is applied to them except from their weight. In real life, brake pads are one opposite the other separated by the disc. This means that a new simulation with the real setup is necessary to be performed. The comparison between the two types of pads position is made by evaluating total losses: both of them in case 0 are equal to 1.338 W. This means the current flow is not disc dependent, but by the two brake pads.

3.2 Current density distribution

Current density distribution hallows to understand how the current flows inside the system, in particular how it spreads inside the brake pads. To be able to perform the distribution the parameters to consider are: resistance value and surface area. In our case the pad area is 7514.25 mm².

In terms of formulas the relation between current and current density is:

$$I = J * A \quad (3.5)$$

Where I stands for the current, J the current density distribution and A the contact area.

For each configuration a mathematical computation has been processed, evaluated both in numerical system and dB system and then compared to the simulation results. During laboratory test applying to the system a voltage drop of 1V

Case 0

$$I = \frac{1}{0.720098} = 1.388 \text{ A}$$

$$J = \frac{1.3887}{2 * 7514.25} = 9.24 * 10^1 \frac{\text{A}}{\text{m}^2}$$

$$dB [J] = 20 * \log_{10} J = 3.93 * 10^1 \text{ dB}$$

Case 1

$$I = \frac{1}{2.487686} = 0.402 \text{ A}$$

$$J = \frac{0.402}{2 * \frac{7514.25}{4}} = 10.699 * 10^1 \frac{\text{A}}{\text{m}^2}$$

$$dB [J] = 20 * \log_{10} J = 4.058 * 10^1 \text{ dB}$$

Case 2

$$I = \frac{1}{2.50941} = 0.3985 \text{ A}$$

$$J = \frac{0.3985}{2 * \frac{7514.25}{4}} = 10.606 * 10^1 \frac{\text{A}}{\text{m}^2}$$

$$dB [J] = 20 * \log_{10} J = 4.051 * 10^1 \text{ dB}$$

Case 3

$$I = \frac{1}{2.536269} = 0.3943 \text{ A}$$

$$J = \frac{0.3943}{2 * \frac{7514.25}{4}} = 10.494 * 10^1 \frac{\text{A}}{\text{m}^2}$$

$$dB [J] = 20 * \log_{10} J = 4.041 * 10^1 \text{ dB}$$

Case 4

$$I = \frac{1}{2.532864} = 0.3948 \text{ A}$$

$$J = \frac{0.3948}{2 * \frac{7514.25}{4}} = 10.508 * 10^1 \frac{\text{A}}{\text{m}^2}$$

$$dB [J] = 20 * \log_{10} J = 4.043 * 10^1 \text{ dB}$$

Case 5

$$I = \frac{1}{1.4203} = 0.7041 \text{ A}$$

$$J = \frac{0.7041}{2 * \frac{7514.25}{2}} = 9.370 * 10^1 \frac{\text{A}}{\text{m}^2}$$

$$dB [J] = 20 * \log_{10} J = 3.943 * 10^1 \text{ dB}$$

Case 6

$$I = \frac{1}{1.4274} = 0.7005 \text{ A}$$

$$J = \frac{0.7005}{2 * \frac{7514.25}{2}} = 9.322 * 10^1 \frac{\text{A}}{\text{m}^2}$$

$$dB [J] = 20 * \log_{10} J = 3.939 * 10^1 \text{ dB}$$

Case 7

$$I = \frac{1}{1.3258} = 0.7542 \text{ A}$$

$$J = \frac{0.7542}{2 * \frac{7514.25}{2}} = 10.037 * 10^1 \frac{\text{A}}{\text{m}^2}$$

$$dB [J] = 20 * \log_{10} J = 4.003 * 10^1 \text{ dB}$$

Case 8

$$I = \frac{1}{1.3341} = 0.7495 \text{ A}$$

$$J = \frac{0.7495}{2 * \frac{7514.25}{2}} = 9.974 * 10^1 \frac{\text{A}}{\text{m}^2}$$

$$dB [J] = 20 * \log_{10} J = 3.997 * 10^1 \text{ dB}$$

This computation gives just an idea of what the value of density current distribution should be around, without taking into consideration all the coupling and mutual effects of the components. All the density distribution values are pretty much the same, the difference between maximum and minimum one is 0.128 dB which is 10.14 A/m^2 not a wide variation since it is 13.6%. This small variation is correct because in each configuration in order to obtain the current is not used a fixed resistance value but the parameter relative to ohmic losses in the interested surface area

Analyzing instead the simulation results it is possible to evaluate not only the average current previously found but the entire spectrum. In the following Figure(31) the density current spectrum of case 0 is shown:

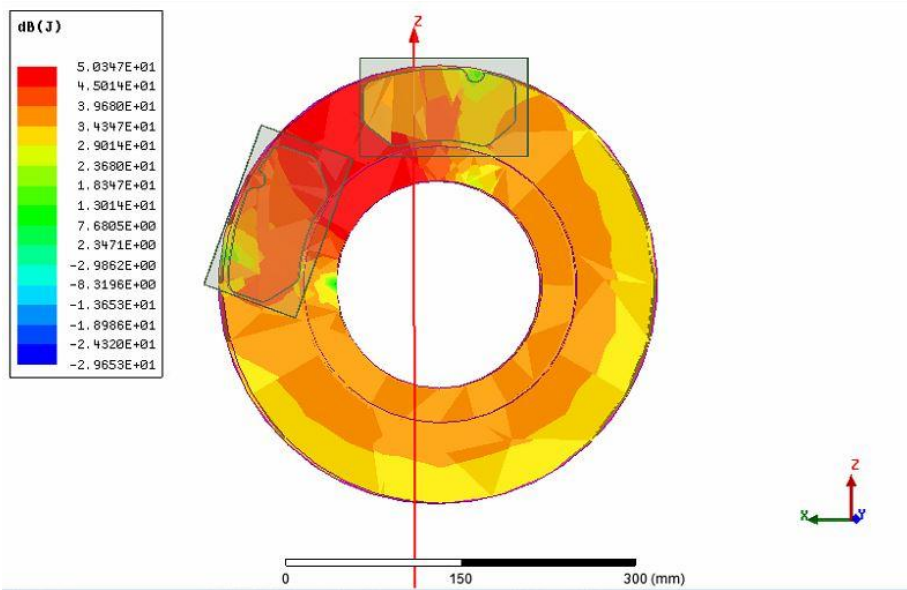


Figure 31: Current density distribution with total contact

It is possible to identify two main current paths. Both of them have in common the initial and final point which are defined by the two clamps placed on the pads. Moreover they are in parallel and the component which generates this type of circuit is the disc. The main difference between the two is the amount of current flowing into and the circuit length. The shortest one is characterized by the highest density current distribution meanwhile the other by the average value.

Comparing the legend in the Figure31 above with the theoretical result it is possible to find a similarity: the average color stands in the window between $2.901 \cdot 10^1$ and $3.968 \cdot 10^1$ dB and the obtained values is $3.93 \cdot 10^1$ dB.

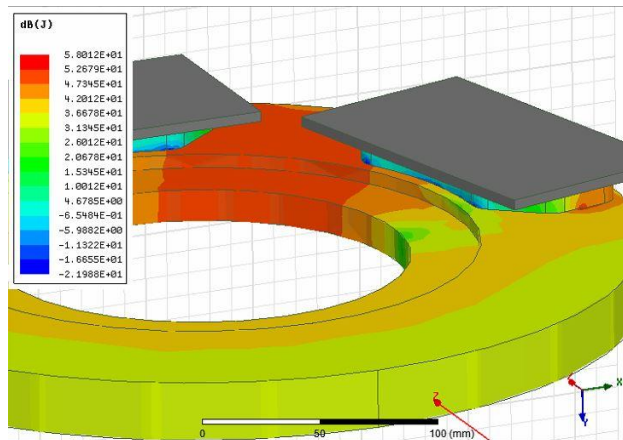
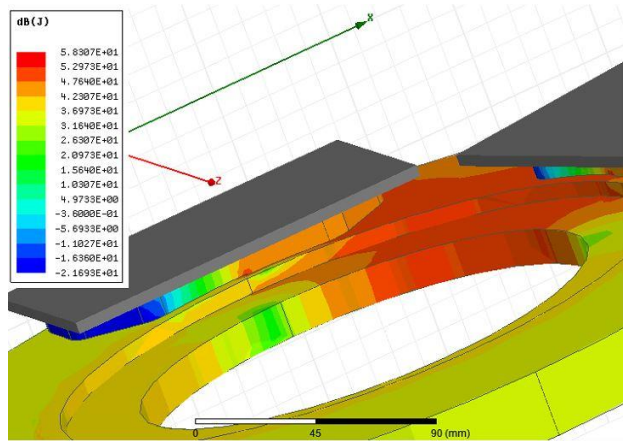
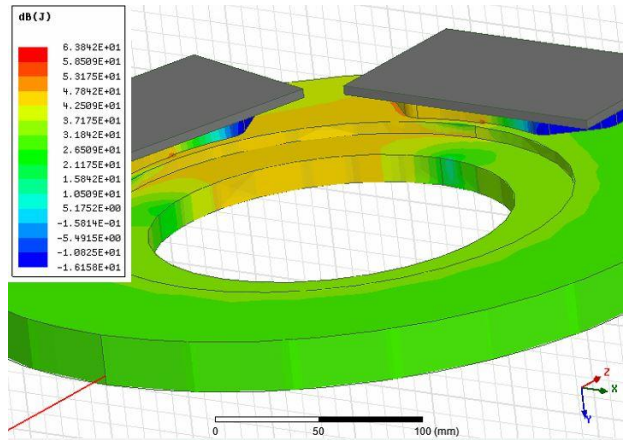


Figure32: Ratio between current density distribution over different contact areas

Considering all the other cases, characterized by a partial contact, the spectrum trend changes as a function of the contact surface area.

Comparing the parallel path of case 0 in the previous image and cases 4 respectively on the top and 5 in the middle and 7 on the bottom of Figure(32) is easy to see how the density current distribution behaves: decreasing surface contact area the length of the two circuits varies, in particular, the shorter one gets longer and the longer one as a sequence gets shorter.

From the numerical point of view the theoretical results in each case are within the orange window of borders $3.96 \cdot 10^1$ - $4.25 \cdot 10^1$ dB.

4.1 Electrostatic Simulations

Electrostatic simulation, also known as Maxwell electrostatic solver, allows to compute the static electric field that exists in a structure given a distribution of DC voltages and static charges. The capacitance matrix can then be calculated from the obtained electric field. Once it is gained is compared with the experimental values.

The simulator solves the electric field using the following relationship:

$$E = -\nabla \Phi \quad (3.6)$$

Where E stands for the electric field and Φ the electrical potential.

For the electrostatic solution, it is assumed that all objects are stationary, so velocity is zero everywhere in the defined region where the electrostatic field is applied. There is no time variation of any of the electromagnetic quantities and no current flow in conductors, thus Joule losses are zero everywhere. All conductors are considered to be perfect and equal-potential such that there is no electric field inside conductors

After E field is calculated, Maxwell writes out solution files and performs an error analysis. In an adaptive analysis, it refines the tetrahedrons with the lowest error, and continues solving until the stopping parameter of 0.05 % error is met.

4.2 Capacitance matrix

To compute the capacitance matrix of the system, in each field simulation, one volt is applied to a single conductor and zero volts to all the other ones. Therefore for a N-conductors system a N field simulations are performed.

The energy stored in each electric field is associated with the capacitance between two conductors can be expressed as:

$$W_{ij} = \frac{1}{2} \int D_i * E_j d\Omega \quad (3.7)$$

where:

- W_{ij} is the energy in the electric field associated with the flux lines that connect charges of conductor i to those on conductor j
- D_j is the dielectric flux density associated with the case in which 1 volt is applied to conductor i
- E_j is the electric field associated with the case in which 1 volt is applied to conductor j

The capacitance matrix can now be developed by:

$$C = \frac{2W_{ij}}{v^2} \quad (3.8)$$

In other expression it can also be evaluated as:

$$C = \int E * D d\Omega \quad (3.9)$$

here

$$D = \epsilon_0 * E \quad (3.10)$$

and vacuum permittivity $\epsilon_0 = 8.854187817 * 10^{-12} \frac{F}{m}$

The Maxwell capacitance matrix provides the relation between applied voltages on a set of conductors, in our case to the brake system elements, and charges on the conductors. For a generic set of conductors the relation is:

$$Q = C * V \quad (3.11)$$

where Q and V are the charge and voltage vectors and C the capacitance matrix.

The brake system is composed of three conductors: two brake pads (considering pad and plate as a unique piece, in orange) and a disc brake (in blue)

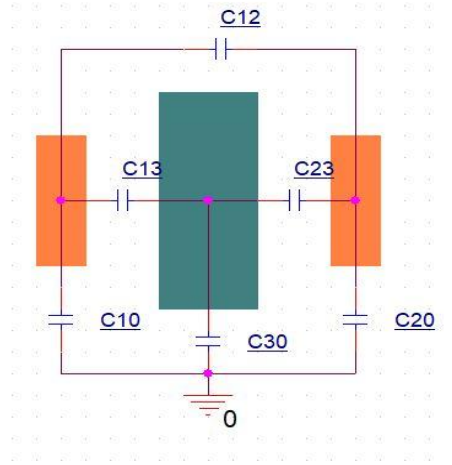


Figure33: Electrical equivalent system of the braking system

In Figure(33) are shown the electrical conductors connected each other by the auto capacitances (C_{10} , C_{20} , C_{30}) and the mutual ones (C_{12} , C_{23} , C_{13}). The electrical system is drawn and it is possible to understand the above

mentioned relation. Important to note is that mutual capacitances are referred towards infinite.

If we take into account brake pad number one (the left one) and give to each conductor its voltage V , charge Q_1 is found as:

$$Q_1 = C_{10} * V_1 + C_{12} * (V_1 - V_2) + C_{13} * (V_1 - V_3) \quad (3.12)$$

which can be arranged as:

$$Q_1 = (C_{10} + C_{12} + C_{13}) * V_1 - C_{12} * V_2 - C_{13} * V_3 \quad (3.13)$$

so the first row of the Maxwell capacitance matrix C is:

$$|C_{10} + C_{12} + C_{13} \quad -C_{12} \quad -C_{13}| \quad (3.14)$$

Repeating this process two times more it is possible to realize the entire capacitance matrix

$$C = \begin{bmatrix} C_{10} + C_{12} + C_{13} & -C_{12} & -C_{13} \\ -C_{21} & C_{20} + C_{21} + C_{23} & -C_{23} \\ -C_{31} & -C_{32} & C_{30} + C_{31} + C_{32} \end{bmatrix} \quad (3.15)$$

This is not the specific capacitance matrix for the system under test. The right configuration is a 5x5 matrix, where brake pad and brake pad plate are considered separated.

For a general case with N conductors the formulation will be:

$$\begin{bmatrix} Q_1 \\ Q_2 \\ \vdots \\ Q_N \end{bmatrix} = \begin{bmatrix} \sum_{i=1}^N C_{1,i} & -C_{12} & \cdots & -C_{1,N} \\ -C_{21} & \sum_{i=1}^N C_{2,i} & \cdots & -C_{2,N} \\ \vdots & \vdots & \ddots & \vdots \\ -C_{N,1} & -C_{N,2} & \cdots & \sum_{i=1}^N C_{N,i} \end{bmatrix} * \begin{bmatrix} V_1 \\ V_2 \\ \vdots \\ V_N \end{bmatrix} \quad (3.16)$$

The diagonal elements are the sum of all capacitances from one conductor to all the others. These terms represent the self-capacitance of the N conductors. The off-diagonal terms are the negative values of the capacitances between the corresponding conductors (mutual effects). Finally it is a symmetric matrix about the diagonal and so the mutual effects between any two conductors are equal. In the studied system there is no reference or ground: this means that the diagonal elements of the matrix won't have the N,0 component.

4.3 Simulation setup

In order to create a simulation as similar as the real laboratory measurements some elements need to be defined. The most important one is how to consider the region around the system in particular which is the volume to take into account. A brief paragraph will show how capacitance matrix is affected by a variation of the region dimension.

Let examine a plane capacitor made up by 3 layers of cast iron and 2 different air region2. Each conductive layer has a base dimension of 10x10 mm and a height of 1 mm one parallel to the other spaced by 1mm, meanwhile the regions are:

1. Same shape of the conductor placed between the layers (light blue)
2. Box in which all layers fit (yellow)

To better define this two volumes the following Figure(34) highlights the differences.

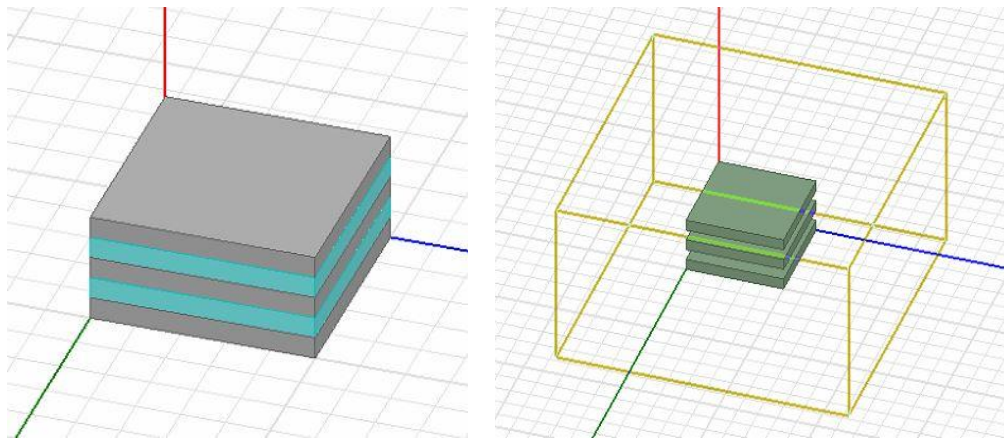


Figure34: Region setup comparison

Applying 1V to the highest plate and 0V to the other two for both cases, the capacitance matrix C_1 and C_2 expressed in pF are:

$$C_1 = \begin{bmatrix} 0.88542 & -0.88542 & 0 \\ -0.88542 & 1.7708 & -0.88542 \\ 0 & -0.88542 & 0.88542 \end{bmatrix}$$

$$C_2 = \begin{bmatrix} 1.2918 & -1.1291 & -0.16271 \\ -1.1291 & 2.2541 & -1.125 \\ -0.16271 & -1.125 & 1.2877 \end{bmatrix}$$

The two matrices are completely different in values. In C_1 is present a 0, which means that upper and lower layer do not interact. In case 2 on the other hand each layer meshes together giving a complete matrix. For the simulation setup due to its better realism the second case has been chosen. A new problem comes out: define how much the surrounding area should be. With same

plane capacitor modifying the region by its percentage offset value in each direction high variations are gained. By decreasing this parameter from 100 to 10 the new matrix $C_{2,1}$ is:

$$C_{2,1} = \begin{bmatrix} 1.0984 & -1.0833 & -0.0151 \\ -1.0833 & 2.1605 & -1.0772 \\ -0.0151 & -1.0772 & 1.0923 \end{bmatrix}$$

Which corresponds to an average 10% smaller to C_2 .

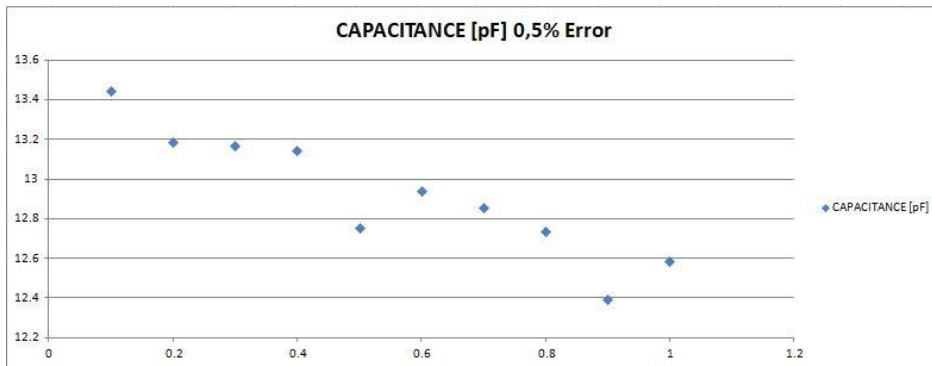
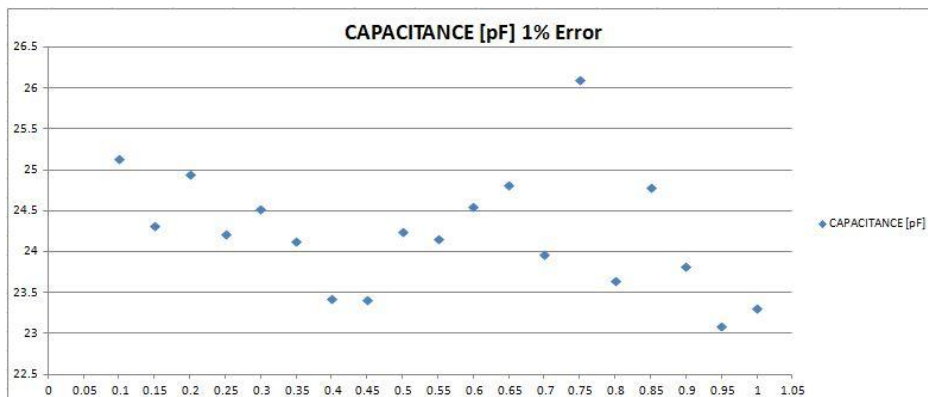
In the braking system due to the particular shape a region area evaluation should be done. Two different regions are analyzed. The first one includes all the components with the percentage offset value set to 100 meanwhile the second one characterized by the portion of area limited between the two parallel braking pad plates without any offset. It has an extremely complex architecture to investigate and even if it would be more precise it doesn't allow to verify all the mutual capacitances along the disc. Due to this reason the first mentioned region has been set as fixed parameter for every simulation.

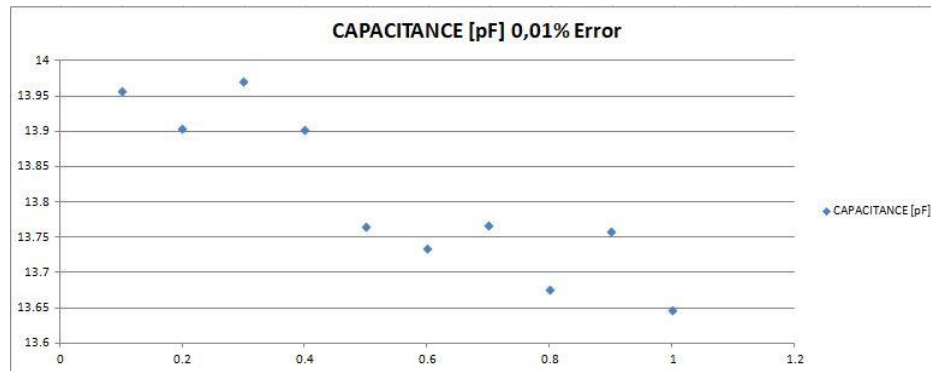
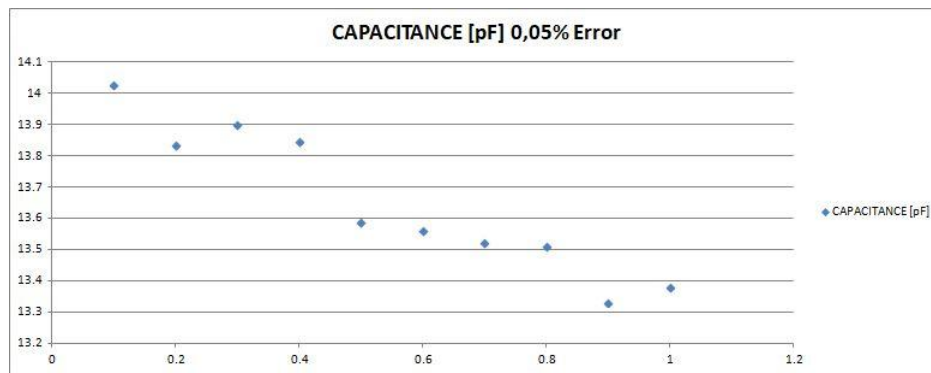
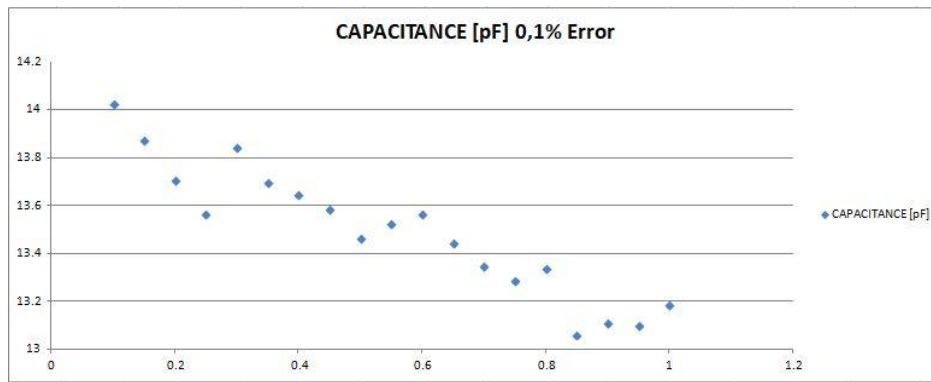
The succeeding parameter to define before being able to proceed with the simulation is to specify the voltages. From the experimental LCR instrument a sinusoid with 2Vpp was used, so the maximum applicable voltage would be in the range between -1V and +1V. At first think the applied voltages would have been three: one for each pad plate and the last one for the disc. The software on the other hand, in order to perform the complete capacitance matrix requires to apply to each component its specific voltage. This means that, having 5 components, five voltages should be applied and the matrix will be a 5x5 in dimension. The established voltages are: +1V, 0V, and -1V. given in this way:

- +1V to the left plate and its pad
- -1V to the right plate and pad
- 0V to the disc since it placed on a Table directly connected to ground.

To the pad and its relative pad plate the same voltage is applied. This is not entirely correct because there is a small voltage drop across the plate. Since the plate resistance is two orders smaller than the total system resistance we can assume it as negligible.

Another specification to be set is the energy percentage error sufficient to stop the simulation and proceed with the matrix computation. Many tests have been done before choosing the right percentage error by comparing the trend of the laboratory test with the simulation results. Once computed the simulations at 0.1mm incremental distance and 0.05mm for same cases, only the first element of the matrix is extracted and inserted in a distance-capacity value Table. The percentage error studied are: 1%, 0.5%, 0.1%, 0.05% and 0.01% and the relative Graphs (10) are shown.





Graph 10: Capacitive simulation trend at different percentage errors

In particular cases 1% and 0.1% have been investigated with an incremental distance of 0.05mm meanwhile 0.5%, 0.05% and 0.01% with 0.1mm increment. From the five cases the chosen one is 0.05% because it has a better decay capacitance-distance and is the lowest value in order to not incur in non convergent solutions. 0.01% could have been better but many divergent simulations occurred and solving time too wide. Defined the error also the incremental distance is fixed to 0.1mm.

First set of simulations has been processed with the aim to verify the trend of capacitance along different configurations setup. The two configurations treated are the one analyzed in the previous chapter: same surface and opposite surface. By comparing the simulations results shown in the Table (27) and respective Graph(11)

DISTANCE [mm]	0.1	0.2	0.3	0.4	0.5	0.6	0.7	0.8	0.9	1
OPPOSITE SURFACE [pF]	14.032	13.837	13.904	13.848	13.546	13.391	13.524	13.514	13.334	13.382
SAME SURFACE [pF]	13.754	13.643	13.616	13.569	13.546	13.391	13.334	13.291	13.045	13.114

Table 27: Comparison between same surface and opposite surface capacitive behavior

Is evident how both configurations have same trend, with a maximum percentage difference between each other of 2,2%. Since the variation is so small we can assume even in the simulation setup that the positions of same surface and opposite surface led to same results. For this reason only the opposite configuration is studied.

For this configuration ten simulation have been performed to be compared with the experimental values and other three to make sure the tendency stay asymptotic, so a total of thirteen matrices 5x5 are computed. The additional

Graph 11: Same surface versus Opposite surface capacitive trend

experimental measurements taken are depicted in Table(28):

DISTANCE [mm]	1.5	2	3
CAPACITANCE [pF]	42	38	24

Table 28: Long distance capacitance measurements

The thirteen distance-capacitance matrixes simulated are

$$C_{0.1mm} = \begin{bmatrix} 11.613 & -5.55665 & -5.7199 & -0.01676 & -0.30998 \\ & \mathbf{684.13} & -678.55 & -0.00115 & -0.01653 \\ & & 1368.5 & -678.51 & -5.7157 \\ & & & 684.27 & -5.7378 \\ & & & & 11.78 \end{bmatrix}$$

$$C_{0.2mm} = \begin{bmatrix} 13.326 & -5.5095 & -7.2932 & -0.01701 & -0.50638 \\ & \mathbf{349.4} & -343.88 & -0.00009 & -0.01698 \\ & & 701.98 & -343.52 & -7.2893 \\ & & & 348.75 & -5.2079 \\ & & & & 13.021 \end{bmatrix}$$

$$C_{0.3mm} = \begin{bmatrix} 13.548 & -5.7218 & -7.3025 & -0.01722 & -0.50621 \\ & \mathbf{237.49} & -231.75 & -0.00009 & -0.01711 \\ & & 478.09 & -231.72 & -7.3115 \\ & & & 237.15 & -5.1956 \\ & & & & 13.241 \end{bmatrix}$$

$$C_{0.4mm} = \begin{bmatrix} 11.53 & -5.485 & -5.715 & -0.0173 & -0.31307 \\ & \mathbf{180.86} & -175.36 & -0.00126 & -0.01752 \\ & & 362.14 & -175.39 & -5.6775 \\ & & & 180.61 & -5.2061 \\ & & & & 11.214 \end{bmatrix}$$

$$C_{0.5mm} = \begin{bmatrix} 12.987 & -5.1556 & -7.3048 & -0.0177 & -0.50894 \\ & \mathbf{146.82} & -141.65 & -0.00104 & -0.01756 \\ & & 298.07 & -141.88 & -7.2399 \\ & & & 147.01 & -5.1085 \\ & & & & 12.875 \end{bmatrix}$$

$$C_{0.6mm} = \begin{bmatrix} 13.068 & -5.295 & -7.2462 & -0.01825 & -0.20899 \\ & \mathbf{124.11} & -118.8 & -0.001 & -0.017 \\ & & 252.15 & -118.78 & -7.2318 \\ & & & 124.09 & -5.1956 \\ & & & & 12.954 \end{bmatrix}$$

$$C_{0.7mm} = \begin{bmatrix} 13.376 & -5.6231 & -7.2261 & -0.01844 & -0.05078 \\ & \mathbf{107.99} & -102.35 & -0.00115 & -0.01854 \\ & & 219.23 & -102.45 & -7.2037 \\ & & & 107.78 & -5.3075 \\ & & & & 13.038 \end{bmatrix}$$

$$C_{0.8mm} = \begin{bmatrix} 12.73 & -5.0258 & -7.1757 & -0.01852 & -0.51031 \\ & \mathbf{95.156} & -90.111 & -0.00117 & -0.0188 \\ & & 194.57 & -90.112 & -7.1736 \\ & & & 95.367 & -5.2358 \\ & & & & 12.939 \end{bmatrix}$$

$$C_{0.9mm} = \begin{bmatrix} 12.693 & -5.0502 & -7.1142 & -0.01873 & -0.50987 \\ & 85.972 & -80.902 & -0.00119 & -0.01905 \\ & & 175.9 & -80.751 & -7.1369 \\ & & & 86.317 & -5.5467 \\ & & & & 13.213 \end{bmatrix}$$

$$C_{1.0mm} = \begin{bmatrix} 12.974 & -5.3021 & -7.1149 & -0.01912 & -0.51138 \\ & 78.397 & -73.075 & -0.00121 & -0.01905 \\ & & 160.42 & -73.113 & -7.1163 \\ & & & 78.256 & -5.1223 \\ & & & & 12.769 \end{bmatrix}$$

$$C_{1.5mm} = \begin{bmatrix} 12.992 & -5.5588 & -6.9134 & -0.02085 & -0.49923 \\ & 55.371 & -49.79 & -0.00149 & -0.02113 \\ & & 113.41 & -49.745 & -6.9653 \\ & & & 58.843 & -5.0757 \\ & & & & 12.561 \end{bmatrix}$$

$$C_{2.0mm} = \begin{bmatrix} 12.939 & -5.6046 & -6.8121 & -0.02243 & -0.49985 \\ & 43.715 & -38.086 & -0.00171 & -0.0225 \\ & & 89.782 & -38.07 & -6.8133 \\ & & & 43.636 & -5.5421 \\ & & & & 12.878 \end{bmatrix}$$

$$C_{3.0mm} = \begin{bmatrix} 12.027 & -4.9676 & -6.5515 & -0.02592 & -0.48233 \\ & 31.158 & -26.163 & -0.00225 & -0.02519 \\ & & 65.386 & -29.138 & -6.533 \\ & & & 31.482 & -5.3162 \\ & & & & 12.357 \end{bmatrix}$$

Represented in the following parameters order:

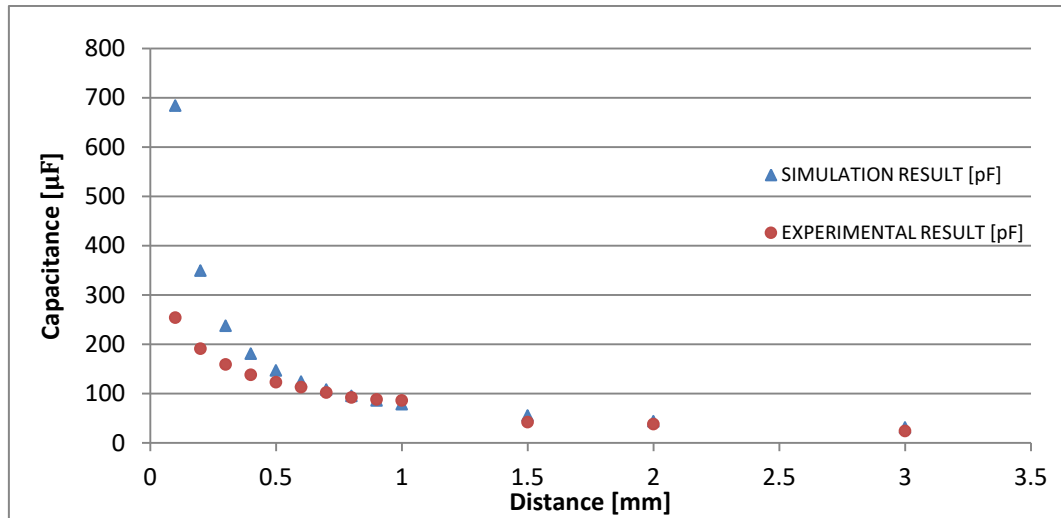
1. Left pad plate
2. Left pad
3. Disc
4. Right pad
5. Right pad plate

The highlighted values correspond to the element C_{22} of the capacitance matrix and represent the capacitance value measured during the experimental test. Also C_{44} could have been taken into account in fact the two elements difference is not bigger than 0.4% in the first 10mm.

Extrapolating the values and comparing them with the experimental one the following Table(29) and Graph(12) are obtained.

DISTANCE [mm]	SIMULATION RESULT [pF]	EXPERIMENTAL RESULT [pF]
0.1	684.13	254
0.2	349.4	191
0.3	237.49	159
0.4	180.86	138
0.5	146.82	123
0.6	124.1	113
0.7	107.99	102
0.8	95.156	92
0.9	85.972	88
1	78.397	86
1.5	55.371	42
2	43.715	38
3	31.158	24

Table 29: Comparison between simulation and experimental results



Graph 12: Simulation versus experimental tests

By looking at the graph is noticeable that experimental and simulation curves are practically the same when the distance is bigger than 0.6mm included. In the distance between 0.1 mm and 0.5mm the two hyperbolas have different slope. The main reason due to this gap is due to the defect introduced by the paper dielectric permittivity set during material assignment. Paper in fact has a dielectric permittivity that varies from 2.3 to 4 depending on the type of paper used; if there is contamination of oil (4) or wax (2.5). For the simulation configuration 2.3 has been imposed. Moreover the used insulator is not properly paper but scotch tape, this means that the chosen value can vary a little due to glue or other adhesive materials.

Another possible error is given by the non-perfect connection of the disc with the ground since it is not cable grounded but place on a wooden Table. This could generate a really small parasitic capacitance that can't be measured. Last approximation is given by the previously definition of the material characteristics especially for the braking pad which as previously said is made up of hundreds of different materials.

Moreover this comparison is valid only for metallic brake pads since no other kind of pads have been tested.

4.4 Final impedance value

Once measured resistance and capacitance values the impedance can be evaluated by its definition:

$$Z = R + jX \quad (3.17)$$

where R stands for resistance and X for reactance. Since the brake pad is made of a compound homogenous in all its volume, the resistance value should not vary along the pad wear out. Due to this assumption the impedance variation is given only by the reactance and so by the capacitance.

Chapter 4

In the final chapter a brief schematic solution is proposed to design a possible industrial product able to perform an impedance measurement and to evaluate unwanted contacts.

During laboratory session the GW Instek LCR 819 has been used. This instrument is really precise with a wide frequency window, many computational modes, but at the same time is heavy (about 5,5 kg) bulky not suitable for fitting inside a car control unit. The solution to the problem is to search for a microchip and then an evaluation board with approximately same specifics or at list the one of interest.

The chosen microchip is the AD5933, meanwhile the evaluation board related to the chip is the EVAL-AD5933EBZ board. The characteristics that led to this choice are:

- Frequency resolution of 27 bits which means less then 0.1 Hz
- Impedance measurement range from 100 to 10M Ω with right configuration
- System accuracy of 0.5%
- Temperature range between -40°C and +125°C
- Qualification for automotive applications

First three features are related to measure itself, how to take it, how precise is the instrument or item used and which is the measurable window. The last two on the other hand are strictly related to the external conditions that may create interferences and so wrong values.

Really important is the temperature range since is perfectly inside the one used during climatic tests in the automotive industry (from -60°C to +150°C). Moreover the qualification for automotive applications allows to create a measuring system that doesn't interact with the surrounding electrical circuits.

4.1 AD5933 system description

The AD5933 is a high precision impedance converter system solution that combines an on board frequency generator with a 12-bit , 1MSPS (1 million samples per second) ADC (analog-digital converter). The frequency generator allows an external complex impedance to be excited with a known frequency. The response signal from the impedance is sampled by the on board ADC and discrete Fourier Transform (DFT) processed by an on-board digital signal process (DSP) engine. The DFT algorithm returns both a real “R” and an imaginary “I” value at each frequency point along the sweep. In the easy process, the impedance magnitude and phase are then easily calculated using the following equations:

$$\text{Magnitude} = \sqrt{(R^2 + I^2)} \quad (4.1)$$

$$\text{Phase} = \tan^{-1} \left(\frac{I}{R} \right) \quad (4.2)$$

In addition it permits to perform frequency sweep with a starting frequency defined by the user, a frequency resolution and a number of points in the sweep. Also the peak to peak value of the output sinusoidal signal as excitation to the unknown impedance connected between input and output voltage (VIN VOUT pins) can be chose by four different values depicted in Table(30).

Range	Output excitation [Vpp]	Output DC Bias level [V]
1	1.98	1.48
2	0.97	0.76
3	0.383	0.31
4	0.198	0.173

Table 30:Peak to peak voltage of the output signal

The block diagram of the micro chip is depicted in Figure(35)

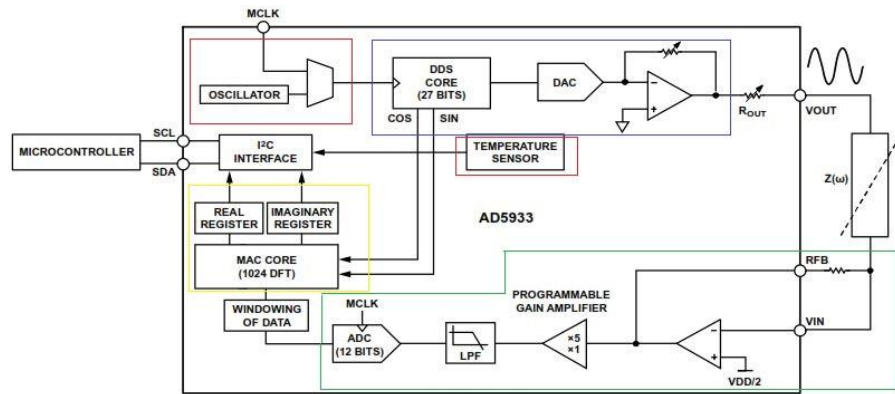


Figure 35: AD5933 board block diagram

It can be divided in five blocks:

- Transmit stage
- Receive stage
- Discrete Fourier Transform
- System clock
- Temperature sensor

Transmit stage is made up of a 27-bit phase accumulator direct digital synthesis (DDS) core which provides the excitation signal at the user chosen frequency. In this specific microchip, the first three bits of the starting frequency are internally set to zero, therefore the user can program the frequency in the range of 24 bits. This block is shown blue in Figure(35).

Receive stage is made up of a current to voltage amplifier followed by a programmable gain amplifier (PGA), an anti-aliasing filter and an analog to digital converter (ADC). It is enclosed in the green box in Figure(35). In the first piece, current to voltage amplifier, the voltage present at pin VIN is a virtual ground with a DC value set at $VDD/2$ (VDD stands for supply voltage). The signal current developed across the unknown impedance flows into the VIN pin and produces a voltage signal to the output of the converter. The gain of this amplifier is dependent to the user-chosen resistor placed between VIN and RFB (external feedback resistor) pins. The second step is the programmable gain amplifier (PGA) which allows to multiply the output of the

current to voltage by a factor of 1 or 5, by selecting a series of switches. Finally the analog signal is low pass filtered and the ADC converts it digital code.

The digital codes reaches the discrete operation block encase in the orange block in Figure(35) where the 1024 point discrete Fourier transform is evaluated for each frequency step of the sweep.

It is represented by the formula:

$$X(f) = \sum_{n=0}^{1023} (x(n)(\cos(n) - j \sin(n))) \quad (4.3)$$

where:

-X(f) is the output sequence at rated frequency f

-x(n) is the digital output of the ADC converter

-cos(n) and sin(n) the vectors provided by the DDS core at rated frequency f

Once the DFT is performed the results of each frequency point f are stored in two registers, one for the real component and one for the imaginary component.

AD5933 microchip allows the possibility to adopt two system clocks: one on-board 16.776MHz oscillator or an external one provided by the user. Time block is defined in Figure(35) in yellow.

The last box in red in Figure(35) represents the temperature sensor. It is characterized by a 14 bits, one limited to the definition of sign. It allows to execute measurement between -40°C to +125°C with an accuracy of ±2°C.

Starting from the results of the DFT the magnitude of the transform is given by (4.1). To get to the impedance value it has to be multiplied by a scaling factor called gain factor. The gain factor is calculated during system calibration with a known impedance connected to the VIN and VOUT pins and is given by the

ratio inverse calibration impedance value over the magnitude. In terms of formulas it is expressed as:

$$Gain\ factor = \left(\frac{1}{\frac{Calibration\ Impedance}{Magnitude}} \right) \quad (4.4)$$

4.2 Measurement setup

As previously mentioned the microchip is fit on an evaluation board named: EVAL-AD5933EB which can be powered from a USB port with a supply voltage that varies from 2.7V to 5.5V. This power supply can be given by a traditional pc.

In the following Figure (36) the connection necessary to let the measurement system function is depicted. The USB port doesn't only provides the power supply but also allows the data transmission from the electronic board to the software. Cable blue and brown are the connection between the impedance measurement point and the reference pad plate eyelets

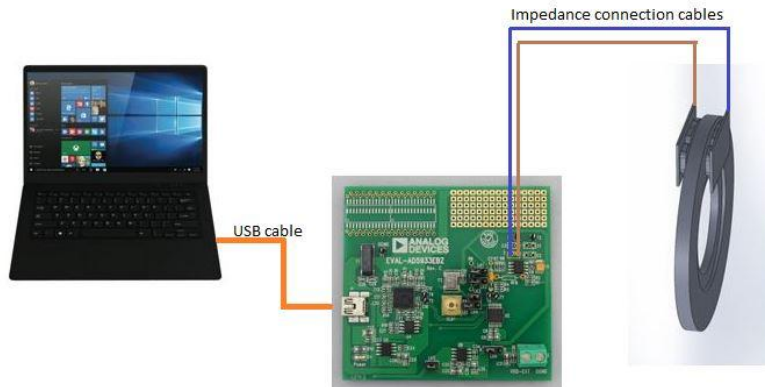


Figure 36: System connections

Inside a vehicle the control unit doesn't furnish the electrical supply itself, but it is given by the 12V battery. Due to this a voltage step down is needed. The data on the other hand are not managed by a portable computer but by an

electronic control unit (ECU).The configuration previously shown changes a bit. In Figure(37) it is possible to see the adjustments.

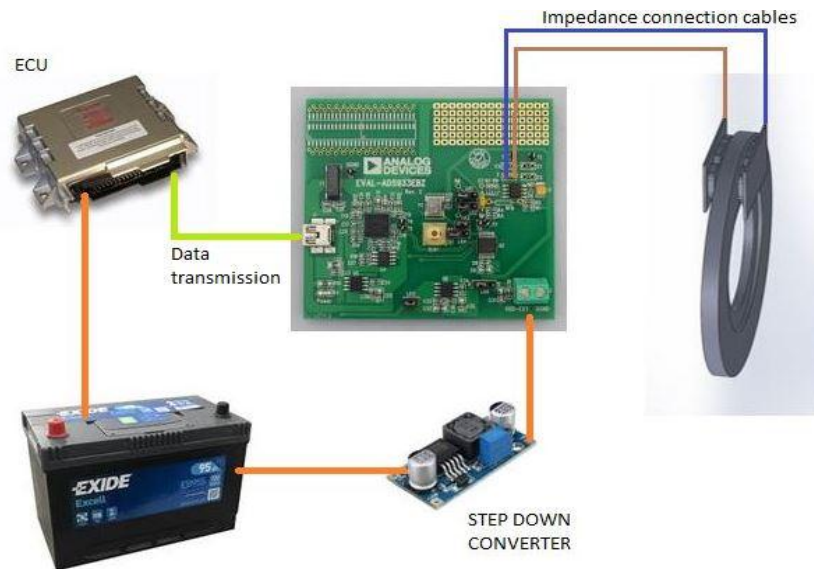


Figure 37: Automotive system connections

4.3 Advantages versus disadvantages

This system has many advantages starting from the fact that it is automotive compatible. This means that it should not interfere with any other electronic system on board and can be placed side by side to the already present braking wear control systems for a better safety efficiency. Moreover with the frequency sweep function, during configuration mode, it can be easily find a window in which measurements are not affected by errors or at least with a small percentage. It is very compact, light and can be integrated next to the ECU.

The main problem related to this approach is that only one impedance measurement can be performed at a time. To solve this problem a possibility is to create a circuit with a multiple switch with at least four channels. For a complete disc brake set up all four are needed meanwhile for the disc-drum configuration only two. Taking into account the complete disc brake configuration, each channel is related to one pair of pads. With same time

interval the switch changes channel and the measurement is taken. This is a complex and fragile solution since all the system depends on a switch. The easiest way to overcome this problem is to divide the entire braking system in two: front axle and rear axle. It would double the measurement units and the switches, but the load is reduced.

Another limitation is the starting frequency fixed at 1kHz which is a frequency one order of magnitude bigger than the one performed during laboratory sessions (100Hz). To overcome this issue is possible to add an external board that allows to decrease the starting frequency.

4.4 Experimental test on the EVAL-AD5933EB board

To analyze the system and perform a frequency sweep along a distance increment the first thing that needs to be done is the calibration of the electronic board. In the instruction scheme this process is well described but the in the requirements a pair of resistor of 200k Ω was needed. Since a 200k Ω resistor is not a common one, during calibration a 220k Ω has been used. In the following Figure (38) this passage is shown.



Figure 38: Calibration setup of the EvalAD5933EBZ board

The two resistor were inserted one in the external feedback resistor (RFB) position and the other between the V_{in} and V_{out} pins of the AD5933. The

system is power supplied by the computer through the usb connection. On the computer the software is opened and the configuration process begins. Once defined all the variable for the sweep , gain and temperature is possible to apply the measurement. The outcome is shown in Figure(39)

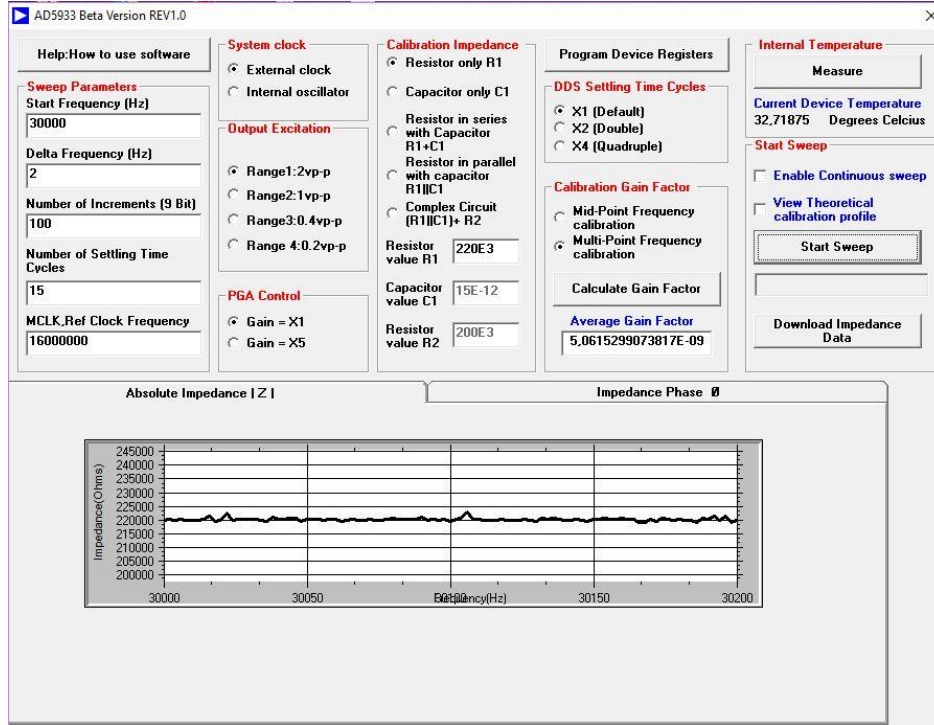


Figure 39: Software parameter for board calibration

And the absolute impedance fluctuate around 220kΩ. Configurations is concluded and is time to find for our system setup the calibration resistance to insert in RFB. Calibration resistance can be expressed as:

$$R_{cal} = \frac{Z_{min} + Z_{max}}{3} \quad (4.5)$$

where

$$|Z_{min}| = \sqrt{\frac{1^2 + (2\pi RC f_{min})^2}{2\pi RC f_{min}}} \quad (4.6)$$

$$|Z_{max}| = \sqrt{\frac{1^2 + (2\pi RC f_{max})^2}{2\pi RC f_{max}}} \quad (4.7)$$

In particular f_{\min} and f_{\max} are the boundary frequencies for the sweep meanwhile R and C are the relative values of the system impedance.

From the experimental measurement at 10KHz $R=40\Omega$ and $C= 850\mu\text{F}$. By considering a sweep between 30000Hz and 30200Hz the calibration resistance equals: $R_{\text{cal}}=54.231\Omega$

Since a resistance of this value is not easily available, the 56Ω is used.

A new calibration has been performed with the new resistance and once concluded the incremental distance can take place. As well as the experimental test with the LCR, also with the evaluation board, ten distances are established each one increased by 0.1mm.

In Figure(40) is represented the simulation setup with the two brake pads placed on the same disc surface, each one connected to the relative board pins. The yellow-red wire has been cut longer than the required for the test and rolled upon itself in order to verify the system stability measurement even at long distances. If this device is placed inside the control unit and has to communicate with the rear brake axle a noticeable distance is present between the components and the measurement should not be altered. The distance between pad and disc has been done as in chapter 2 with use of scotch tape and wire were not soldered. A better performance could be done using an analog front end (AFE) which allows to measure smaller impedances.

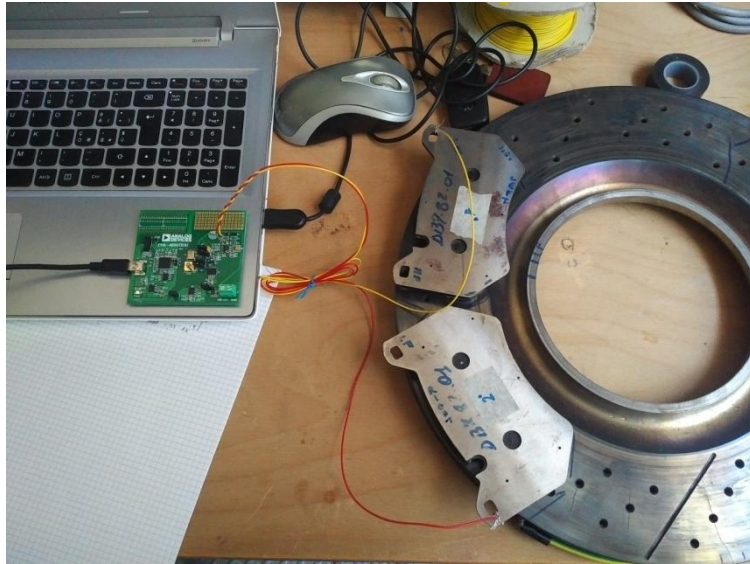
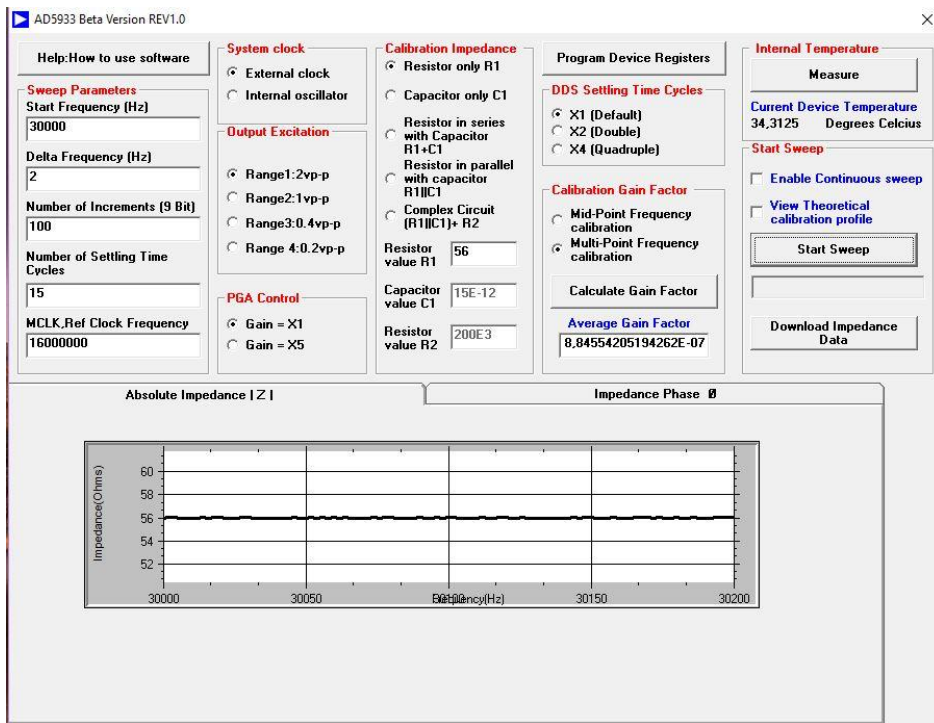


Figure 40: Impedance measurement setup

All the ten simulation are depicted in the following Figure(41):



AD5933 Beta Version REV1.0

Help:How to use software

Sweep Parameters

Start Frequency (Hz)
30000

Delta Frequency (Hz)
2

Number of Increments (9 Bit)
100

Number of Settling Time Cycles
15

MCLK_Ref Clock Frequency
16000000

System clock

External clock
 Internal oscillator

Output Excitation

Range1:2vp-p
 Range2:1vp-p
 Range3:0.4vp-p
 Range 4:0.2vp-p

PGA Control

Gain = X1
 Gain = X5

Calibration Impedance

Resistor only R1
 Capacitor only C1

Resistor in series with Capacitor R1+C1
 Resistor in parallel with capacitor R1||C1
 Complex Circuit (R1||C1)+ R2

Resistor value R1: 56
Capacitor value C1: 15E-12
Resistor value R2: 200E3

Program Device Registers

DDS Settling Time Cycles

X1 (Default)
 X2 (Double)
 X4 (Quadruple)

Calibration Gain Factor

Mid-Point Frequency calibration
 Multi-Point Frequency calibration

Calculate Gain Factor

Average Gain Factor
8.84554205194262E-07

Internal Temperature

Measure

Current Device Temperature
34.4375 Degrees Celcius

Start Sweep

Enable Continuous sweep
 View Theoretical calibration profile

Start Sweep

Download Impedance Data

Absolute Impedance |Z| Impedance Phase θ

AD5933 Beta Version REV1.0

Help:How to use software

Sweep Parameters

Start Frequency (Hz)
30000

Delta Frequency (Hz)
2

Number of Increments (9 Bit)
100

Number of Settling Time Cycles
15

MCLK_Ref Clock Frequency
16000000

System clock

External clock
 Internal oscillator

Output Excitation

Range1:2vp-p
 Range2:1vp-p
 Range3:0.4vp-p
 Range 4:0.2vp-p

PGA Control

Gain = X1
 Gain = X5

Calibration Impedance

Resistor only R1
 Capacitor only C1

Resistor in series with Capacitor R1+C1
 Resistor in parallel with capacitor R1||C1
 Complex Circuit (R1||C1)+ R2

Resistor value R1: 56
Capacitor value C1: 15E-12
Resistor value R2: 200E3

Program Device Registers

DDS Settling Time Cycles

X1 (Default)
 X2 (Double)
 X4 (Quadruple)

Calibration Gain Factor

Mid-Point Frequency calibration
 Multi-Point Frequency calibration

Calculate Gain Factor

Average Gain Factor
8.84554205194262E-07

Internal Temperature

Measure

Current Device Temperature
34.375 Degrees Celcius

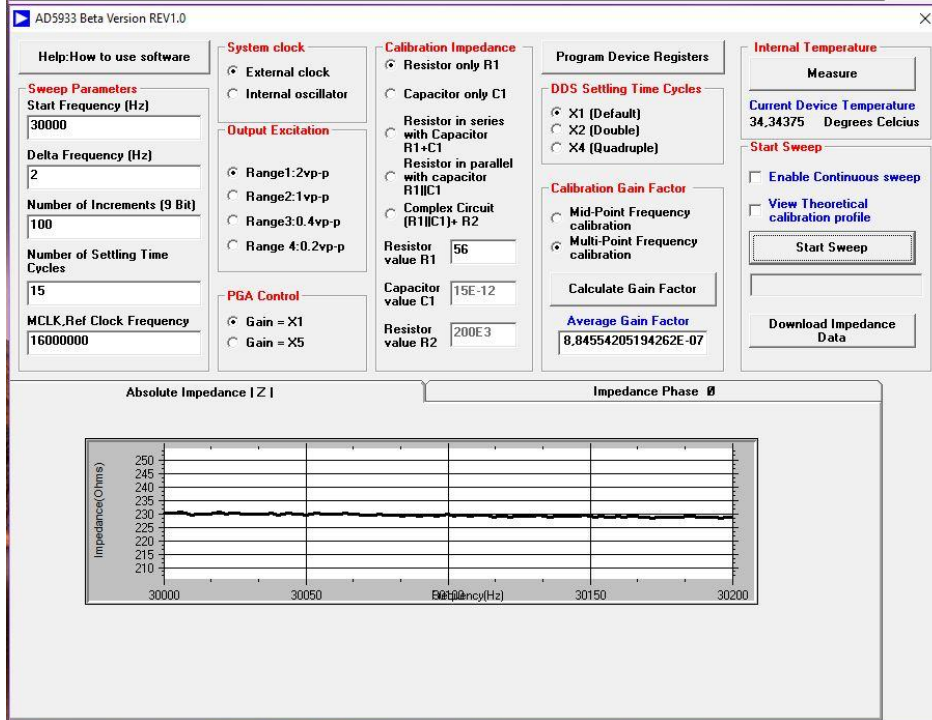
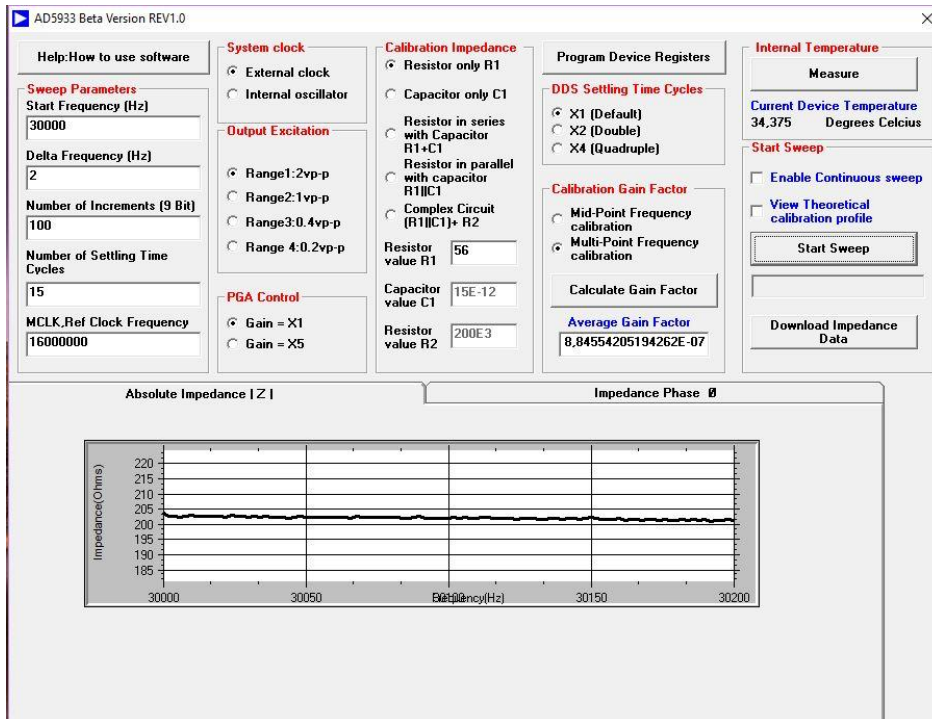
Start Sweep

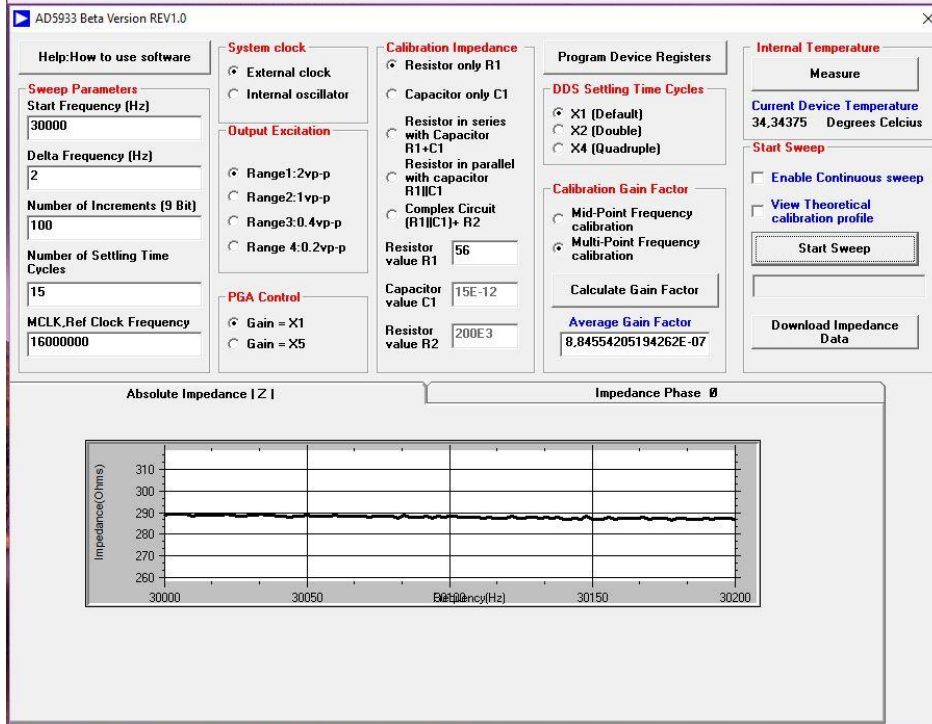
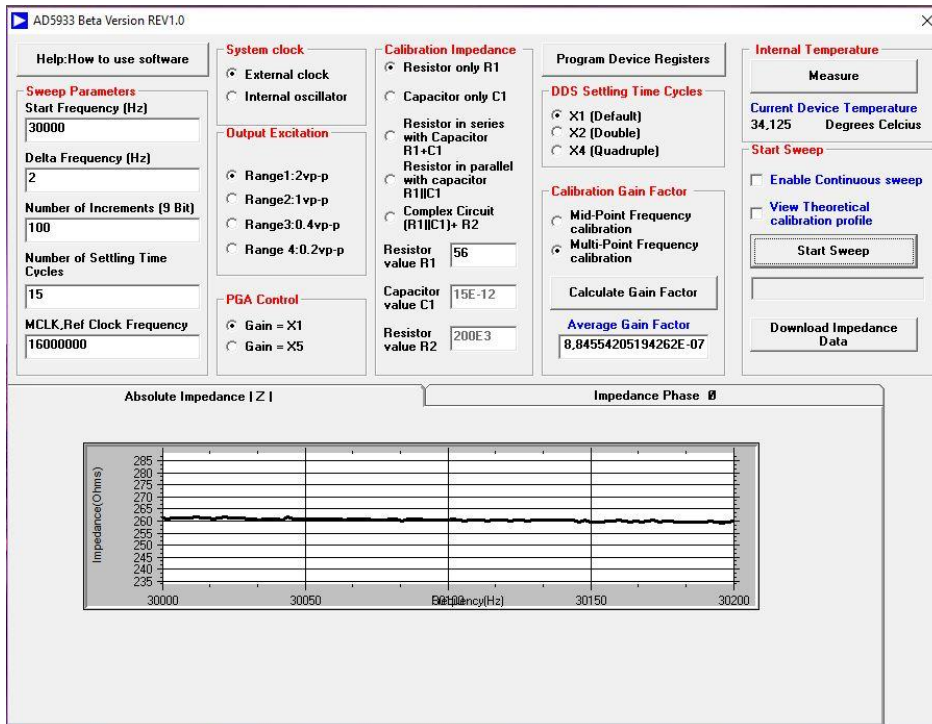
Enable Continuous sweep
 View Theoretical calibration profile

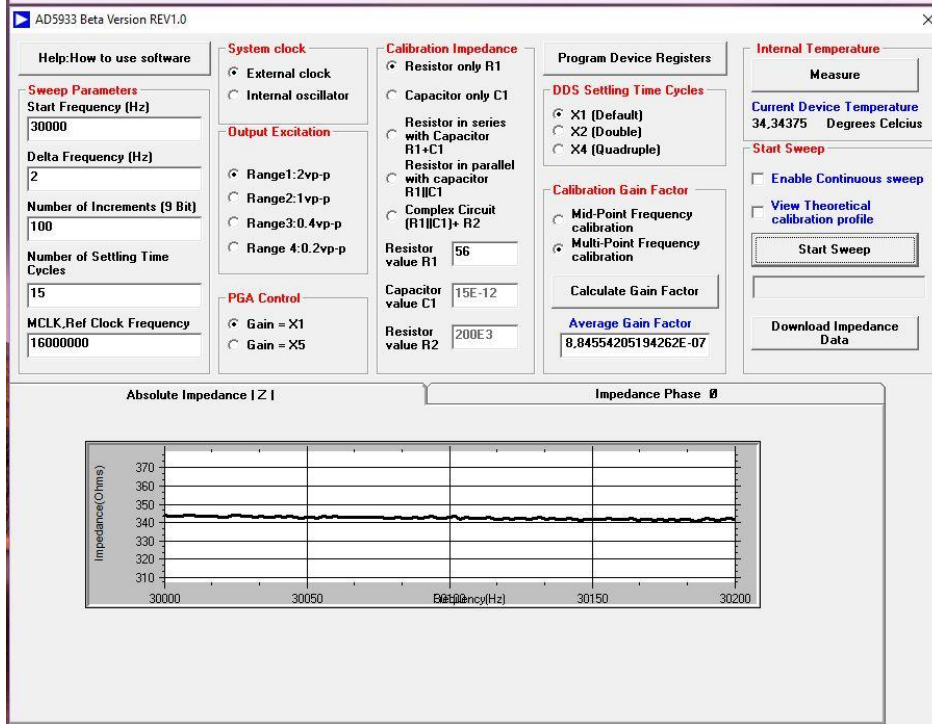
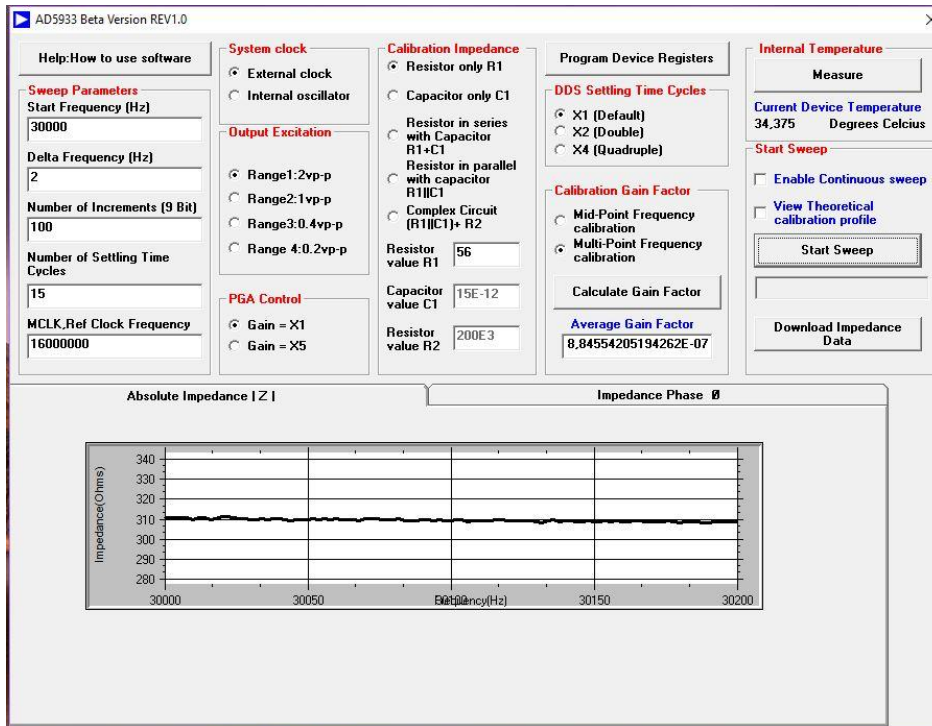
Start Sweep

Download Impedance Data

Absolute Impedance |Z| Impedance Phase θ







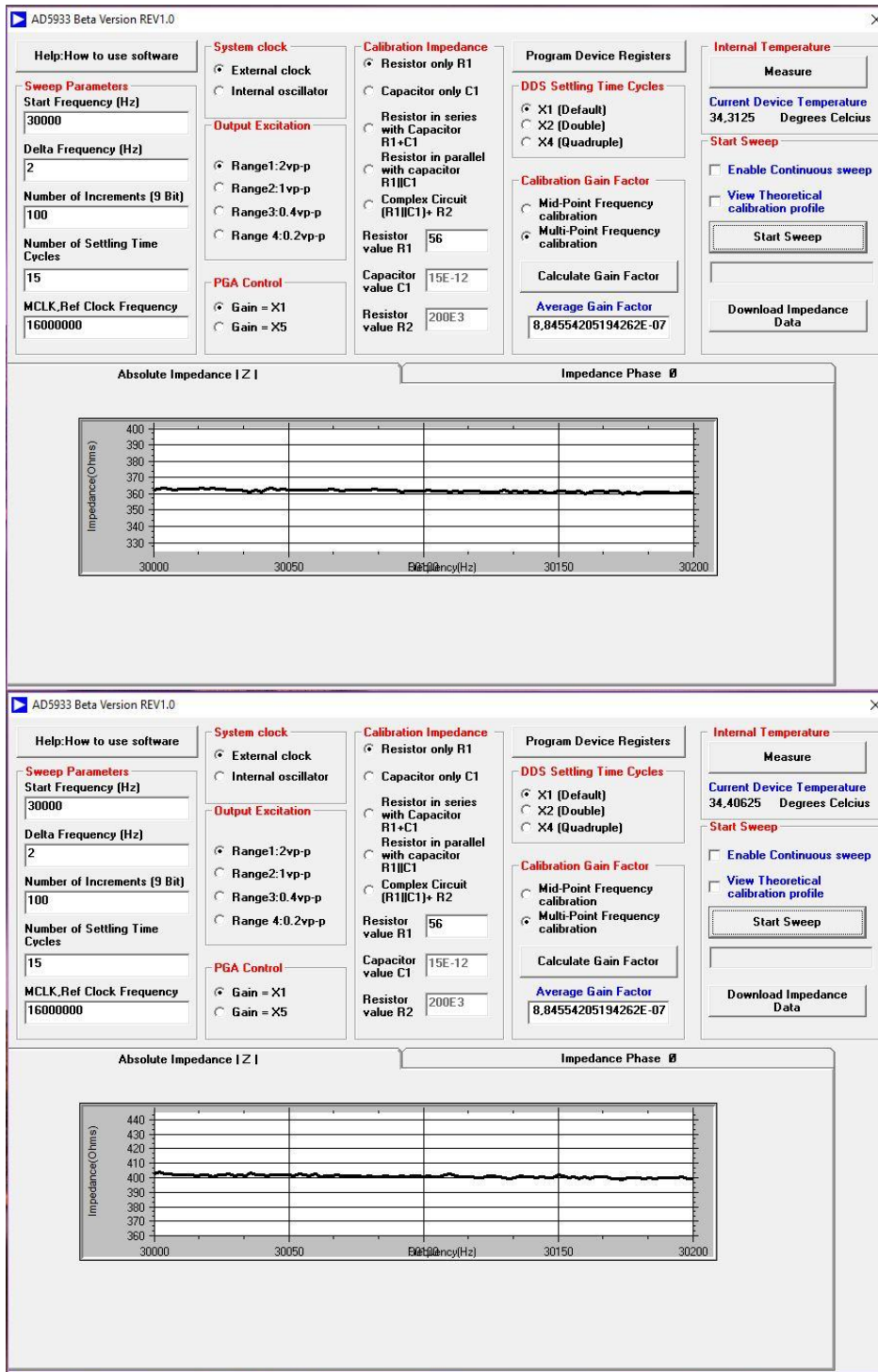


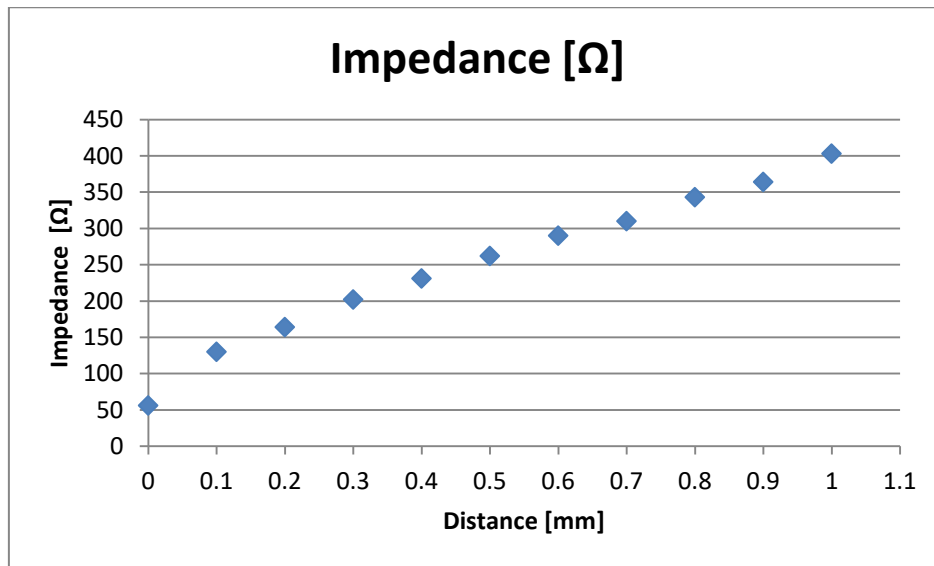
Figure 41: 11 impedance simulation with EvalAD5933EBZ board

In the region of frequency analyzed measurement are stable and do not perform any kind of oscillation. The trend of each graph is to show an impedance decrease within the frequency increase. This is correct since the reactive component is inverse proportional to the frequency which rises along the established window.

The results can be sum up into the Table(31) and relative Graph(13)

Distance[mm]	Impedance [Ω]
0	56
0.1	130
0.2	164
0.3	202
0.4	231
0.5	262
0.6	290
0.7	310
0.8	343
0.9	364
1	403

Table 31: Impedance at incremental distance



Graph 13: Impedance at incremental distance

Looking at the results to an increase in distance corresponds an increase of impedance. This is correct since reminding equation 2.4 , 3.17 and the expression of capacitance as:

$$C = \varepsilon \frac{S}{d} \quad (4.8)$$

where “S” stands for normal surface and “d” for armature distance.

Impedance can be written as:

$$Z = \rho \frac{d}{S} - \frac{j}{2\pi f \varepsilon \frac{S}{d}} \quad (4.9)$$

In terms of absolute value:

$$|Z| = \sqrt{\left(\rho \frac{d}{S}\right)^2 + \left(\frac{d}{2\pi f \varepsilon S}\right)^2}$$

Increasing the distance d, present in both terms in the numerator, the absolute value of impedance will rise.

Conclusion

The presented analysis has dealt with one of the problems caused by vehicles: air pollution. This phenomena occurs not only when the driver wants to decelerated and stops, but also without noticing during ordinary driving. The defect stays in the possible contact of brake pads with the disc when braking actions are not required. However a smart design of the brake caliper can mitigate the impact of this phenomenon and even contribute to alleviate the pads wear. From a literature point of view there aren't many studies related to the topic of interest. The only research attributable to the mentioned issue has been developed in China but it is not accessible since it is under patent. This thesis analyzed a strategy solution to the proposed problem by evaluating through an LCR measurement equipment the impedance absolute value of the system: brake pad pair and brake disc at different distances. The type of solution adopted is able, once characterized all the braking system components, to detect the presence of unwanted contacts just by a comparison of two impedance values: the measure one and the reference. The system should work continuously in order to have always an updated comparison and so the actual state of the system. Some counteractions can be adopted when the unwanted contact has risen. The easiest one consist in creating a clamp that connects each pad plate with its caliper piston and apply when required a negatives pressure to the braking system and drift apart the pads. This type of project involves several components and a very high number of possible aspects and variable parameters. Therefore, the presented solution is only one side of the braking system study, which needs to be deepened and applied in the future of the ultimate industrial product. Several criticalities must still be analyzed and several improvements can still be outlined. Therefore, this work aims at acting as a springboard for the future of the synthetic inertia studies.

Bibliography

- [1] James D. Halderman, "Brake Systems", 7th Edition, January 2016.
- [2] James D. Halderman, "Automotive Technology: principles, diagnosis and service", Fifth Edition, January 2015.
- [3] Milenko Braunovic, Valery V. Konchits, and Nikolai K. Myshkin, "Fundamentals of Electrical Contacts", CRC Press, 2007.
- [4] Holm, R., "Electrical Contacts, Springer", New York, 1979
- [5] Roberto Dante, "Handbook of Friction Materials and their Application", 1st Edition, Elsevier Ltd., 2016.
- [6] Glossbrenner, E. W., "Sliding contact for instrumentation and control, In Electrical Contacts: Principles and Applications", Marcel Dekker, New York, pp. 885–941, 1999.
- [7] Hutchings, I. M., Tribology: Friction and Wear of Engineering Materials, Edward Arnold, London, 1992.
- [8] B.N.J.Persson, E.Tosatti, "Physics of Sliding Friction", Springer, 1995
- [9] Peter J. Blau, "Composition, Functions, and Testing of Friction Brake Materials and their Additives", „August 2001
- [10] A. E. Anderson, "Friction and Wear of Automotive Brakes," in ASM Handbook, Friction Lubrication and Wear Technology, Volume 18, ASM International, Materials Park, Ohio, pp. 569- 577, 1992.
- [11] Analog Device, « [AD5933](#) Datasheet".
- [12] [Analog](#) Device "UG-364".
- [13] G.P. Ostermeyer, "Modeling friction and wear of brake systems", Institute of Dynamics and Vibrations, Technische Universität Braunschweig, 2001.
- [14] Ýlker Sugözü, Ýbrahim Mutlu, Ahmet Keskin, "Friction and wear behaviour of ulexite and cashew in automotive brake pads", 2015.

Appendix

TABLE OF MATERIALS USED INSIDE A BRAKE PAD.

Material Name	Main Function	Other Functions	Percentage Found In Pads	Conduction properties
Fiberglass	Binder	Works both as a binder and as a structural material	5-25%	Insulator
Phenolic Resin, which may or may not be derived from Cashew Nut Shells	Binder	Works a binder but also as performance additive	10-20%	Insulator
Cashew Resin which may or may not be used in "friction dust"	Performance	A special type of phenolic resin that improves brake performance, resists fade, and can help make brakes operate more quietly	0-20%	. insulator
Mineral wool fibers	Structure	These fibers typically reinforce the structure of the pad, but they can also help manage temperatures and reduce fade. Fibers can be spun from silica, alumina, calcia, and magnesia. Vermiculite is also a mineral fiber.	10-20%	insulator
Mineral fillers, typically quartz or synthetic silicates	Abrasive	Unlike mineral <i>fibers</i> , fillers are used as an abrasive to boost friction.	5-35%	.insulator for quartz and semiconductor for synthetic silicates
Metal Oxides, typically aluminum oxide and iron oxide	Abrasive	An abrasive that boosts friction, but also a filler/binder in a metallic or semi-metallic pad.	0-70%	insulator

Carbon (Graphite)	Performance	Carbon comes in many forms. It may be used to increase friction, but could also be used as a lubricant.	0-35%	conductor
Brass filings or chips	Abrasive	A cheap abrasive that boosts pad performance in wet weather.	0-5%	conductor
Friction Dust or Friction Powder	Performance	A proprietary mix of compounds that have a wide variety of uses - everything from reducing noise to acting as a flame retardant.	0-25%	
Metal sulfides, including copper sulfide, antimony sulfide, and lead sulfide	Performance	Work to stabilize friction coefficients at various temperatures	0-5%	insulator
Petroleum coke	Performance	Stabilizes and modifies friction performance - very cheap material.	??%	
Asbestos	Structure	Filler, structural reinforcement, and heat resistance	0-35%	insulator
Barium Sulfate, a.k.a. Barytes	Filler	Very common filler material.	0-35%	conductor
Lime (Calcium Hydroxide)	Performance	Inhibits corrosion in metallic pads	0-5%	insulator
Potassium Titanate	Filler	Common filler material	0-30%	insulator
Steel Wool	Filler	Another common filler material	0-30%	conductor

Rubber or Rubber Scrap from recycled tires	Filler	Filler material can increase wear resistance.	0-10%	insulator
Ceramic Microspheres	Performance	Works as a filler, friction modifier, and brake dust inhibitor	0-20%	insulator
Finely ground bituminous coal, known as Sea Coal	Filler	Cheap filler material	??%	insulator
Kevlar [®] and Kevlar [®] Pulp	Performance	Friction enhancer -	0-3%	insulator
Copper	Performance	Copper provides heat resistance, improves cold weather performance, and acts as a lubricant to prevent squeaking. Frequently found in ceramic brake pads. May be replaced with hexagonal boron nitride (pending legislation).	0-25%	conductor
Ceramics	Structure	Ceramic compounds come in an incredible number of varieties and are capable of performing all functions.	0-100%	insulator
Carbon Fiber	Binder	Carbon fiber is an up-and-coming pad material that acts as a binder and abrasive. However, it's very expensive and relatively exotic.	0-100%	conductor.